



LUND UNIVERSITY

Deformations and Critical Loads of Steel Beams Under Fire Exposure Conditions

Thor, Jörgen

1973

[Link to publication](#)

Citation for published version (APA):

Thor, J. (1973). *Deformations and Critical Loads of Steel Beams Under Fire Exposure Conditions*. (Bulletin of Division of Structural Mechanics and Concrete Construction, Bulletin 35; Vol. Bulletin 35). Lund Institute of Technology.

Total number of authors:

1

General rights

Unless other specific re-use rights are stated the following general rights apply:

Copyright and moral rights for the publications made accessible in the public portal are retained by the authors and/or other copyright owners and it is a condition of accessing publications that users recognise and abide by the legal requirements associated with these rights.

- Users may download and print one copy of any publication from the public portal for the purpose of private study or research.
- You may not further distribute the material or use it for any profit-making activity or commercial gain
- You may freely distribute the URL identifying the publication in the public portal

Read more about Creative commons licenses: <https://creativecommons.org/licenses/>

Take down policy

If you believe that this document breaches copyright please contact us providing details, and we will remove access to the work immediately and investigate your claim.

LUND UNIVERSITY

PO Box 117
221 00 Lund
+46 46-222 00 00

LUND INSTITUTE OF TECHNOLOGY · LUND · SWEDEN · 1973
DIVISION OF STRUCTURAL MECHANICS AND CONCRETE CONSTRUCTION · BULLETIN 35

JÖRGEN THOR

DEFORMATIONS AND CRITICAL LOADS OF
STEEL BEAMS UNDER FIRE EXPOSURE
CONDITIONS

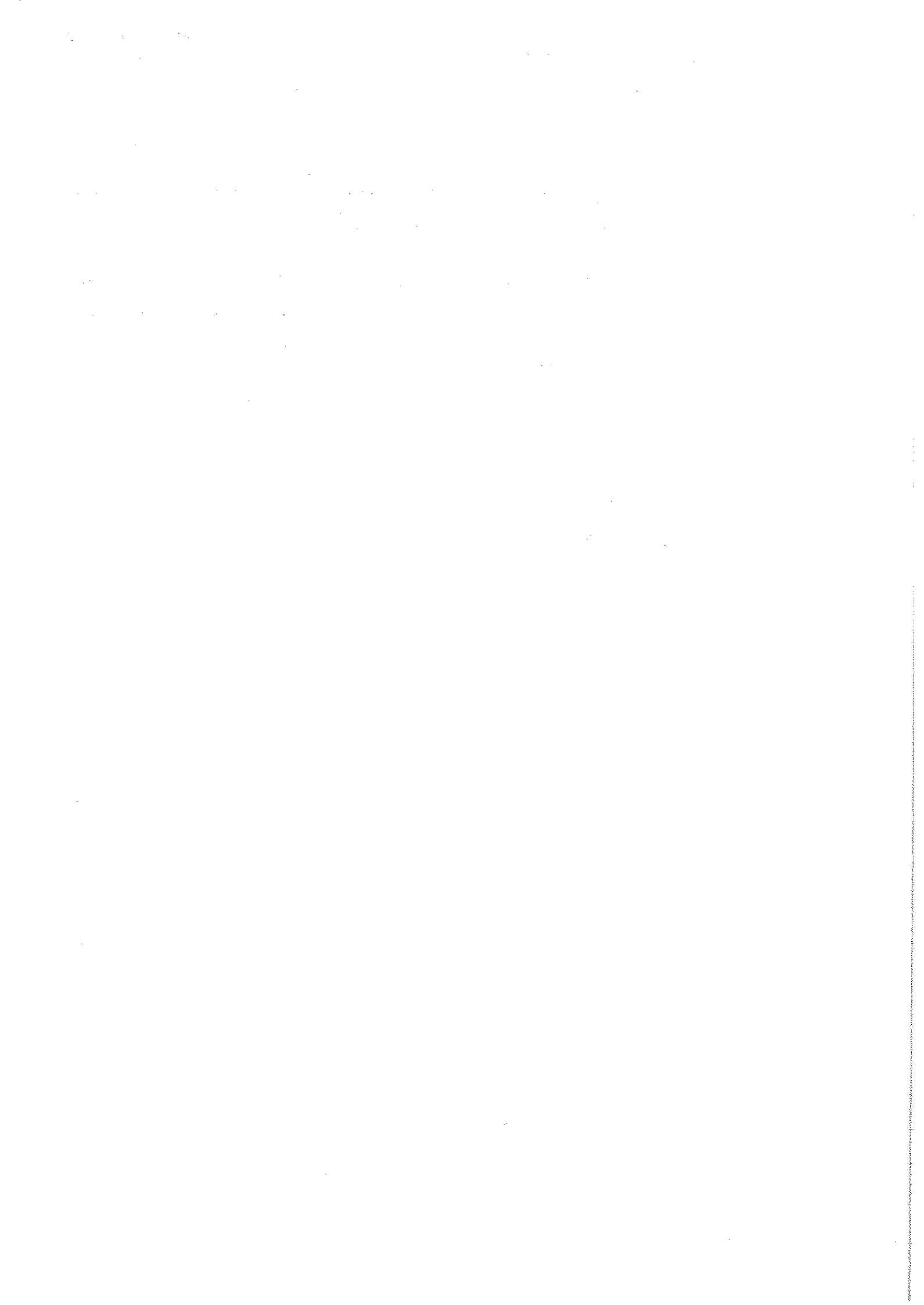
Document

D16:1973

**Deformations and critical
loads of steel beams under
fire exposure conditions**

Jörgen Thor

**National Swedish
Building Research**



Brandpåverkade stålbalkars deformation och kritiska belastning

Jörgen Thor

En nyanserad brandteknisk dimensionering tillämpad på bärande stålkonstruktioner kan ge avsevärda kostnadsbesparingar.

Detta Document summerar de viktigaste resultaten i författarens doktorsavhandling "Behaviour of Steel Structures Exposed to Fire". En metod för beräkning av brandpåverkade stålbalkars deformationsförlopp presenteras. Modellen gör det möjligt att säkrare bedöma bärförmåga och brottrisk och att beakta de speciella förhållanden som kan råda för olika konstruktioner. Det har visat sig att en stålbalk utsatt för brand oftast har en avsevärt större bärförmåga än vad en schablonmässig bestämning ger som resultat.

Dimensionering

I jämförelse med den relativt noggranna dimensionering en bärande konstruktion underkastas för statisk last måste dimensioneringen av samma konstruktion för påverkan av brand oftast karakteriseras som slentrianmässig. Den brandtekniska dimensioneringen baseras nämligen vanligtvis på schablonartat uppställda krav på motståndstider mot brand relaterade till en påverkan enligt ett standardiserat temperatur-tidförlopp, den s.k. standardbrandkurvan. Enligt gällande svenska bestämmelser tillåts dock en mer nyanserad brandteknisk dimensionering. Vid en sådan dimensionering, där brand betraktas som ett lastfall bland andra, krävs ett påvisande av att konstruktionen uppfyller sin funktion vid den verkliga brandpåverkan den kan bli utsatt för i aktuell typ av byggnad. Tillämpat på en bärande stålkonstruktion resulterar ofta en sådan noggrannare dimensionering i att avsevärda kostnadsbesparingar för att uppnå erforderligt brandskydd kan göras.

Vid en nyanserad brandteknisk dimensionering beräknas stålkonstruktionens temperatur-tidförlopp genom värmebalanskvationer, varefter bärförmågan bedöms med ledning av materialets deformations- och hållfasthetsegenskaper vid ifrågavarande temperaturer. För en bärande stålbalk baseras därvid denna bedömning ofta på materialets 0,2-gränspåkänning. Denna gränspåkänning ersätter sträckgränspåkänningen eftersom vanliga konstruktionsstål saknar utpräglade sträckgränsområden vid högre temperaturer. En bedömning av bärförmågan baserad på 0,2-

gränspåkänningen har dock vissa nackdelar. Påkänning-töjningskurvorna från varmdragprov uppvisar mycket mjukt avrundade förlopp vilket innebär att påkänningen ofta kan höjas avsevärt över 0,2-gränspåkänningen utan att töjningarna blir kritiska. Vidare är det svårt att på ett tillfredsställande sätt beakta materialets kryptöjning vid en bedömning av bärförmågan baserad på 0,2-gränspåkänningen.

Beräkningsmodell

Hänsyn till påkänning-töjningskurvornas mjukt avrundade förlopp samt till inverkan av kryptöjningen kan däremot tas vid en bedömning av bärförmågan baserad på balkens deformationsförlopp. En modell för beräkning av brandpåverkade stålbalkars deformationsförlopp har därför uppställts. Som ingångsdata i modellen används fullständiga påkänning-töjningskurvor framtagna genom varmdragprov med så hög belastningshastighet att kryptöjningens inverkan på dessa kurvsamband kan anses försumbar. Hänsyn till krypning tas i stället genom en speciell beräkning av kryptöjningen. För krypberäkningen nödvändiga materialdata har bestämts för ett antal olika konstruktionsstål genom krypförsök och resultaten har sammanställts i tabellform.

Test av modellen

För att verifiera den uppställda beräkningsmodellen har ett 20-tal brandförsök med belastade stålbalkar utförts. Vid försöken uppmätta och med modellen beräknade balknedböjningar jämfördes. Resultatet exemplifieras i FIG. 1 för en av de brandprovade balkarna. Den goda överensstämmelse som genomgående erhöles mellan beräknade och uppmätta nedböjningsförlopp bekräftar att modellen generellt kan användas för beräkning av brandpåverkade stålbalkars nedböjningsförlopp.

Kritisk belastning

Beräkningen av en brandpåverkad stålbalks nedböjningsförlopp innebär ett omfattande arbete. För att förenkla den praktiska användningen har därför hjälpmedel framtagits. Ett mycket stort antal systematiska beräkningar av brandpåverkade stålbalkars nedböjningsförlopp har genomförts på dator. Genom att använda ett till nedböjningens storlek kopplat brottkriterium, som

Byggforskningen Sammanfattningar

D16:1973

Nyckelord:

stålbalkar, brandpåverkan, bärförmåga, deformation, varmhållfasthet, krypning, beräkningsmodell

Document D16:1973 avser anslag C 742 från Statens råd för byggnadsforskning till Stålbjggnadsinstitutet.

UDK 624.072.2:624.014.2
620.193.5

SfB Hh2, Gh2

ISBN 91-540-2210-X

Sammanfattning av:

Thor, J, 1973, *Deformations and critical loads of steel beams under fire exposure conditions*. Brandpåverkade stålbalkars deformation och kritiska belastning. (Statens institut för byggnadsforskning) Stockholm. Document D16: 1973, 124 s., ill. 23 kr.

Skriften är skriven på engelska med svensk och engelsk sammanfattning.

Distribution:

Svensk Byggtjänst
Box 1403, 111 84 Stockholm
Telefon 08-24 28 60

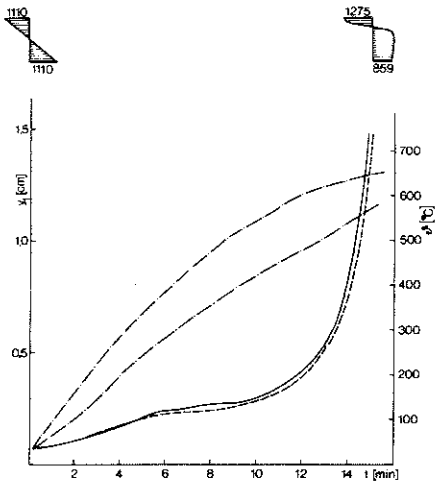


FIG. 1. Exempel på jämförelse mellan uppmätt (linjekurva) och beräknad (streckad kurva) mittpunktsnedböjning y_1 för balkdelen mellan lastangreppspunkterna som funktion av tiden t . Balkens temperaturförlopp ($\vartheta-t$) i mittsnittets överfläns och underfläns framgår av den undre respektive övre streckprickade kurvan. Beräknad påkänningsfördelning i början och slutet av försöket framgår av de infällda figurerna.

visat sig praktiskt väl tillämpbart har kritisk belastning kunnat bestämmas ur de beräknade nedböjningsförloppen. Resultaten har redovisats i diagram, ur vilka kritisk belastning för brandpåverkade stålbalkar vid olika lasttyper och statiska system kan bestämmas som funktion av under branden uppkommen maximal ståltemperatur och balkens uppvärmningshastighet. Exemplet i FIG. 2 gäller för fritt upplagd balk med jämnt fördelad belastning. Balkens avsvälningshastighet har genomgående förutsatts vara en tredjedel av uppvärmningshastigheten. Detta förhållande mellan uppvärmnings- och avsvälningshastighet har med stöd av resultat från brandprovningar visat sig vara en visserligen grov men i detta sammanhang tillräckligt god approximation av de verkliga förhållandena. Uppvärmningshastigheten kan grovt bedömas med hjälp av FIG. 3.

Bärförmåga och brottrisk

Med beräkningsmodellen kan man även studera hur avvikelser från ideala för-

hållanden påverkar deformationsförlopp och bärförmåga. Bland sådana genomförda studier kan nämnas inverkan av ojämnt fördelad temperatur i balken samt inverkan av förhindrad längdutvidgning.

Genom beräkning av en brandpåverkad stålbalks deformationsförlopp möjliggörs en säkrare bedömning av bärförmåga och brottrisk än vad som är möjligt med enbart 0,2-gränspåkänningen som underlag. En bedömning av bärförmågan baserad på deformationsförloppet visar också att bärförmågan för en brandpåverkad stålbalk oftast är avsevärt större än vad som kan bedömas på basis av 0,2-gränspåkänningen.

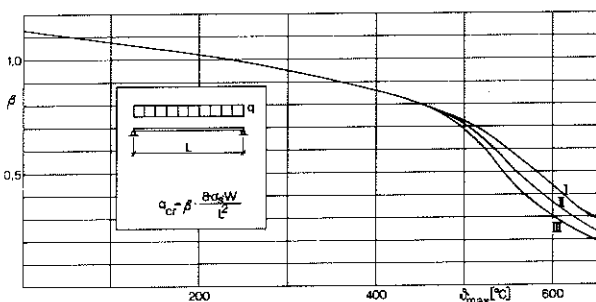


FIG. 2. Diagram för bestämning av kritisk belastning q_{cr} för brandpåverkad fritt upplagd balk med jämnt fördelad belastning som funktion av den maximala ståltemperaturen vid olika uppvärmnings- och avsvälningshastigheter.

| Kurva | I | II | III |
|--------------------------------|------|------|------|
| Uppvärmningshastighet (°C/min) | 100 | 20 | 4 |
| Avsvälningshastighet (°C/min) | 33,3 | 6,67 | 1,33 |

W = balkens elastiska böjmotstånd
 σ_s = materialets sträckgränspåkänning vid rumtemperatur

FIG. 3. Genomsnittlig uppvärmningshastighet a som funktion av brandbelastning q vid olika värden på brandcellens öppningsfaktor $A\sqrt{h}/A_1$ och olika maximala ståltemperaturer ϑ_{max} .
 A = brandcellens sammanlagda öppningsyta (m^2)
 h = ett med hänsyn till öppningarnas storlek vägt medelvärde av deras utsträckning i höjded (m)
 A_1 = brandcellens totala omslutningsyta (m^2)

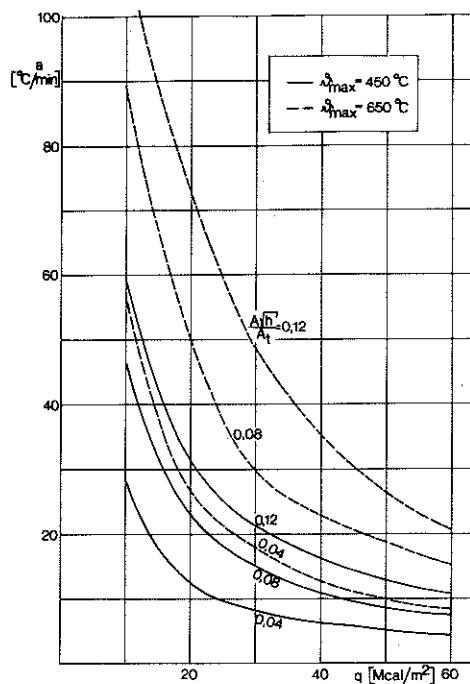


FIG. 3

Deformations and critical loads of steel beams under fire exposure conditions

Jörgen Thor

Application of rational fire engineering design to loadbearing steel structures can result in appreciable savings in cost.

This Document summaries the most important results in the Author's dissertation entitled "Behaviour of Steel Structures Exposed to Fire". A method is presented for the analysis of the deformation process in steel girders under fire exposure conditions. The model makes it possible for the loadbearing capacity and risk of failure to be estimated more safely, and for the special conditions which may apply to various structures to be taken into consideration. It has been found that a steel girder when exposed to fire will in most cases have an appreciably higher loadbearing capacity than is indicated by a standardised procedure.

Design

In comparison with the relatively accurate design process to which a loadbearing structure carrying a static load is subjected, design of the same structure with regard to the action of fire must often be characterised as a standardised procedure. Fire engineering design is usually based on standardised requirements as to periods of fire resistance which are related to action according to a standardised temperature-time process, the standard fire curve. According to current Swedish regulations, however, a more rational fire engineering design is permitted. In this rational design where fire is regarded as one loading condition among others, it must be demonstrated that the structure is capable of performing its function when subjected to such an action of fire which is likely to occur in the type of building in question. When applied to a loadbearing steel structure, such rational fire design, compared with the standardised fire design procedure, often results in appreciable savings in cost in attaining the required fire resistance.

In rational fire engineering design, the temperature-time curve of the steel structure is calculated by means of heat balance equations, after which the loadbearing capacity is estimated on the basis of the deformation and strength characteristics of the material at the temperatures considered. For a loadbearing steel beam this estimation is often based on the 0.2 % proof stress of the material instead of its yield stress, since ordinary structural steel has no pronounced yield region at elevated temperatures. Estimation of the loadbearing capacity on the basis of the 0.2 % proof stress has certain drawbacks, however, since the stress-strain curves obtained

during tensile tests at elevated temperatures are very softly rounded, with the result that the stress can often be raised appreciably above the 0.2 % proof stress without the strains becoming critical. Furthermore, it is difficult satisfactorily to take into account the creep strain of the material in estimating the loadbearing capacity on the basis of the 0.2 % proof stress.

Calculation model

If the loadbearing capacity is estimated on the basis of the deformations of the beam, however, it is possible to take into account the softly rounded shapes of the stress-strain curves and the influence of the creep strain. A model has therefore been constructed for calculation of the deformation process of steel beams exposed to the action of fire. Complete stress-strain curves, recorded in elevated temperature tensile tests at such high rates of loading that the effect on these curves of the creep strain may be considered negligible, have been used as input data in the model. Creep is instead taken into consideration by separate calculation of the creep strain. Material data necessary for calculation of creep have been determined by creep tests for a number of structural steels and the results summarised in a table.

Verification of the model

Some twenty fire tests have been performed on loaded steel beams in order to verify the calculation model. The beam deflections recorded during the tests have been compared with those calculated using the model. The results are exemplified in FIG. 1 for one of the beams subjected to a fire test. The satisfactory agreement consistently obtained between calculated and recorded deflection curves confirms that the model can be used generally for calculation of the deflections of steel beams under fire exposure conditions.

Critical load

Calculation of the deflections of a steel beam when this is exposed to the action of fire entails extensive work, and a large number of systematic calculations of deflections have therefore been performed on a computer in order to simplify practical application of the results. By using a criterion of failure related to the magnitude of the deflection, which has been found appropriate to apply in practice, the critical load has been determined on the basis of the calculated deflection curves. The results are given in the form of diagrams, for different types

National Swedish Building Research Summaries

D16:1973

Key words:

steel girders, fire exposure, loadbearing capacity, deformation, strength at elevated temperatures, creep, calculation model

Document D16:1973 relates to Grant C 742 from the National Swedish Council for Building Research to Swedish Institute of Steel Construction.

UDC 624.072.2:624.014.2
620.193.5
SfB Hh2, Gh2
ISBN 91-540-2210-X

Summary of:

Thor, J., 1973, *Deformations and critical loads of steel beams under fire exposure conditions*. (Statens institut för byggnadsforskning) Stockholm. Document D16:1973, 124 p., ill. 23 Sw. Kr.

The document is in English with summaries in Swedish and English.

Distribution:

Svensk Byggtjänst
Box 1403, S-111 84 Stockholm
Sweden

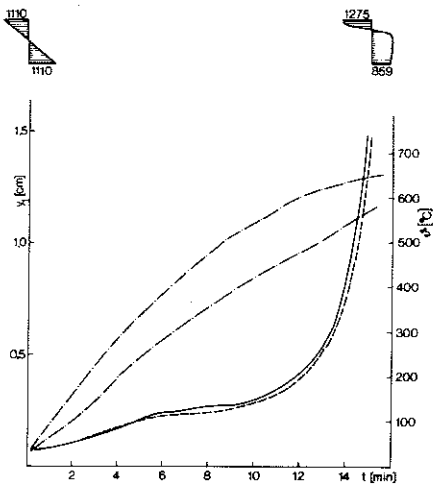


FIG. 1 Example of comparison between during fire tests recorded (full line curve) and calculated (dashed line curve) central deflections y , for the portion of beam between the points of application of the load, as a function of the time t . The temperature-time ($\vartheta-t$) curve for the top and bottom flange at the mid-section are shown by the lower and upper chain line respectively. The insets show the calculated stress distribution at the beginning and end of the test.

of loads and static systems, from which the critical load for steel beams under fire exposure conditions, can be determined as a function of the maximum steel temperature attained during the fire and as a function of the rate of heating of the beam. The example in FIG. 2 is valid for a simply supported beam with a uniformly distributed load. The rate of cooling of the beam has in all cases been assumed to be one third of the rate of heating. This relationship between the rates of heating and cooling has been found, on the basis of fire tests, to be an approximation of actual conditions which, although rough, is nevertheless sufficiently good in this context. The rate of heating can be roughly estimated with the help of FIG. 3.

Loadbearing capacity and risk of failure

The calculation model enables studies to be undertaken concerning the effect of deviations from ideal conditions on the deformation process and the loadbearing capacity. Among such studies which have been performed may be mentioned those concerning the influence of uneven temperature distribution in

the beam and the influence of a restraint on longitudinal expansion.

Calculation of the deformation process of a steel beam under fire exposure conditions makes possible safer estimation of the loadbearing capacity and the risk of failure than a process based only on the 0.2 % proof stress. Estimation of the loadbearing capacity based on the deformation process also demonstrates that the real loadbearing capacity of a steel beam, under fire exposure conditions, is very often appreciably higher than that obtained when estimation is based on the 0.2 % proof stress.

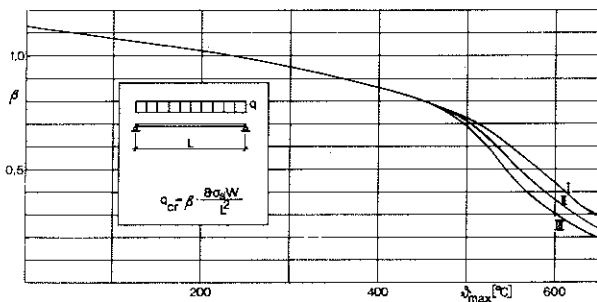


FIG. 2. Diagram for determination of the critical load q_{cr} for a simply supported steel beam with a uniformly distributed load under fire exposure conditions as a function of the maximum steel temperature ϑ_{max} for different rates of heating and cooling.

| | | | |
|--------------------------|------|------|------|
| Curve | I | II | III |
| Rate of heating (°C/min) | 100 | 20 | 4 |
| Rate of cooling (°C/min) | 33.3 | 6.67 | 1.33 |

W = elastic modulus of section
 σ_s = yield stress of the material at room temperature

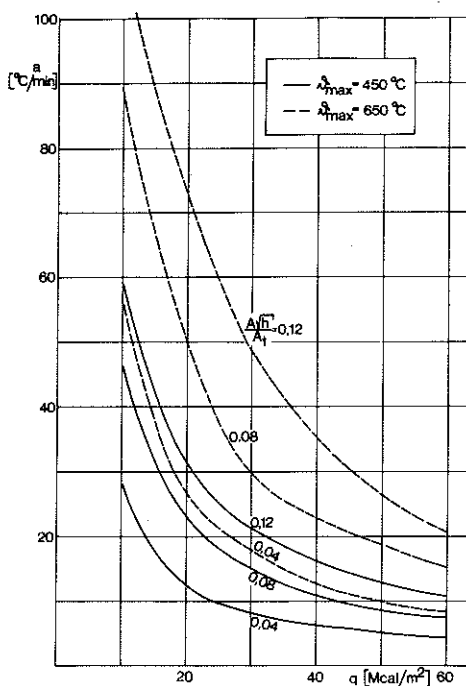


FIG. 3

FIG. 3. Average rate of heating a as a function of the fire load q for different values of the opening factor $A\sqrt{h}/A_t$ of the fire cell and for different maximum steel temperatures ϑ_{max} .
 A = total opening area of the fire cell (m²).
 h = mean value of the vertical extents of the openings, weighted in view of their sizes (m)
 A_t = total surface area of the fire cell (m²)

Document D16:1973

DEFORMATIONS AND CRITICAL LOADS OF STEEL BEAMS
UNDER FIRE EXPOSURE CONDITIONS

by Jörgen Thor

This document refers to Grant C 742 from the Swedish Council for
Building Research to the Swedish Institute of Steel Construction.

The National Swedish Institute för Building Research
Box 27 163, S-102 52 Stockholm 27, Sweden
ISBN 91-540-2210-X

Rotobekman AB, Stockholm 1973

FOREWORD

This Report summarises the most important results comprised in the following reports:

- Thor, J: The Effect of Creep on the Loadbearing Capacity of Steel Beams Exposed to Fire. Swedish Institute of Steel Construction, Publication No 24, Stockholm 1971.
- Thor, J: Undersökning av olika konstruktionsståls krypegenskaper under brandförhållanden (Investigation of the Creep Properties of Various Types of Structural Steel Exposed to Fire). Jernkontorets Forskning, Series D, No 40, Stockholm 1972.
- Thor, J: Statiskt bestämda stål balkars deformation och bär-förmåga vid brandpåverkan - experimentell och teoretisk undersökning (Deformation and Loadbearing Capacity of Statically Determinate Steel Beams Affected by Fire - an Experimental and Theoretical Study). Jernkontorets Forskning, Series D, No 54, Stockholm 1972.
- Thor, J: Beräkning av brandpåverkade statiskt bestämda och statiskt obestämda stål balkars deformation och kritiska belastning (Calculation of the Deformation and Critical Load of Statically Determinate and Indeterminate Steel Beams Exposed to Fire). Swedish Institute of Steel Construction, Report No 22:9, Stockholm 1972.

These reports form part of a composite doctoral thesis entitled "Behaviour of Steel Structures Exposed to Fire" which includes the following report in addition to the above:

- Thor, J: Strålningspåverkan på oisolerade eller undertaksisolerade stålkonstruktioner vid brand (Radiation Effects of Fire on Steel Structures with no Insulation or Insulation in the Form of a Ceiling), Structural Mechanics and Concrete Construction, Lund Institute of Technology, Bulletin No 29, Lund 1972.

Work on the thesis has mainly been carried out at the Swedish Institute of Steel Construction and has also been financed by the Institute. The publication of this Document has been assisted by a grant from the Swedish Council for Building Research.

The Author wishes to express his sincere thanks to the Head of the Swedish Institute of Steel Construction, Lars Wallin, for his support and encouragement and to Professor Ove Pettersson, Head of the Division of Structural Mechanics and Concrete Construction at Lund Institute of Technology, for his valuable advice and views during the whole of this work. Thanks are furthermore due to Mr L.J. Gruber for translation of the manuscript into English,

Stockholm, February 1973

Jörgen Thor

CONTENTS

| | | |
|-------|---|----|
| 1 | INTRODUCTION | 7 |
| 2 | DETERMINATION OF STRESS-STRAIN CURVES BY TENSILE TESTS AT ELEVATED TEMPERATURES | 11 |
| 3 | DETERMINATION OF THE CREEP STRAIN | 14 |
| 3.1 | Creep theory | 14 |
| 3.2 | Determination of the creep parameters $\Delta H/R$, Z and ϵ_{t_0} from conventional creep tests | 16 |
| 3.3 | Creep tests at variable temperatures | 23 |
| 4 | MODEL FOR CALCULATION OF THE DEFORMATION PROCESS OF STEEL BEAMS EXPOSED TO THE ACTION OF FIRE | 27 |
| 4.1 | Statically determinate beams | 27 |
| 4.2 | Statically indeterminate beams | 38 |
| 5 | COMPARISON OF CALCULATED BEAM DEFORMATIONS WITH THOSE RECORDED DURING TESTS | 42 |
| 5.1 | Beam tests performed in Sweden | 42 |
| 5.1.1 | Testing equipment | 42 |
| 5.1.2 | Material data used in the calculations | 47 |
| 5.1.3 | The results of tests and calculations | 48 |
| 5.2 | Beam tests performed under the aegis of the European Convention for Constructional Steelwork | 51 |
| 6 | CRITERION OF FAILURE | 55 |
| 7 | THE INFLUENCE OF VARIOUS FACTORS ON THE DEFORMATION PROCESS OF STEEL BEAMS EXPOSED TO THE ACTION OF FIRE | 61 |
| 7.1 | Maximum temperature | 61 |
| 7.2 | Rates of heating and cooling | 64 |
| 7.3 | Statical system | 64 |
| 7.4 | Type of loading | 66 |
| 7.5 | Magnitude of load | 69 |
| 8 | CRITICAL LOADS FOR STEEL BEAMS EXPOSED TO THE ACTION OF FIRE AS DETERMINED BY MEANS OF CALCULATED DEFORMATIONS | 70 |
| 8.1 | Calculation method | 70 |
| 8.2 | Diagrams for determination of the critical load for certain given conditions | 72 |
| 8.3 | Estimation of critical load under conditions different from those in Section 8.2 | 77 |
| 8.3.1 | Other types of loading | 77 |
| 8.3.2 | Continuous beams | 83 |
| 8.3.3 | Other grades of steel | 84 |

| | | |
|-------|---|-----|
| 8.3.4 | Different shape of cross section | 90 |
| 8.3.5 | Variation in the cross section along the beam | 94 |
| 8.3.6 | Different ratio between the rates of heating and cooling | 97 |
| 8.3.7 | Variation in temperature across the cross section | 98 |
| 8.3.8 | Variation in temperature along the beam | 101 |
| 8.3.9 | Restraint on longitudinal expansion | 103 |
| 9 | COMPARISON, FOR STEEL BEAMS EXPOSED TO THE ACTION OF FIRE, OF THE CRITICAL LOADS DETERMINED FROM CALCULATED DEFORMATIONS WITH THOSE DETERMINED ON THE BASIS OF THE YIELD STRESS OR 0.2 % PROOF STRESS AT ELEVATED TEMPERATURES | 115 |
| | REFERENCES | 122 |

1 INTRODUCTION

In order to estimate the loadbearing capacity of steel structures when exposed to fire, it is necessary to know the strength properties and deformational characteristics of the steel under fire exposure conditions. When the structural members under consideration are subjected to tension or bending, such estimates are most frequently based on the yield stress at elevated temperatures or the 0.2% proof stress of the steel.

The relations between the high temperature yield stress or the 0.2% proof stress and the temperature, which have been published in the literature, may differ considerably even when they apply to the same or similar grades of steel. See FIG. 1. One of the causes of the inadequate agreement at comparatively high temperatures may be the effect of creep. In fact, at temperatures in excess of about 400°C, the creep of ordinary structural steel begins to be noticeable, and the rate of creep becomes very high at temperatures above 600°C. Consequently, the rate of loading in a high temperature tensile test may have great influence on the shape of the stress-strain curve and hence on the evaluation of the 0.2% proof stress. On the other hand, the magnitude of creep strain in a steel structure exposed to fire depends not only on the load level and the maximum temperature attained, but also on the rates of heating and cooling which are, in turn, dependent on the fire load and the ventilation conditions in the fire cell, the insulation capacity of the fire insulation, etc. (5).

Another cause of the differences between the reported 0.2% proof stresses may be the uncertainty in assessing the slope of the tangent, at the origin, to the stress-strain curves determined in high temperature tests. At elevated temperatures the linear relationship between stress and strain ceases for quite low values of the stress, and owing to this uncertainty regarding the slope of the tangent, assessment of the 0.2% proof stress is also uncertain.

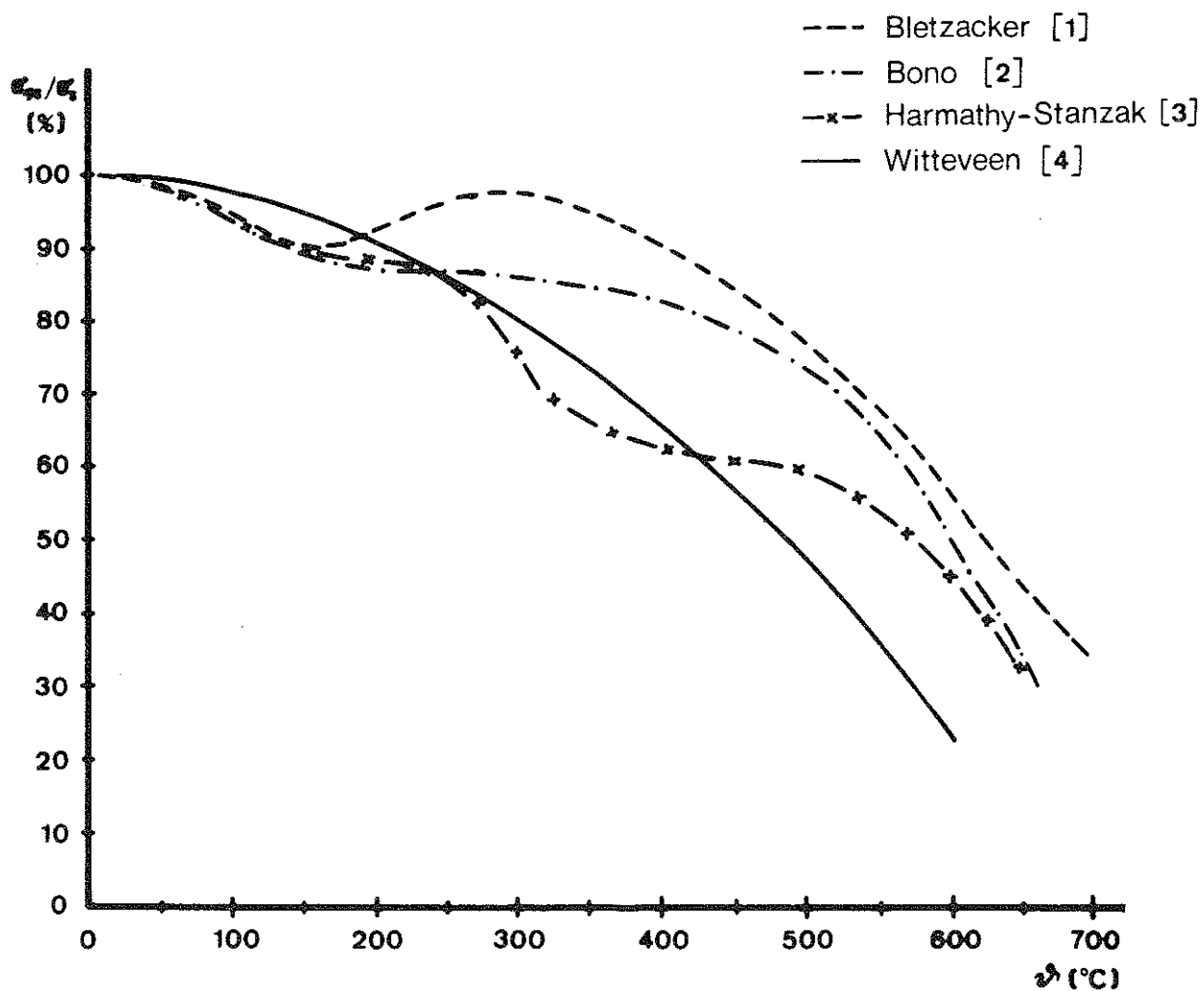


FIG. 1. Yield stress at elevated temperatures, or 0.2% proof stress, of structural mild steels expressed as a percentage of the yield stress at room temperature, plotted as a function of the temperature θ .

Another point which should be noted in this connection is that the stress-strain curve at elevated temperatures is softly rounded (see FIG. 3). Therefore, a moderate increase in stress above the 0.2% proof stress need not necessarily give rise to a critical increase in deformation. There is thus an obvious need for a criterion better than the yield stress at elevated temperatures, or the 0.2% proof stress alone, in order to provide a reliable basis for the estimation of the loadbearing capacity of steel structures exposed to fire.

One method which permits more reliable estimation of the loadbearing capacity of steel beams exposed to fire is based on the deformation of the beams during the fire, account being taken of the softly rounded shape of the stress-strain curve and also the effect of creep strain. A model has therefore been constructed for the calculation of the deformation of a steel beam which is exposed to fire. This calculation is based, inter alia, on stress-strain curves obtained in tensile tests at elevated temperatures which were performed at such high rates of loading that the influence of creep strain on these curves may be considered negligible. The effect of creep at elevated temperatures is taken into account by separate calculation of the magnitude of the creep strain. Various tests have been performed in order to obtain data relating to the materials and to verify the calculation model.

High temperature tensile tests have been carried out on test pieces taken from a batch of steel beams in order to determine the stress-strain curves at different temperatures. Test pieces were also taken from the same beams for determination of the creep properties of the material. A number of fire tests have also been performed on the same steel beams, loaded and simply supported, the temperatures and deflection curves of the beams being determined in these tests. The deformation process of the beams was then calculated with the calculation model, using the material data obtained in the tensile tests at elevated temperatures and in the creep tests, and the results compared with the deformations recorded in the tests. Collapse criteria, associated with the deformation process, have also been studied by means of the tests and the

calculation model. Finally, the influence of various factors on the deformation could be studied by systematic calculations of the deformation processes of steel beams exposed to fire, and the loadbearing capacity, associated with a deformation criterion, could be determined for different types of load and different statical systems.

2 DETERMINATION OF STRESS-STRAIN CURVES BY TENSILE TESTS AT ELEVATED TEMPERATURES

The material of the beams from which the test pieces were taken was an ordinary structural grade mild steel Type 1411 according to Swedish Standard SIS 14 14 11. The yield stress at room temperature was found to be 3400 kgf/cm^2 . The analysis of the material is shown in TABLE I in Section 3.2. The thickness of the test pieces used in the elevated temperature tensile tests was 3 mm. Their other dimensions are shown in FIG. 2. The temperature of the test pieces was kept constant during each test. Load was increased gradually at a constant rate and the load and strain were recorded continuously during the test. FIG. 3 shows the recorded stress-strain curves at different temperatures. The rate of loading during the tests is equivalent to an increase in stress of $975 \text{ kgf/cm}^2 \cdot \text{min}$, which means that the influence of creep strain on the stress-strain curve is very small. The curves shown in the Figure have been used in the course of calculations with the calculation model previously referred to. Elevated temperature tensile tests were also carried out on the same material at considerably lower rates of loading. More detailed description of the test series will be found in an Appendix to (6). (Determination of the $\sigma - \epsilon$ curve for structural steels at different constant temperature levels and different constant rates of loading, A Hultgren and S E Magnusson).

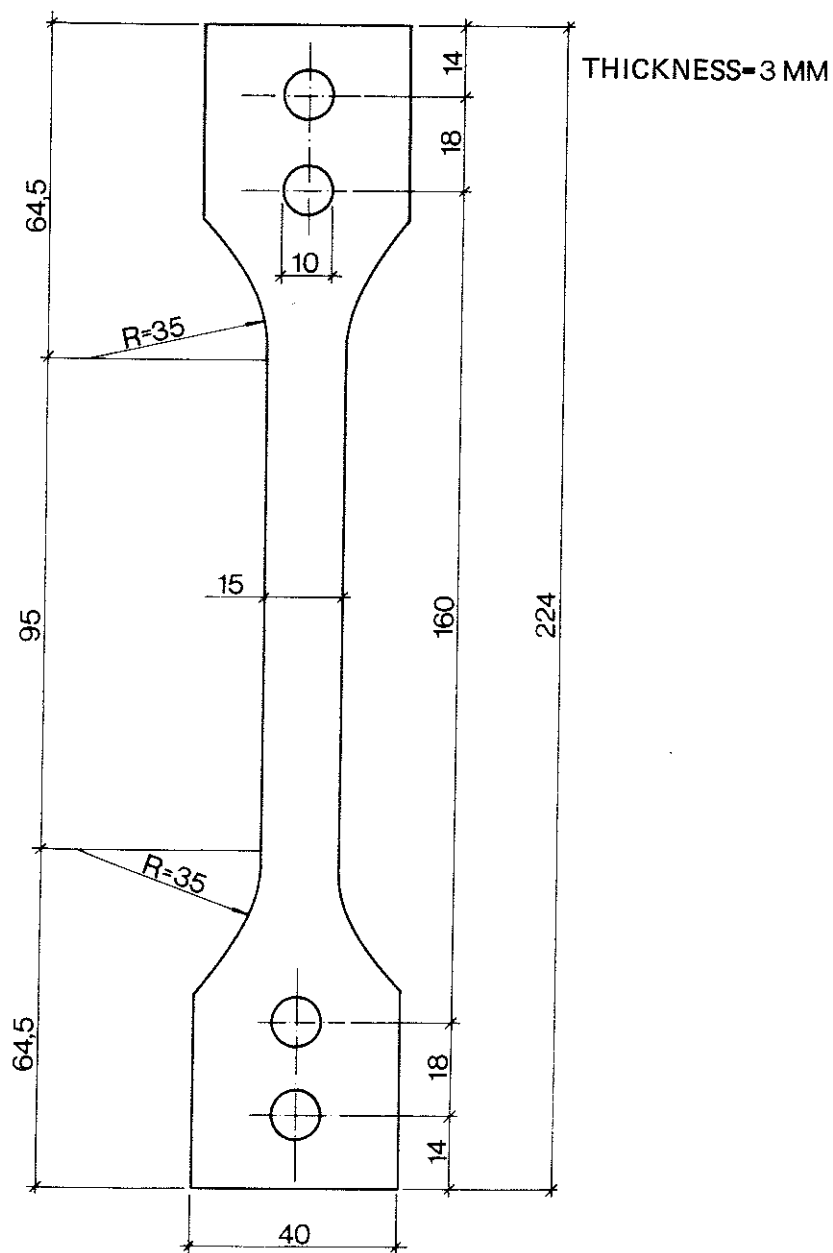


FIG. 2. Dimensions of test piece used in tensile tests.

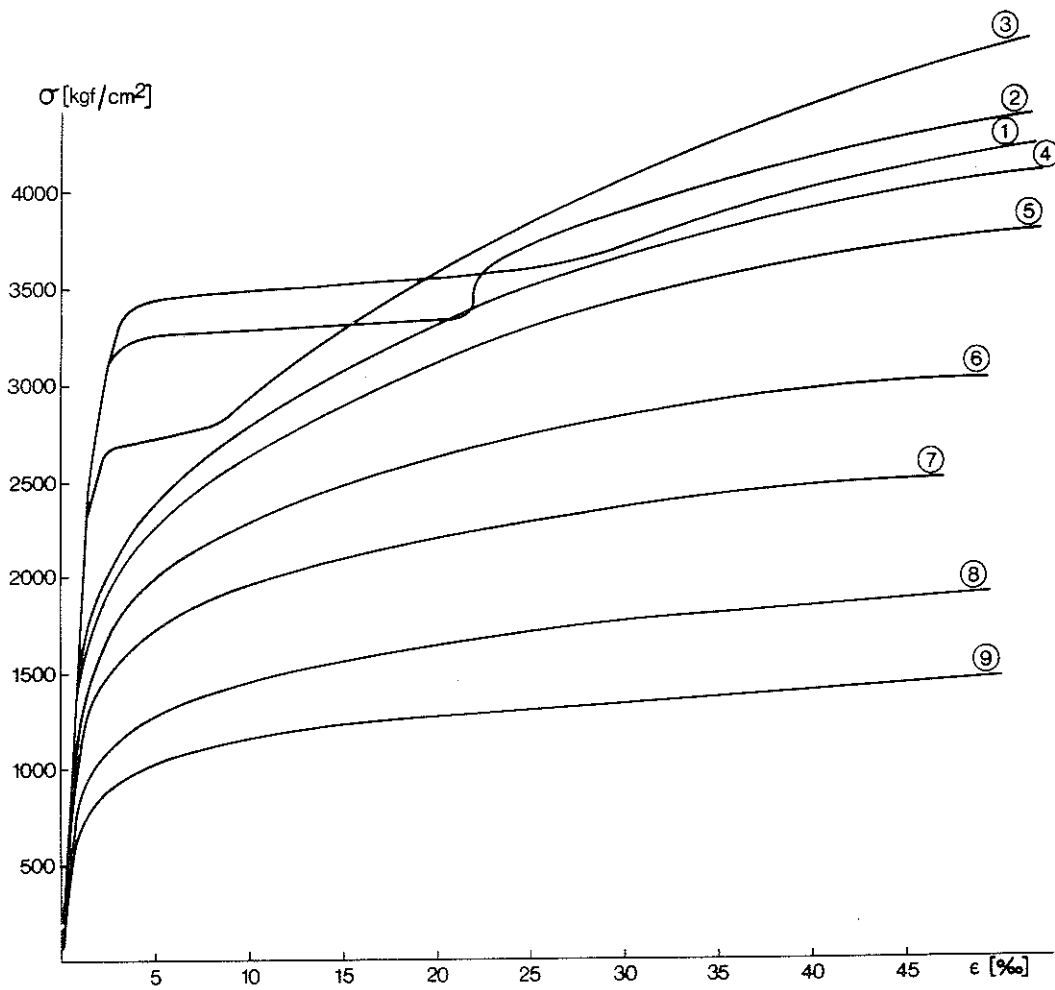


FIG. 3. Stress-strain ($\sigma - \epsilon$) curves determined in tensile tests at elevated temperatures at a rate of loading of 975 kgf/cm². min. Temperatures °C: ① 25, ② 100, ③ 300, ④ 400, ⑤ 450, ⑥ 500, ⑦ 550, ⑧ 600, ⑨ 650.

3 DETERMINATION OF THE CREEP STRAIN

3.1 Creep theory

A creep theory put forward by Dorn (7) has been found suitable for use in estimating the magnitude of the creep strain. In contrast to several other creep theories, Dorn's theory permits consideration of the effect of a temperature which varies with time. It is assumed that the creep strain ϵ_t for a certain grade of steel is dependent on the magnitude of the stress σ and on a temperature-compensated time θ , defined by the relation

$$\theta = \int_0^t e^{-\Delta H/RT} dt \quad (\text{h}) \quad (1)$$

where ΔH = the activation energy required for creep (cal/mol)
 R = universal gas constant (cal/mol . degrees Kelvin)
 T = temperature (degrees Kelvin)
 t = time (hours)

The curve expressing the relation between the creep strain ϵ_t and the temperature-compensated time θ , for different stresses σ , contains a portion of constant slope. This slope $d\epsilon_t/d\theta$ is denoted Z and is stated to be dependent only on the magnitude of the stress. The intersection of the "Z line" with the strain axis is denoted ϵ_{t_0} and is also stated to be dependent only on the magnitude of the stress (see FIG. 4).

Harmathy (8) has indicated a mathematical relationship between the creep strain ϵ_t and the quantities θ , Z and ϵ_{t_0} .

$$\epsilon_t = (\epsilon_{t_0} / \ln 2) \cosh^{-1} (2^{Z\theta/\epsilon_{t_0}}) \quad (2)$$

If the value of $\Delta H/R$ is known for a grade of steel, the temperature-compensated time θ can be calculated for any temperature-time curve with the aid of Equation (1). If the relation between the stress and Z and the relation between the stress and ϵ_{t_0} is also known the creep strain ϵ_t of the steel at the appropriate value of θ can be calculated for any stress using Equation (2)

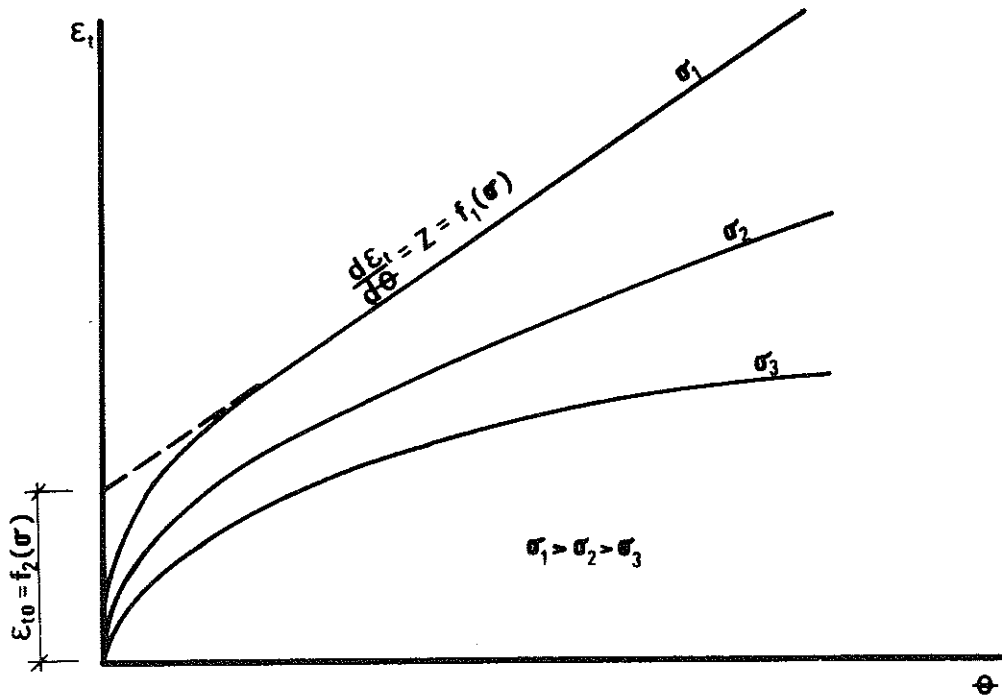


FIG. 4. $\epsilon_t - \theta$ curves for different stresses σ .

3.2 Determination of the creep parameters $\Delta H/R$, Z and ϵ_{t_0} from conventional creep tests

The value of $\Delta H/R$ and the relation between the stress and Z or ϵ_{t_0} can be determined by means of conventional creep tests, i.e. creep tests at constant temperature and stress. At constant temperature, Equation (1) may be written

$$\theta = e^{-\Delta H/(R.T)} \cdot t \quad (3)$$

Since the magnitude of the creep strain is assumed to be dependent only on the magnitude of the stress and on θ , the value of θ in two tests must be the same if the creep strains in the two tests are of the same magnitude at the same stress, i.e.

$$e^{-\Delta H/(R.T_1)} \cdot t_1 = e^{-\Delta H/(R.T_2)} \cdot t_2 \quad (4)$$

where T_1, T_2 = temperature ($^{\circ}K$) in test 1 and 2
 t_1, t_2 = times(h) at which the strains attained in test 1 and test 2 are the same.

Equation (4) can be solved for $\Delta H/R$

$$\frac{\Delta H}{R} = \frac{T_2 \cdot T_1 \cdot \ln(t_2/t_1)}{T_2 - T_1} \quad (5)$$

As regards Z ,

$$Z = \left(\frac{d\epsilon_t}{d\theta}\right) = \left(\frac{d\epsilon_t}{dt} \cdot \frac{dt}{d\theta}\right) = \dot{\epsilon}_{ts} \cdot e^{\Delta H/(R.T)} \quad (6)$$

where $\dot{\epsilon}_{ts}$ = rates of creep during the secondary creep stages of the conventional creep tests

Once $\Delta H/R$ has been determined according to Equation (5) and the rates of creep $\dot{\epsilon}_{ts}$ have been evaluated from each test, the value of Z appropriate to each test can be calculated from Equation (6). If the calculated values of Z are plotted in a diagram as a function of the magnitude of the stress in each test, it is found that the points relating to high stresses are usually reasonably close to a straight line in a diagram plotted with one axis

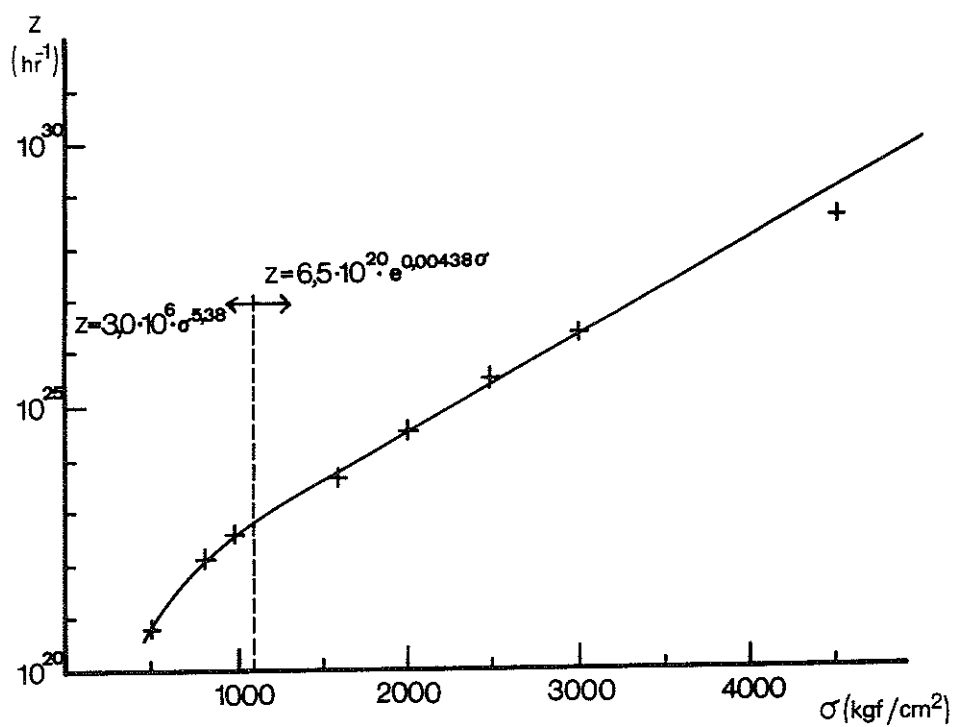


FIG. 5. The relation between Z and the stress σ plotted in a diagram with the Z-axis to a logarithmic scale, Steel 2172.

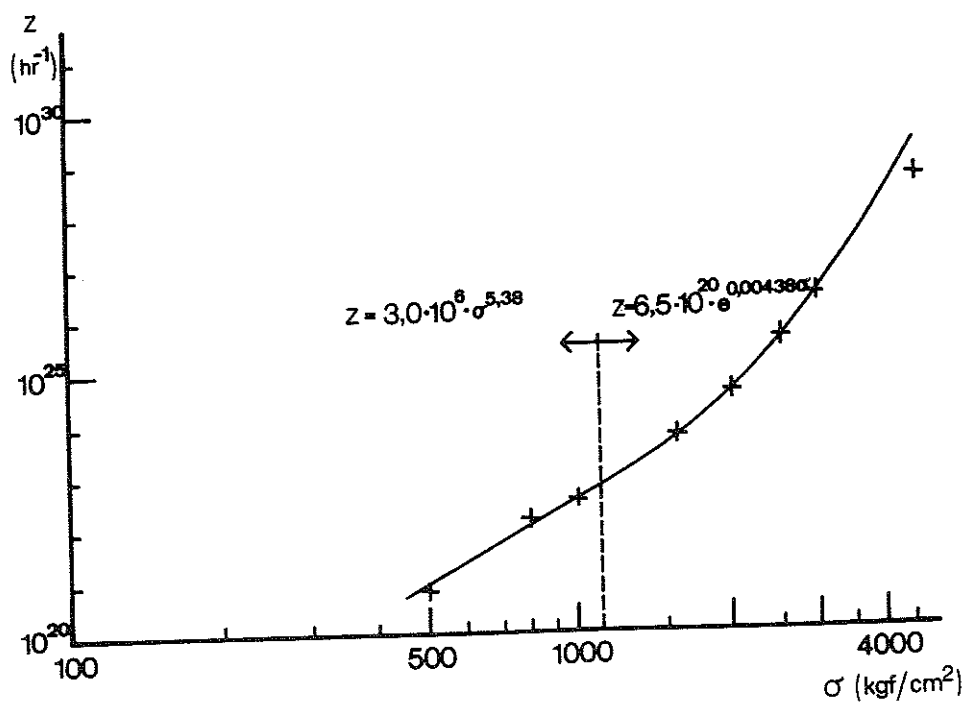


FIG. 6. The relation between Z and the stress σ plotted in a diagram with both axes to a logarithmic scale, Steel 2172.

(the Z-axis) to a logarithmic scale. For small stresses, the points are usually fairly close to a straight line in a diagram in which both variables are plotted to a logarithmic scale.

At the Domnarvet Iron Works, short-term creep tests have been performed on a grade 2172 steel to SIS 14 21 72 and also on a steel grain-refined with aluminium, with a basic analysis corresponding to steel 2172 (9). From the first test, the value of $\Delta H/R$ for steel 2172 has been found to be $50,000^\circ\text{K}$ (10). The values of Z determined in the same test have been plotted as a function of the stress, in FIG. 5 with one variable to a logarithmic scale and in FIG. 6 with both variables to a logarithmic scale (11). The Figures also contain the functional relations between Z and the stress which best agree with the curve plotted.

The value of ϵ_{t_0} is determined from conventional creep tests as the intersection in a strain-time diagram between the strain axis (the ϵ_t -axis) and the projection of the straight line which is drawn through the points relating to the secondary stage of the creep process. The values of ϵ_{t_0} relating to the appropriate test are plotted as a function of the stress in a diagram with both axes to a logarithmic scale. FIG. 7 shows the values of ϵ_{t_0} plotted as a function of the stress for the 2172 steel tested by the Domnarvet Iron Works. The Figure also gives the equation which most closely agrees with the line drawn through the points (10).

The creep strain curve has been calculated theoretically for the temperatures and stresses used in the conventional creep tests, on the basis of the value of $\Delta H/R = 50,000^\circ\text{K}$ and using the relation between stress and Z and stress and ϵ_{t_0} found in the tests for steel 2172. Equations (1) and (2) have been used in calculating the creep strain. Both the theoretically calculated and recorded creep curves are shown in FIG. 8.

The value of $\Delta H/R$ and the relation between the stress and Z and the stress and ϵ_{t_0} have also been determined for the material of the beams described in Chapter 1, which was an ordinary mild carbon steel Type 1411 to Swedish Standard SIS 14 14 11. The creep parameters have also been determined for carbon steel Type 1312 to SIS 14 13 12 and also for grain-refined carbon-manganese steel.

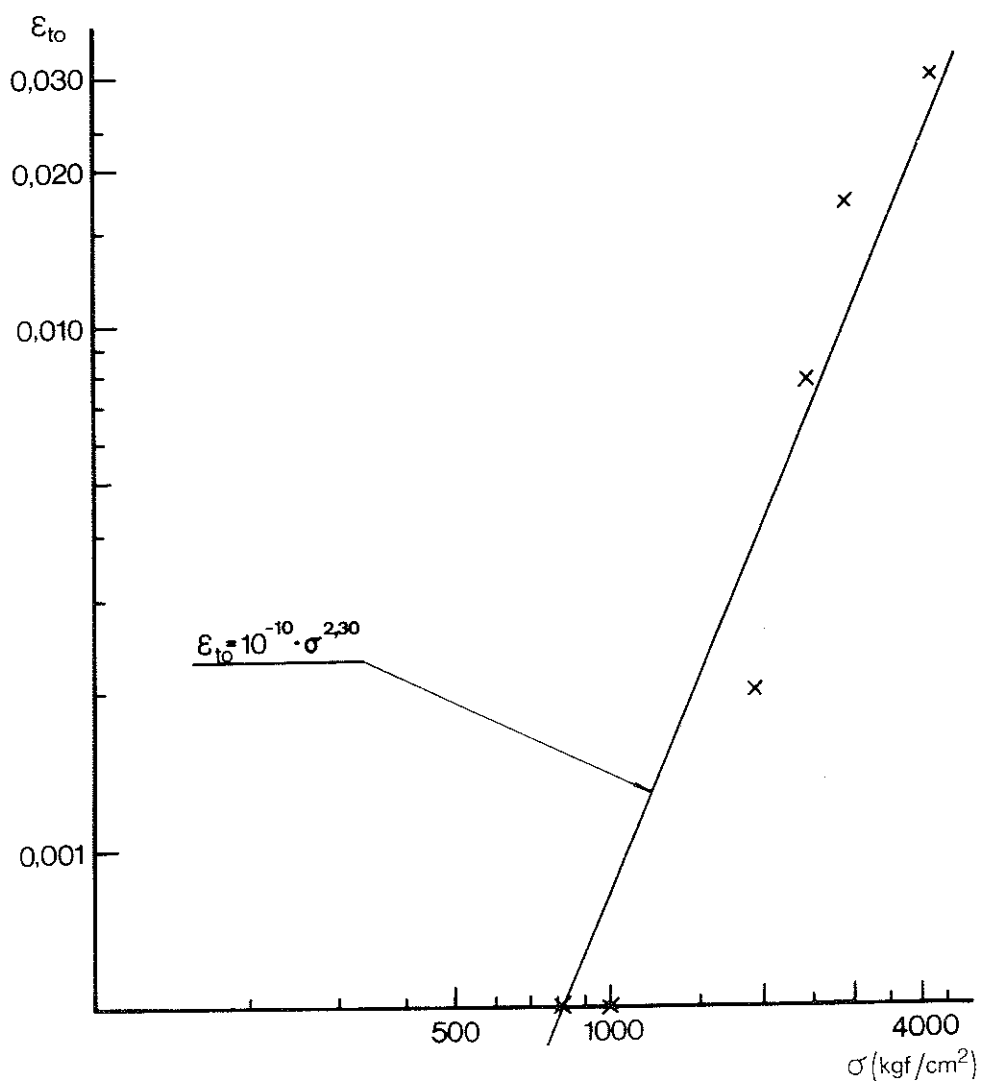


FIG. 7. The relation between ϵ_{to} and the stress σ plotted in a diagram with both axes to a logarithmic scale, Steel 2172.

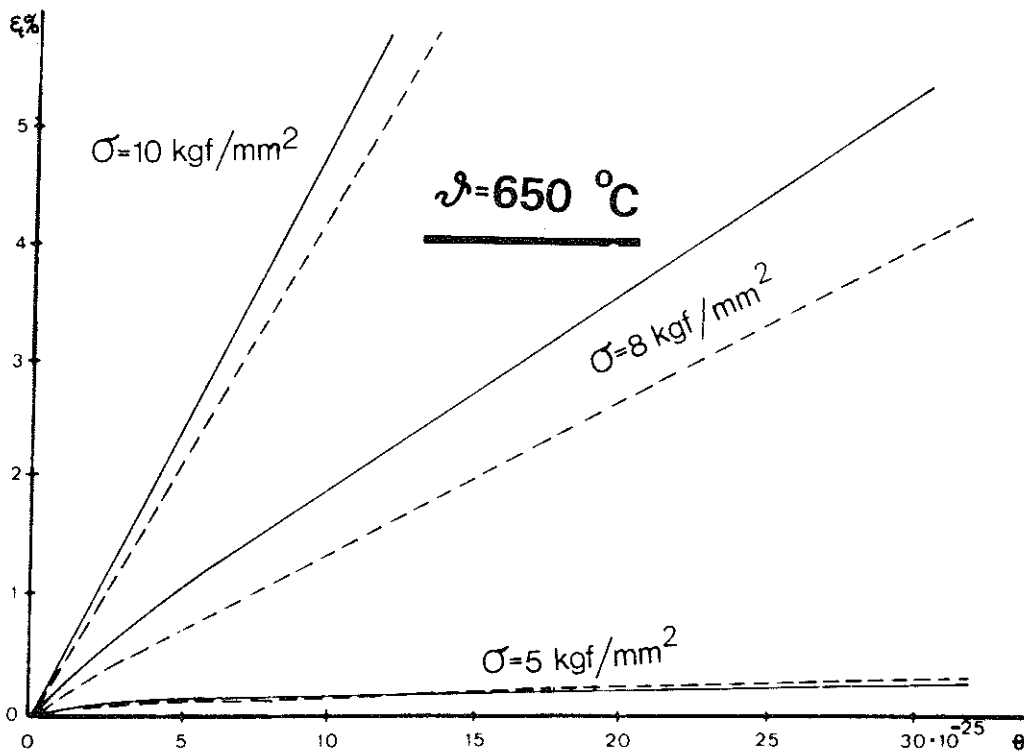
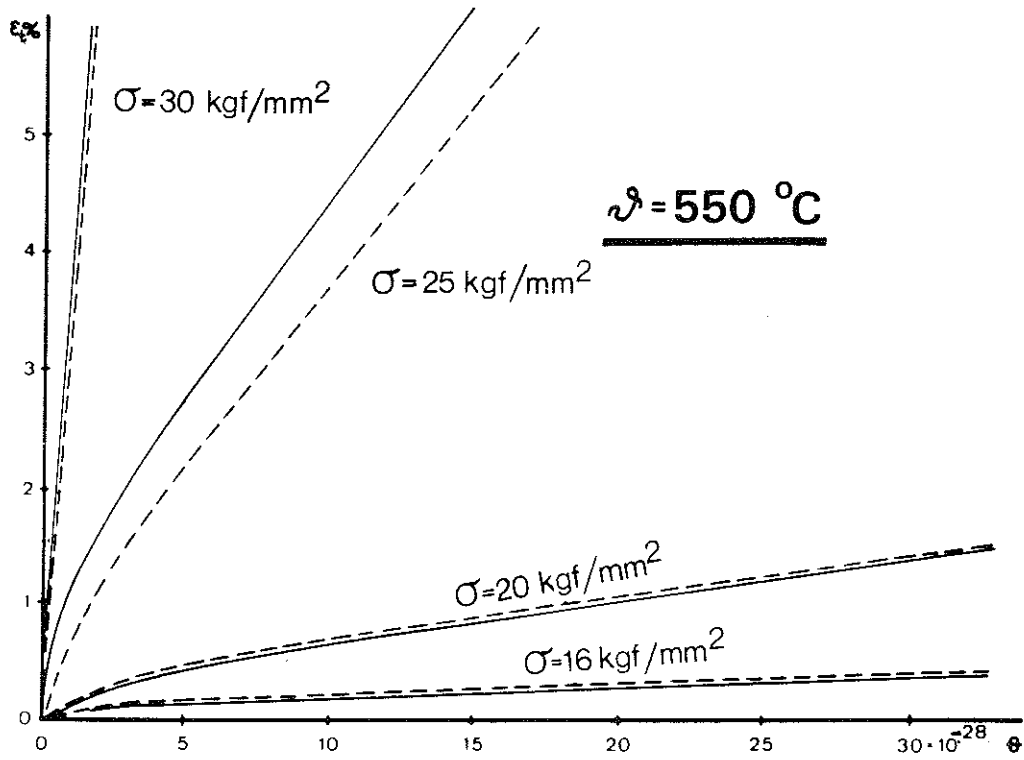


FIG. 8. $\epsilon_t - \theta$ curves for Steel 2172 according to SIS 14 21 72 at different stresses σ for steel temperatures θ of 550°C and 650°C .

———— Recorded strain
 - - - - - Calculated strain

Harmathy and Stanzak (3) have given values of $\Delta H/R$ and the relation between stress and Z and stress and ϵ_{t_0} for steel A36 and steel G.40.12. Steel A36 closely resembles steel 1412 to SIS 14 14 12 and steel G.40.12 closely resembles steel 2172 to SIS 14 21 72.

TABLE I lists the values of $\Delta H/R$ and the functional relations between the stress and Z and the stress and ϵ_{t_0} for all steels (12).

The steels have been divided into three principal groups, carbon steels, carbon manganese steels and grain-refined steels. The Table also gives the analyses of the various steels and their yield stresses at room temperature.

It will be seen from Table I that the values of $\Delta H/R$ and the relationship between the stress and Z and the stress and ϵ_{t_0} show relatively large differences in some cases, even when steels in the same group are compared. It is found on comparing creep tests on similar grades of steel that the creep strain is less for a steel which has a higher yield stress at room temperature than for a steel with a lower yield stress at room temperature, when these are subjected to the same temperatures and stresses. It is seen in Table I that the yield stresses are different even for steels in the same group, and this may therefore explain some of the above differences in the values of the creep parameters. Another reason why these differences occur may be that the determination of $\Delta H/R$ is sometimes sensitive and may therefore be subject to some inaccuracy. The values of $\Delta H/R$ in turn affect the magnitude of Z determined in accordance with Equation (6). Some uncertainty in the value of $\Delta H/R$ can normally be accepted, however, since it is not the values of $\Delta H/R$ or Z in themselves but a combination of these which is decisive with regard to the agreement between the creep curve calculated with Equations (1) and (2) and those plotted on the basis of tests. Agreement is primarily affected by the accuracy with which the values of Z , calculated on the basis of Equation (6) and plotted as a function of the stress, conform to a straight line at low values of stress in a diagram with both variables plotted to a logarithmic scale,

TABLE I. Yield stress at room temperature, analysis, the values of $\Delta H/R$, Z and ϵ_{to} as functions of the stress σ (kgf/cm²) for different structural steels.

| Steel group | Steel | Yield stress at room temperature (kgf/cm ²) | Analysis (%) | | | | | | | | | | | | | $\Delta H/R$ (h ⁻¹) | Z (h ⁻¹) | ϵ_{to} |
|-------------------------|---------------------------------|---|--------------|-----|------|------|------|------|------|------|------|------|----------|-------|--|---|---|-----------------|
| | | | C | Si | Mn | P | S | Cr | Cu | N | Al | Nb | Ni | Mo | | | | |
| Carbon steels | 1312 (Test 1) | 2590 | .11 | .05 | .57 | .025 | .036 | .028 | .006 | .008 | - | - | - | - | 55800 | für $\left\{ \begin{array}{l} \sigma \leq 1100 \quad 4,89 \cdot 10^3 \cdot \sigma^{7,808} \\ \sigma > 1100 \quad 8,3 \cdot 10^{24} \cdot e^{-0,00567 \cdot \sigma} \end{array} \right.$ | $1,02 \cdot 10^{-7} \cdot \sigma^{1,722}$ | |
| | 1312 (Test 2) | 2680 | .13 | .07 | .75 | .010 | .026 | .035 | .052 | .005 | - | - | - | 53900 | für $\left\{ \begin{array}{l} \sigma \leq 1100 \quad 10,53 \cdot 10^2 \cdot \sigma^{7,644} \\ \sigma > 1100 \quad 3,0 \cdot 10^{23} \cdot e^{-0,00590 \cdot \sigma} \end{array} \right.$ | $1,44 \cdot 10^{-9} \cdot \sigma^{2,248}$ | | |
| | 1411 | 3400 | .18 | .13 | .73 | .035 | .020 | .020 | .015 | .013 | - | - | - | 66000 | für $\left\{ \begin{array}{l} \sigma \leq 1200 \quad 1,37 \cdot 10^8 \cdot \sigma^{8,4619} \\ \sigma > 1200 \quad 1,45 \cdot 10^{29} \cdot e^{-0,00592 \cdot \sigma} \end{array} \right.$ | $2,82 \cdot 10^{-9} \cdot \sigma^{2,08}$ | | |
| | A36-66 | 3100 | .19 | .09 | .71 | .007 | .030 | - | - | - | - | - | - | 38900 | für $\left\{ \begin{array}{l} \sigma \leq 1050 \quad 6,80 \cdot 10^3 \cdot \sigma^{4,70} \\ \sigma > 1050 \quad 1,2 \cdot 10^{16} \cdot e^{-0,00426 \cdot \sigma} \end{array} \right.$ | $7,00 \cdot 10^{-8} \cdot \sigma^{1,75}$ | | |
| Carbon-manganese steels | 2172 | 3380 | .17 | .33 | 1,57 | .023 | .020 | - | - | .010 | - | - | - | 50000 | für $\left\{ \begin{array}{l} \sigma \leq 1100 \quad 3,00 \cdot 10^6 \cdot \sigma^{5,38} \\ \sigma > 1100 \quad 6,50 \cdot 10^{20} \cdot e^{-0,00438 \cdot \sigma} \end{array} \right.$ | $1,00 \cdot 10^{-10} \cdot \sigma^{2,30}$ | | |
| | G40,12 | 3400 | .19 | .02 | 1,40 | .015 | .019 | .010 | .080 | - | <.01 | - | .03 spát | 36100 | für $\left\{ \begin{array}{l} \sigma \leq 1050 \quad 1,50 \cdot 10^6 \cdot \sigma^{3,25} \\ \sigma > 1050 \quad 3,70 \cdot 10^{14} \cdot e^{-0,00313 \cdot \sigma} \end{array} \right.$ | $1,80 \cdot 10^{-6} \cdot \sigma^{1,00}$ | | |
| Grain-refined steels | Grain refinement with aluminium | 3730 | .21 | .30 | 1,48 | .017 | .019 | - | - | .005 | .022 | - | - | 40900 | für $\left\{ \begin{array}{l} \sigma \leq 1300 \quad 2,10 \cdot 10^{17} \cdot \sigma^{5,78} \\ \sigma > 1300 \quad 8,00 \cdot 10^{16} \cdot e^{-0,00455 \cdot \sigma} \end{array} \right.$ | $1,48 \cdot 10^{-9} \cdot \sigma^{2,15}$ | | |
| | Grain refinement with niobium | 4050 | .17 | .43 | 1,31 | .018 | .020 | .018 | .014 | .007 | .007 | .021 | - | 45000 | für $\left\{ \begin{array}{l} \sigma \leq 1250 \quad 5,03 \cdot \sigma^{8,644} \\ \sigma > 1250 \quad 1,2 \cdot 10^{19} \cdot e^{-0,00434 \cdot \sigma} \end{array} \right.$ | $4,78 \cdot 10^{-9} \cdot \sigma^{1,95}$ | | |

and to a straight line for large values of stress in a diagram in which only one of the variables is plotted to a logarithmic scale (see FIGs. 5 and 6). If the values of Z agree well with these straight lines, agreement between the theoretically calculated and recorded creep curves will be satisfactory even if there is some uncertainty as regards the value of $\Delta H/R$. A study (12) also shows that calculated creep strains at stresses which are the same in relation to the yield stress of the steel concerned at room temperature exhibit satisfactory agreement within the same principal group, in spite of the above differences in the values of $\Delta H/R$ and Z .

A difference between the values of $\Delta H/R$ for two similar steels is "neutralised" by a difference in the Z function. It will be evident from the foregoing that the value of $\Delta H/R$ and the relationship between Z and ϵ_{t_0} and the stress are to be regarded not as exact material data but rather as empirical values and relationships which, when used in Equations (1) and (2), produce creep curves in good agreement with those plotted on the basis of tests.

3.3 Creep tests at variable temperatures

Contrary to conditions in conventional creep tests, the temperature of a steel structure which is exposed to fire is not constant but exhibits large variations with time. For the calculation of creep strains in case of fire, it is therefore important to know what agreement may be expected between theoretically calculated creep strains at variable temperatures and those recorded during tests. In order to obtain information on this point, some 20 creep tests have been performed on test pieces subjected to different loads and a temperature which varied greatly with time (12). One steel from each group in Table I was used for the study, i.e. steel 1411, steel 2172 and steel grain-refined with aluminium.

Round test pieces of 4.5 mm diameter and a gauge length of 75 mm were used. The temperature of the test piece was recorded by three thermocouples attached to the surface of the test piece. Load was applied to the test piece by weights by means of a system of levers. Changes in the length of the test piece were recorded by dial gauges connected to the ends of the test pieces. FIG. 9 shows the test piece and the test rig.

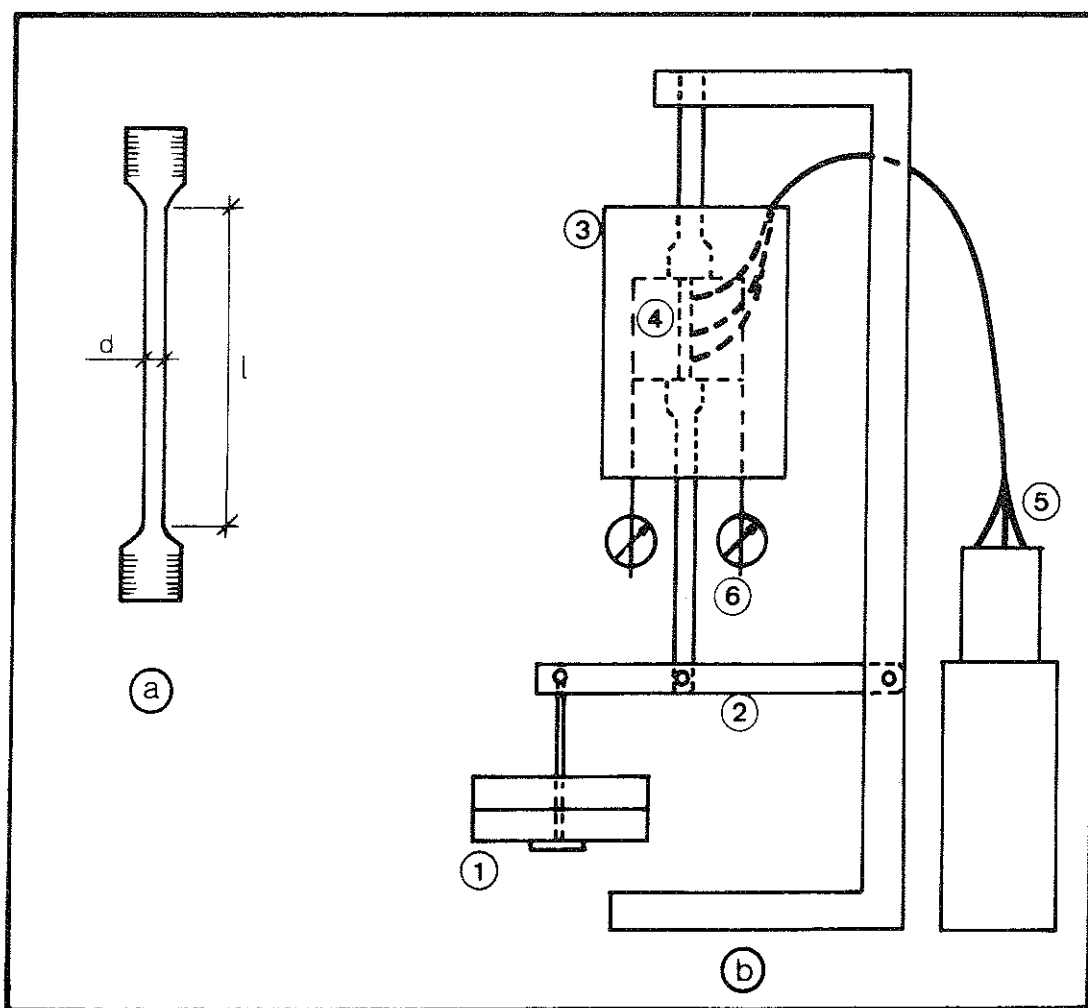


FIG. 9. a) Test piece, gauge length $l = 75$ mm, diameter $d = 4.5$ mm.
 b) General arrangement of test rig; (1) weights, (2) system of levers, (3) furnace, (4) test piece with thermocouples, (5) temperature recorder, (6) dial gauges.

During the tests, the test pieces were first heated to 400°C . Short-term creep is considered negligible up to this temperature. Temperature was allowed to stabilise at 400°C for 5 - 10 minutes and the test pieces were then heated in a few minutes to the temperature range $600 - 650^{\circ}\text{C}$ and then allowed to cool in air.

The test pieces and the linkages which transmitted changes in the length of the test piece to the dial gauges had different coefficients of thermal expansion. Owing to this, a certain part of the dial gauge reading was due to the difference in thermal expansion. In order to determine the strain, every test was repeated without load, and by subtracting the gauge readings in the latter tests from those recorded at the same times in tests in which load was applied to the test pieces, the changes in length of the test pieces due to the strain were obtained.

The creep strain curve was calculated with Equation (2) for each test for purposes of comparison. The values of Z and ϵ_{t_0} used in Equation (2) were calculated on the basis of the equations given in Table I for these quantities. The θ function was calculated with Equation (1) using the values of $\Delta H/R$ in Table I. An example of the results is given in FIG. 10 which compares the calculated and recorded creep strains in one of the tests.

Apart from two tests, the results of which were influenced by errors of a purely procedural nature, the agreement between the recorded and calculated creep strains may be regarded very satisfactory. This demonstrates that Dorn's creep theory and the relation between ϵ_t and the quantities θ , Z and ϵ_{t_0} given by Harmathy is well suited for a description of the creep strain of a steel when subjected to temperatures representative of those encountered during a fire.

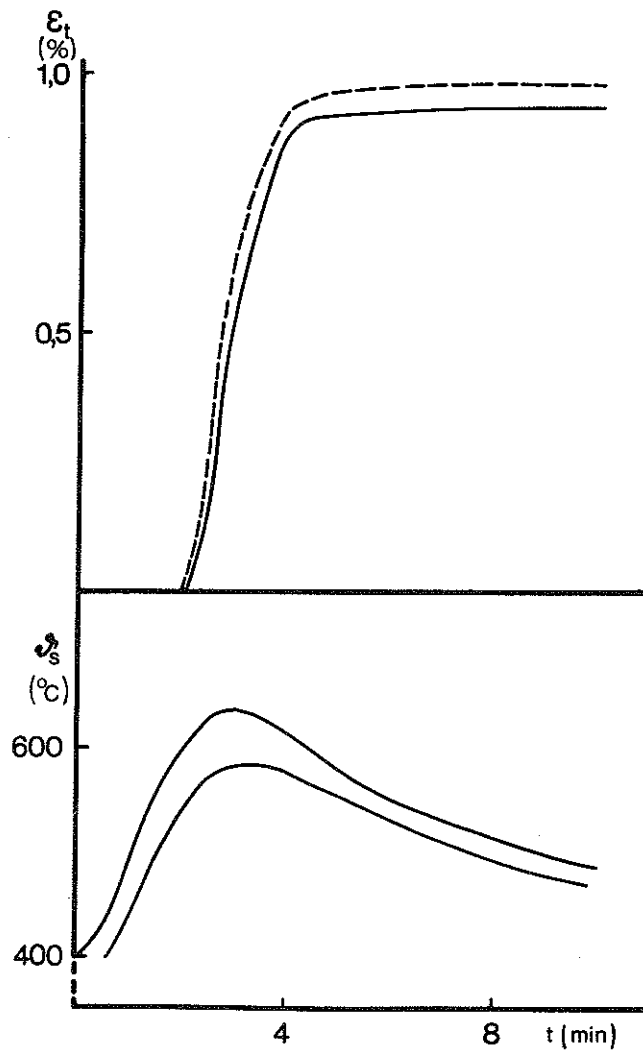


FIG. 10. Comparisons of recorded (—) and calculated (----) creep strains ϵ_t at varying temperatures ϑ_s for test pieces of Steel 2172 (upper figure). The temperature-time (ϑ_s - t) curve of the test pieces is shown in the bottom figure. This gives the maximum and minimum temperatures of the test pieces at the various times. Stress = 1520 kgf/cm².

4 MODEL FOR CALCULATION OF THE DEFORMATION PROCESS OF STEEL BEAMS EXPOSED TO THE ACTION OF FIRE

4.1 Statically determinate beams

In the calculation model, the fire sequence is divided up into a number of time intervals whose lengths are chosen with regard to the temperatures and stresses (6). The deflection of the beam at the midsection is calculated at the end of each time interval. In order that this calculation may be performed, the curvature along the beam must be known, and this is determined by division of the beam into a number of sections for which the curvature is calculated. The strain distribution across each cross section must first be determined in order that the curvature may be calculated, and this is done by breaking down the cross section into a number of elements for which the stress and strain are computed. The principles of the division into time, cross sections and elements are shown in FIG. 11.

Owing to the fact that the temperature in a beam exposed to fire changes during a time interval, the strain and generally also the stress change during the time interval in each element of cross section, since the strength and deformation properties of steel are temperature dependent. The change in strain and stress during the time interval Δt from the time t_n to the time t_{n+1} is studied for an arbitrarily chosen cross section element i . The temperature, in $^{\circ}\text{C}$, is θ_{n+1} at the time t_{n+1} . The stress-strain ($\sigma - \epsilon$) curve at the temperature θ_{n+1} , determined on the basis of tensile tests at elevated temperatures (see also Chapter 2), is approximated to a straight line between the points 0, a, b, c, d, e, f etc as seen in FIG. 12. The total residual strain resulting from previous time stages (both instantaneous strain and time dependent plastic strain) is ϵ_{t_n} at the time t_n . If the mean temperature during the time interval Δt , from the time t_n to the time t_{n+1} , is so low that no creep occurs, then the relation between stress and strain at time t_{n+1} will be described for the element by the line A-B (FIG. 12), provided that the stress does not exceed the value corresponding to the point of intersection between the line A-B and the approximate

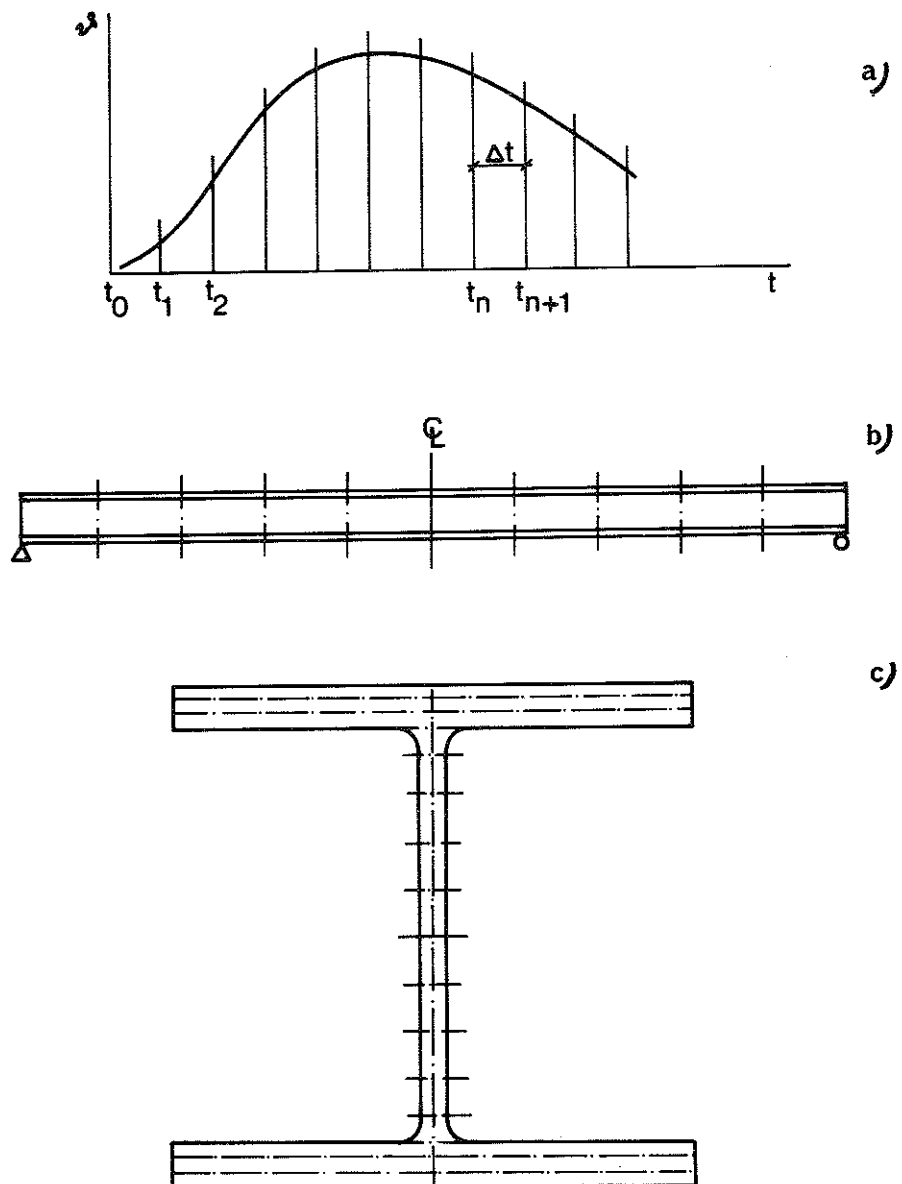


FIG. 11. Principles of division into a) time, b) cross sections and c) elements in the calculation model.

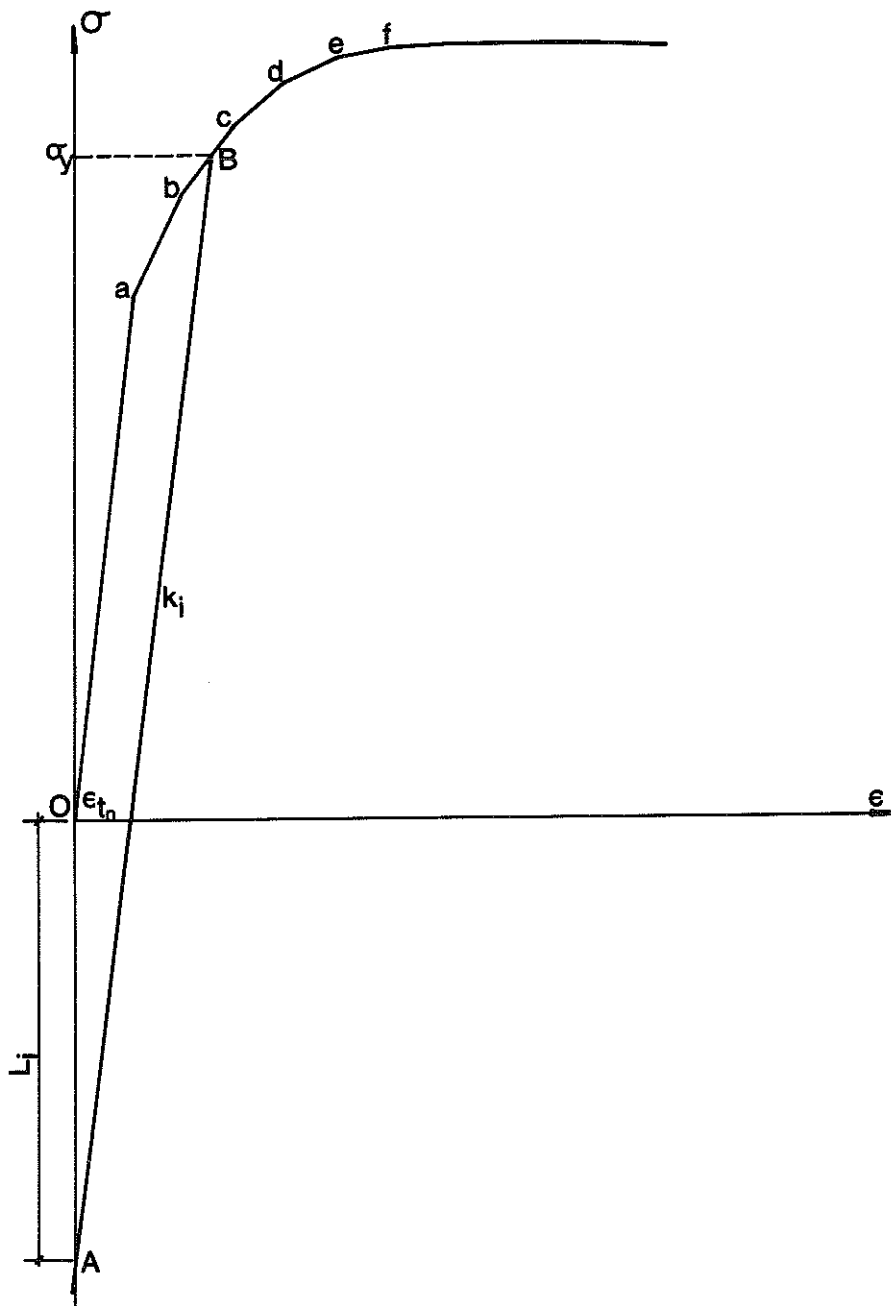


FIG. 12. Relations between the stress σ and strain ϵ which were used in the calculation model for temperatures at which the effect of creep is negligible.

elevated-temperature stress-strain curve (point y in FIG. 12). The direction coefficient of line A-B is denoted k_i and is identical with the modulus of elasticity of the material at the temperature θ_{n+1} . Using the symbols in FIG. 12, the equation of line A-B may be written

$$\sigma = k_i \varepsilon + L_i \quad (7)$$

The appropriate positive or negative values of the quantities concerned are to be inserted into Equation (7).

If, on the other hand, the stress at time t_{n+1} exceeds the value σ_y , then the relation between stress and strain for the element will conform to the curve (-- B, c, d, e, f --). Equation (7) may however continue to be used to describe the relation between stress and strain, if the values of k_i and L_i in the Equation are replaced by the corresponding values obtained from the line of the approximate elevated-temperature stress-strain curve for the appropriate strain.

If the temperature during the time interval Δt is so high that the effect of the creep strain in the material shows, then the relation between stress and strain will be different. As before, the total residual strain from the previous time stages is ε_{t_n} at the time t_n . As before, the elevated-temperature tensile curve at the temperature θ_{n+1} is approximated by the straight lines between the points 0, a, b, c, d, e, f, etc, as shown in FIG. 13. The sum of the residual strain from previous time stages and the creep strain which occurs during the time interval Δt may be calculated by the creep equations described in Section 3.1, i.e.

$$\theta = \int_0^t e^{-\Delta H/RT} dt \quad (8)$$

$$\varepsilon_t = (\varepsilon_{t_0} / \ln 2) \cosh^{-1} (2^{Z\theta/\varepsilon_{t_0}}) \quad (9)$$

where θ = temperature-compensated time (h)

ΔH = the activation energy required for creep to occur
(cal/mol)

R = universal gas constant (cal/mol . degrees Kelvin)

T = temperature (degrees Kelvin)

t = time (hours)

ϵ_{t0} , Z = creep parameters which are dependent on the magnitude of the stress

The value of $\Delta H/R$ and the relation between the stress and ϵ_{t0} and the stress and Z are determined by means of conventional creep tests (see also Section 3.2). The values of Z and ϵ_{t0} are calculated from these relations for the stress σ_n applicable to the time t_n . The calculated values of Z and ϵ_{t0} are inserted into Equation (9), and at the same time the strain ϵ_t in the equation is put equal to the residual strain ϵ_{t_n} from previous time intervals. Equation (9) will then yield that value of θ , θ_n , which corresponds to the stress σ_n and the residual strain ϵ_{t_n} from previous time intervals. The increase $\Delta\theta$ in the temperature-compensated time during the time interval Δt can then be calculated with Equation (8) re-written in the form

$$\Delta\theta = e^{-\Delta H/R.T} \Delta t \quad (10)$$

The value of T used is the mean temperature during the time interval Δt , i.e. $T = (\theta_n + \theta_{n+1})/2 + 270$. The new value of θ at time t_{n+1} will then be $\theta_{n+1} = \theta_n + \Delta\theta$. Provided that the stress is constant and equal to σ_n during the time interval Δt , Equation (9) will yield the value of the residual strain $\epsilon_{t_{n+1}}$ at time t_{n+1} when this value of θ and the values of Z and ϵ_{t0} calculated for the stress σ_n are substituted in the equation. The elastic strain corresponding to the stress σ_n is then added to this strain. The elastic strain is equivalent to σ_n/E , where E is the modulus of elasticity at temperature θ_{n+1} . This gives the position of point A in FIG. 13. As pointed out, however, the stress is usually not constant during a time interval but varies, and if the change in stress from time t_n to time t_{n+1} is assumed to be $\Delta\sigma$, the mean stress σ_m during the time interval Δt is $\sigma_m = \sigma_n + \Delta\sigma/2$.

The values of Z and ϵ_{t0} are calculated for the stress σ_m . With these values of Z and ϵ_{t0} and the value of θ_{n+1} , Equation (9) then yields the value of the strain $\epsilon_{t_{n+1}}$. This is the residual

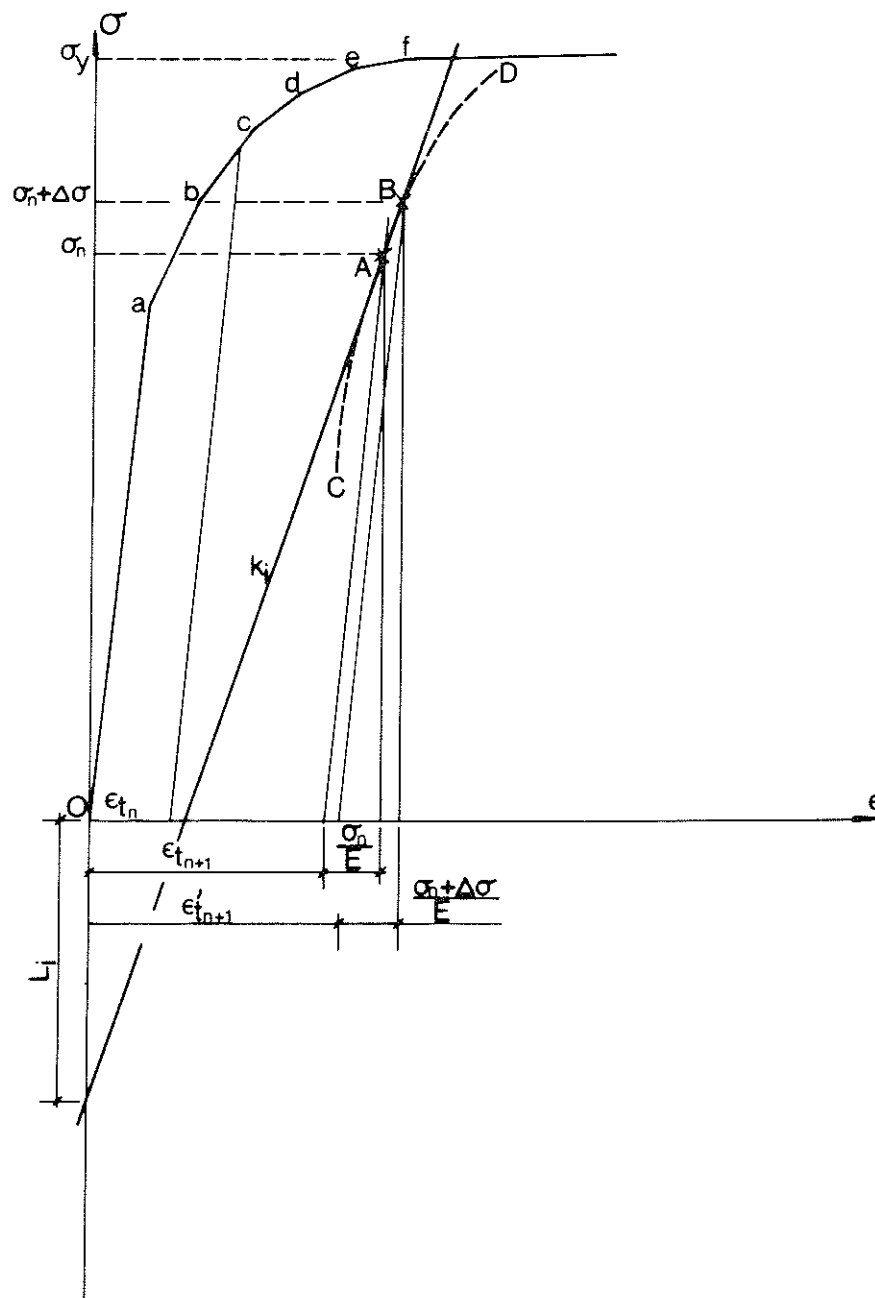


FIG. 13. Relations between the stress σ and strain ϵ which were used in the calculation model for temperatures at which the effect of creep is not negligible.

strain at the time t_{n+1} for a mean stress of σ_m during the time interval Δt . To this strain must be added the elastic strain equivalent to the stress $\sigma_n + \Delta\sigma$, which may be written $(\sigma_n + \Delta\sigma)/E$. This gives the position of the point B in FIG. 13. The points A and B are connected by a straight line. The direction coefficient of this line is denoted k_1 and its intercept with the σ -axis L_1 . The equation of the line A-B is the same as Equation (7). It is assumed that the relation between stress and strain, for stresses below σ_y , is described by the line A-B. This is naturally an approximation since the relation between stress and creep strain is not linear. It is probable that the actual relation between stress and strain is better described by a curve similar to C-D in FIG. 13, but explicit determination of this relation appears to be impossible. The line A-B may therefore be taken as a sufficiently good approximation of the actual relation between stress and strain for limited changes in the stress during a time interval. The change in stress can easily be limited during a time interval Δt by making the length of this interval the smaller, the more the temperature and therefore the tendency to creep increase. Comparisons between deformations calculated with time intervals of different lengths have also shown that computational accuracy is not particularly sensitive to the length of the interval.

If the stress exceeds σ_y , it is assumed as before that the relation between stress and strain is described by a line of the approximate elevated-temperature stress-strain curve which corresponds to the appropriate strain.

Analogous calculations of the relations between stress and strain at the time t_{n+1} are performed for all elements of the cross section by means of Equation (7). It is assumed that Bernoulli's hypothesis concerning plane cross sections is valid. This implies that the total relative expansion of the elements in the cross section, which comprises both strain and thermal expansion, must be linearly distributed over the depth of the beam. An arbitrary distribution of the expansion over the depth of the beam, as shown in FIG. 14, can always be broken down into an expansion of absolute value e_n which is uniformly distributed, and an expansion symmetrically distributed about the neutral

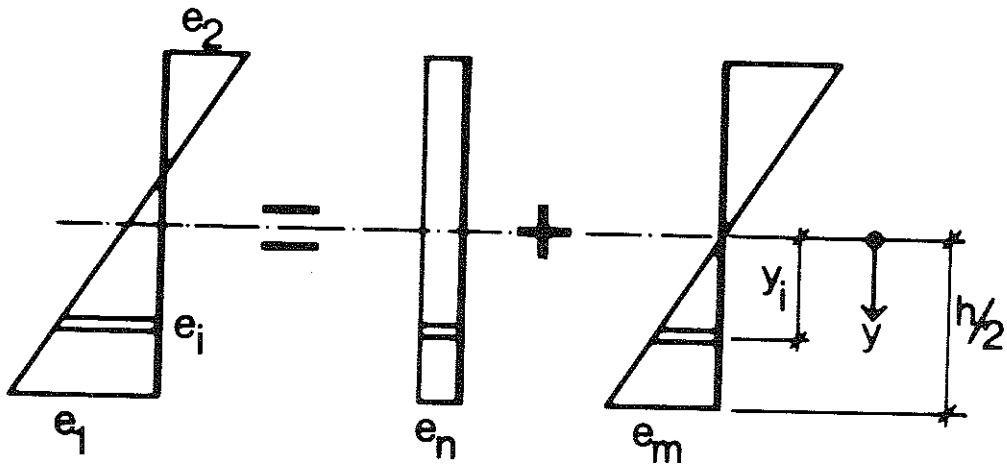


FIG. 14. Distribution of the relative expansion over the depth of the beam.

axis of the section with maximum and minimum values of $+e_m$ and $-e_m$ respectively. The relative expansion e_i at any cross sectional element may then be written

$$e_i = e_n + \frac{2y_i}{h} \cdot e_m \quad (11)$$

where y_i = the distance between the i^{th} element and the neutral axis

h = the depth of the beam

The symbol e has been chosen for the total relative expansion in order to emphasise the difference between this and the strain ϵ .

The strain in the i^{th} element may be written

$$\epsilon_i = e_i - e_{t_i} = e_n + \frac{2y_i}{h} \cdot e_m - e_{t_i} \quad (12)$$

where e_{t_i} = the relative thermal expansion in the i^{th} element at the appropriate temperature

If this expression for ϵ_i is substituted into Equation (7), we get the stress σ_i in the i^{th} element

$$\sigma_i = k_i \epsilon_i + L_i = k_i \left(e_n + \frac{2y_i}{h} \cdot e_m - e_{t_i} \right) + L_i \quad (13)$$

The sum over all the cross sectional elements of the product of the stress σ_i and the elemental areas A_i must be equal to the external normal force acting on the cross section, i.e.

$$\sum_i \left\{ k_i \left(e_n + \frac{2y_i}{h} \cdot e_m - e_{t_i} \right) + L_i \right\} A_i = N \quad (14)$$

The sum over all the cross sectional elements of the product of the stress σ_i and the elemental areas A_i , multiplied by the distance y_i to the neutral axis, must further be equal to the external moment acting on the cross section, i.e.

$$\sum_i \left\{ k_i \left(e_n + \frac{2y_i}{h} \cdot e_m - e_{t_i} \right) + L_i \right\} A_i y_i = M \quad (15)$$

Equations (14) and (15) will yield the values of e_m and then e_n

$$e_m = \frac{h}{2} \cdot \frac{(M + \sum_i k_i A_i y_i e_{t_i} - \sum_i L_i A_i y_i) k_i A_i - (N + \sum_i k_i A_i e_{t_i} - \sum_i L_i A_i) k_i A_i y_i}{\sum_i k_i A_i y_i^2 \cdot \sum_i k_i A_i - (\sum_i k_i A_i y_i)^2} \quad (16)$$

$$e_n = \frac{N + \sum_i k_i A_i e_{t_i} - \sum_i L_i A_i - \frac{2}{h} e_m \sum_i k_i A_i y_i}{k_i A_i} \quad (17)$$

Using these values of e_m and e_n in Equations (12) and (13), the strain ϵ_i and the stress σ_i in all cross sectional elements are calculated. These stresses are compared with those corresponding to the approximate stress-strain curves from the elevated-temperature tensile tests (Fig 12, Fig 13) at the temperature of the different elements at the time t_{n+1} . If the stress in any of the elements exceeds that according to the appropriate elevated-temperature stress-strain curve for the calculated strain ϵ_i , the values of k_i and L_i for these elements are adjusted so as to satisfy the equation of the straight line of the approximate elevated-temperature stress-strain curve at the strain ϵ_i . New values of e_m and e_n are calculated with Equations (16) and (17), using these adjusted values of k_i and L_i , and when these new values of e_m and e_n are substituted into Equations (12) and (13), new values of the strain ϵ_i and stress σ_i are obtained for the various elements. This iteration procedure is repeated until all the calculated stresses σ_i are situated on or below the elevated-temperature stress-strain curve for the temperature of the different elements at time t_{n+1} . Stress and strain are thus known at time t_{n+1} for the whole of the cross section. The expression

$$\epsilon_{t_{n+1}} = e_n + \frac{2y_i}{h} e_m - e_{t_i} - \frac{\sigma_i}{E_i} \quad (18)$$

holds for the residual strain $\epsilon_{t_{n+1}}$ in the i^{th} element at this time,

where E_i = modulus of elasticity at time t_{n+1} for the i^{th} element.

The residual strain in the different elements, as calculated by Equation (18), is to form the basis of the calculations for the stresses and strains in the elements at the time t_{n+2} .

When the final values of e_m and e_n have been calculated as above for a cross section at the time t_{n+1} , the curvature K in this section can be calculated.

$$K = \frac{e_m}{h/2} \quad (19)$$

where h = the depth of the beam.

The above method of calculating the strains, stresses and curvatures at the time t_{n+1} is performed for all the sections into which the beam has been divided. The central deflection of the beam at the time t_{n+1} is then computed by numerical integration of the curvatures of the different sections. The general differential equation for the central deflection y of the beam may be written

$$y'' = \{1 + (y')^2\}^{3/2} \cdot K \quad (20)$$

For deflections which are small in relation to the length of the beam, Equation (20) can be simplified to

$$y'' = K \quad (21)$$

In spite of the fact that the deflection of a beam which is exposed to fire may be considerably larger than its deflection at room temperature, calculation using Equation (21) yields a result which is fully acceptable in this context. It has been found in comparing deflections calculated by Equations (20) and (21) respectively for some representative cases that the error in the deflection calculated by means of Equation (21) is no more than a few per cent.

If the statically determinate beam, for instance, is divided into 10 equal parts (11 cross sections), numerical integration of Equation (21) yields the following central deflection when due attention is paid to the boundary conditions

$$y = \frac{L^2}{h \cdot 200} (0.5e_{m_1} + 2e_{m_2} + 4e_{m_3} + 6e_{m_4} + 8e_{m_5} + 9e_{m_6} + 8e_{m_7} + 6e_{m_8} + 4e_{m_9} + 2e_{m_{10}} + 0.5e_{m_{11}}) \quad (22)$$

where L = length of beam

h = depth of beam

$e_{m_1}, e_{m_2}, e_{m_3} \dots$ = the values of e_m at the appropriate cross section, calculated by means of Eq. (16)

When the central deflection at the time t_{n+1} has been calculated according to Equation (22), the procedure described above is repeated for the time t_{n+2} , and so on.

4.2 Statically indeterminate beams

In a statically indeterminate beam there is usually a re-distribution of the moment along the beam when deformation increases during a fire, which is not the case for a statically determinate beam. This re-distribution of moment must be determined in order that the deformation process in a statically indeterminate beam may be calculated. This may be done by consideration of the rules applicable to the change in inclination of the beam at the sections where it is restrained. For a beam which is **rigidly restrained at one or both ends, there must be no change in inclination at the sections where the restraint is applied.** In practice, calculation of the deformation process of a steel beam exposed to the action of fire, which is e.g. **rigidly restrained at both ends, is performed in the following way.** The curvatures at the various cross sections at the end of a time interval are calculated in the same way as for a statically determinate beam for the moment distribution in the beam which applied at the end of the previous time interval. A check is made by numerical integration of the curvatures thus obtained whether there is any change in inclination at the sections where the restraint is applied. If this is the case, then the moment distribution assumed in calculating the curvatures is incorrect, and the supposed moment distribution is adjusted by increasing or decreasing the restraining moments, depending on whether the changes in inclination at the restraint sections are positive or

negative. The curvatures at the various sections of the beam are again calculated for the new moment distribution, and the curvatures calculated for this moment distribution by numerical integration are again checked with respect to changes in inclination at the restraint sections. The iteration procedure is repeated until a moment distribution is obtained which produces no change in inclination at the restraint sections. The central deflection of the beam at the time concerned is finally obtained by numerical integration of the curvatures calculated for this moment distribution.

The re-distribution of moments in a statically indeterminate beam which is exposed to fire has great influence on the deformation of the beam during the fire. Since re-distribution of moments is dependent on the type of loading, among other things, the deformation will also depend on this, as shown in FIG. 15. This shows the calculated deflection-time ($y - t$) curve for a beam of constant cross section which is restrained at both ends and is exposed to fire, the load in one case being concentrated at the centre and uniformly distributed in the other. The material data used in the calculation are the same as those described below in Section 5.1.2.

It has been assumed in both cases that the extreme fibre stresses at the section where the stress is highest are 55% of the yield stress at room temperature. The temperature-time ($\theta - t$) curve for the beams, which has been assumed to be equal in both cases and equal all along the length of the beam, is also shown in the Figure. It has also been assumed that there is no restraint to longitudinal expansion of the beams. It will be seen in the deformation curves shown that deflection is considerably greater for a concentrated load than for a distributed load. The reason for this is that in a beam with a concentrated load, the moment M_f at midsection and the absolute values of the restraint moments M_s are equal at room temperature ($M_s = - PL/8$, $M_f = PL/8$), and the points of contraflexure are therefore situated at the quarter points of the beam and moment distribution is symmetrical about these points. Owing to this symmetry, the increases in curvature in portions of the beam subjected to a positive moment

are the same as the increases in curvature in portions subjected to a negative moment, and the initial moment distribution in the beam is therefore maintained unchanged during the entire fire.

For a beam with a uniformly distributed load, however, the moment at midpoint at room temperature is only a half of the absolute values of the restraint moments. ($M_s = -qL^2/12$, $M_f = qL^2/24$). The increase in curvature which occurs as the temperature rises and the strength and deformational stiffness decrease is therefore dependent in magnitude on the moment. Since a change in inclination at the restraint sections is prevented, the absolute values of the moments at these sections must become smaller and the moment in the span become larger during the fire. Owing to this moment re-distribution which results in a reduction in the restraint moment, this beam is subjected to a slower and therefore lesser total deformation than the beam with a concentrated load in which the initial moment distribution is retained. FIG. 15 shows the calculated restraint moments M_s as a function of the time t in a beam with a uniformly distributed load. At the assumed load level and temperature load, the absolute value of the restraint moment drops during the fire from $0.0833qL^2$ at time 0 to $0.0683qL^2$ at time 180 minutes. For the same beam consisting of an ideal elastoplastic material, the absolute value of the restraint moment as calculated by the limit state theory, is $0.0627qL^2$. The inset figure in FIG. 15 shows the calculated moment distribution along the beam at time 0 and time 180 minutes. The moment distribution according to the limit state theory is also shown for purposes of comparison.

The re-distribution of moment during the fire is less extensive as that predicted by the limit state theory. In order that a moment distribution according to the limit state theory may be achieved, which presupposes that the cross section is fully plastic, considerable deformations are required during fire, owing to the softly rounded shapes of the stress-strain curves at elevated temperatures (13).

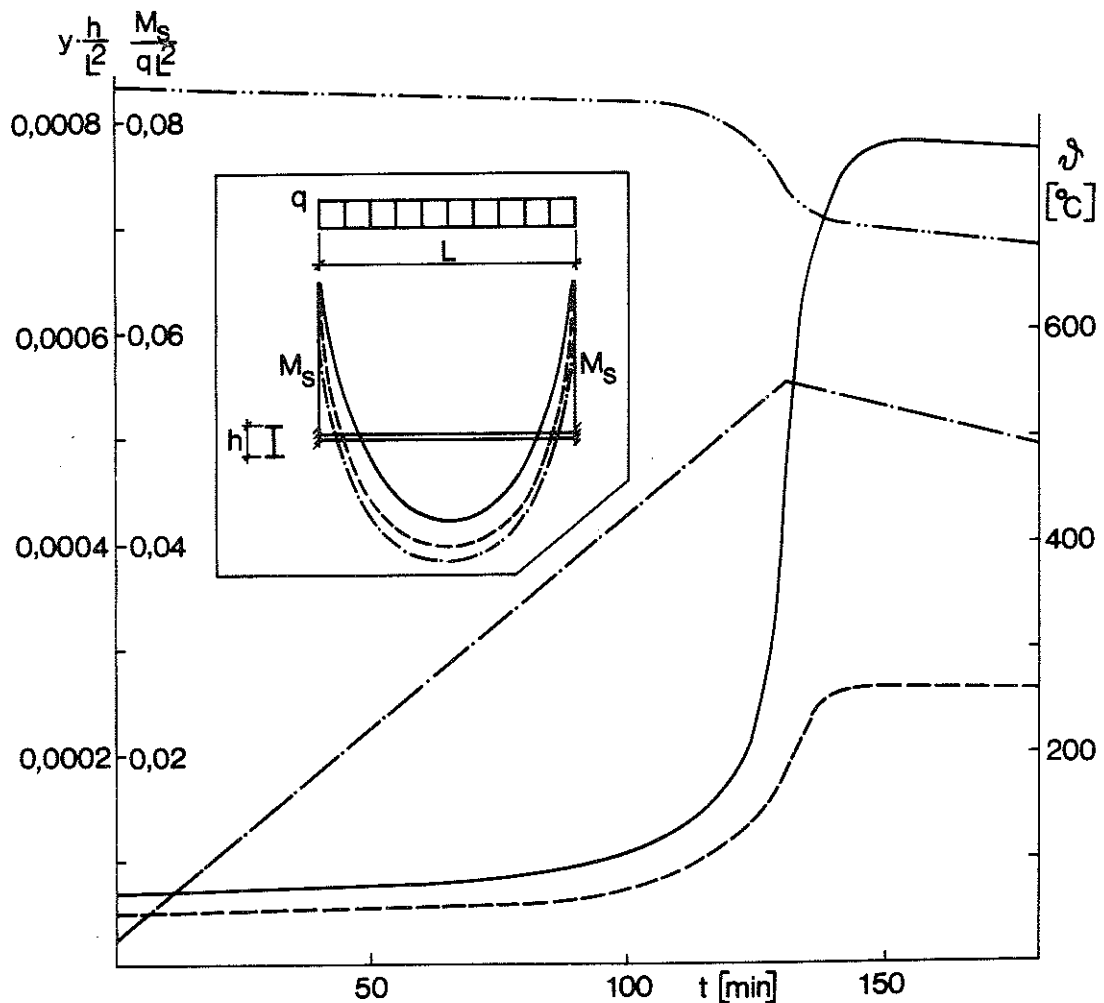


FIG. 15. Comparison, under fire exposure conditions, of the calculated central deflections y as a function of the time t in a beam of carbon steel of constant I section which is rigidly restrained at both ends, for the cases where the load is uniformly distributed (---) and concentrated at the centre (—) (13). It is assumed in both cases that the extreme fibre stresses at the most highly stressed sections are 55% of the yield stress of the material at room temperature. The temperature-time ($\Delta - t$) curve for the beams, which is assumed to be equal in the two cases and to be the same all along the beam, is shown by the chain line. The deflection curves are calculated on the assumption that there is nothing to prevent longitudinal expansion of the beams. The calculated support moment M_s is shown for the beam with uniformly distributed load as a function of the time t (-.-.-).

The inset figure shows the calculated moment distribution in the beam with uniformly distributed load at the beginning of the fire (—) and at the final stage of the fire (---). The moment distribution according to the limit state theory (—), on the assumption that the material is an ideal elasto-plastic one, is also shown for purposes of comparison.

5 COMPARISON OF CALCULATED BEAM DEFORMATIONS WITH THOSE RECORDED DURING TESTS

5.1 Beam tests performed in Sweden

5.1.1 Testing equipment

Some twenty fire tests have been carried out on loaded, statically determinate steel beams in order to verify the calculation model described in the previous Chapter (6). The material of the beams was Steel 1411 according to Swedish Standard SIS 14 14 11 (see Chapter 2). The beams were HE100A sections with a span of 2.5 m.

The fire tests were performed at the Division of Structural Mechanics and Concrete Construction, Lund Institute of Technology, in a bottled gas-fired furnace whose temperature was controlled manually. The temperature of the furnace was recorded at 5 points and that of the beam at 12 points. The thermocouples were affixed to the beam in drilled holes about 3 mm deep which were covered by a thin sheet of asbestos. Placing of the thermocouples is shown in FIG. 16. The temperature-time curves recorded in one of the tests (Beam 8-1) are shown in FIG. 17 as an example.

Load was applied to the test beams by means of a loading yoke in the form of two point loads placed symmetrically about the midpoint of the beam. The loading yoke was connected through a system of wires to a spreading beam carrying two loading containers, situated on the floor below the furnace. The load applied to the test beams was regulated by the quantity of water in these containers. FIG. 18 shows the general arrangement of the loading system.

The total deflection of the beam and also the difference between this deflection and that at the points of application of the load were determined during the test. Deflection of the midpoint was recorded by means of a ruler resting on the top flange of the beam, the ruler being guided by a sleeve against which the reading was made. The deformation of the portion of the beam between the load points was measured by a dial gauge affixed to a bar rigidly connected to the two legs of the loading yoke. The point of the

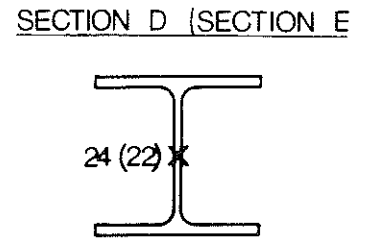
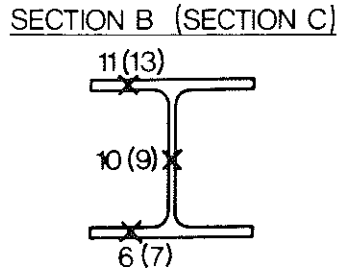
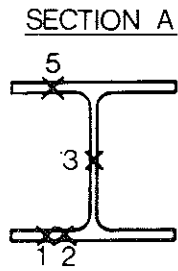
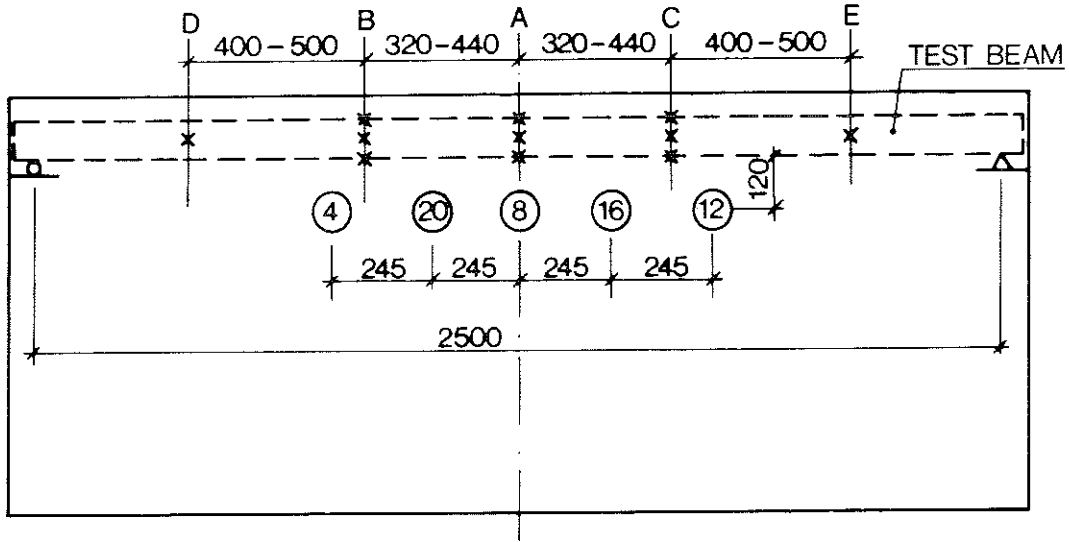


FIG. 16. Placing and numbering of thermocouples. O = furnace, X = beam. The thermocouples in the top flange were placed in holes drilled from the top of the flange. The thermocouples in the bottom flange, with the exception of No 2 which was placed in a hole drilled from the top of the flange, were placed in holes drilled from the bottom of the flange.

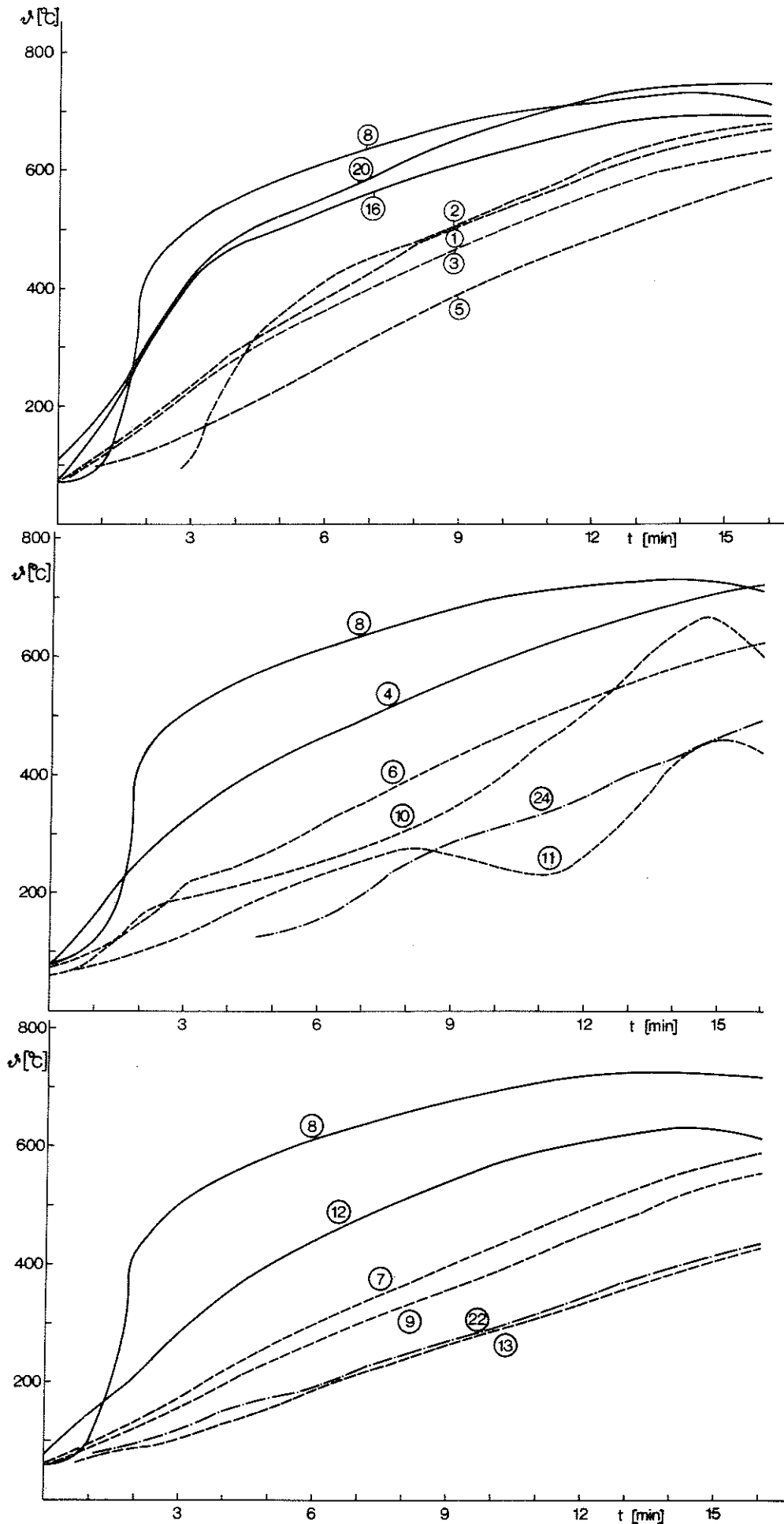


FIG. 17. Temperature-time ($\Delta - t$) curves recorded in the furnace and on the beam, in the case of test beam 8-1. The numbers against the curves are the numbers allocated to the thermocouples as shown in FIG. 16.

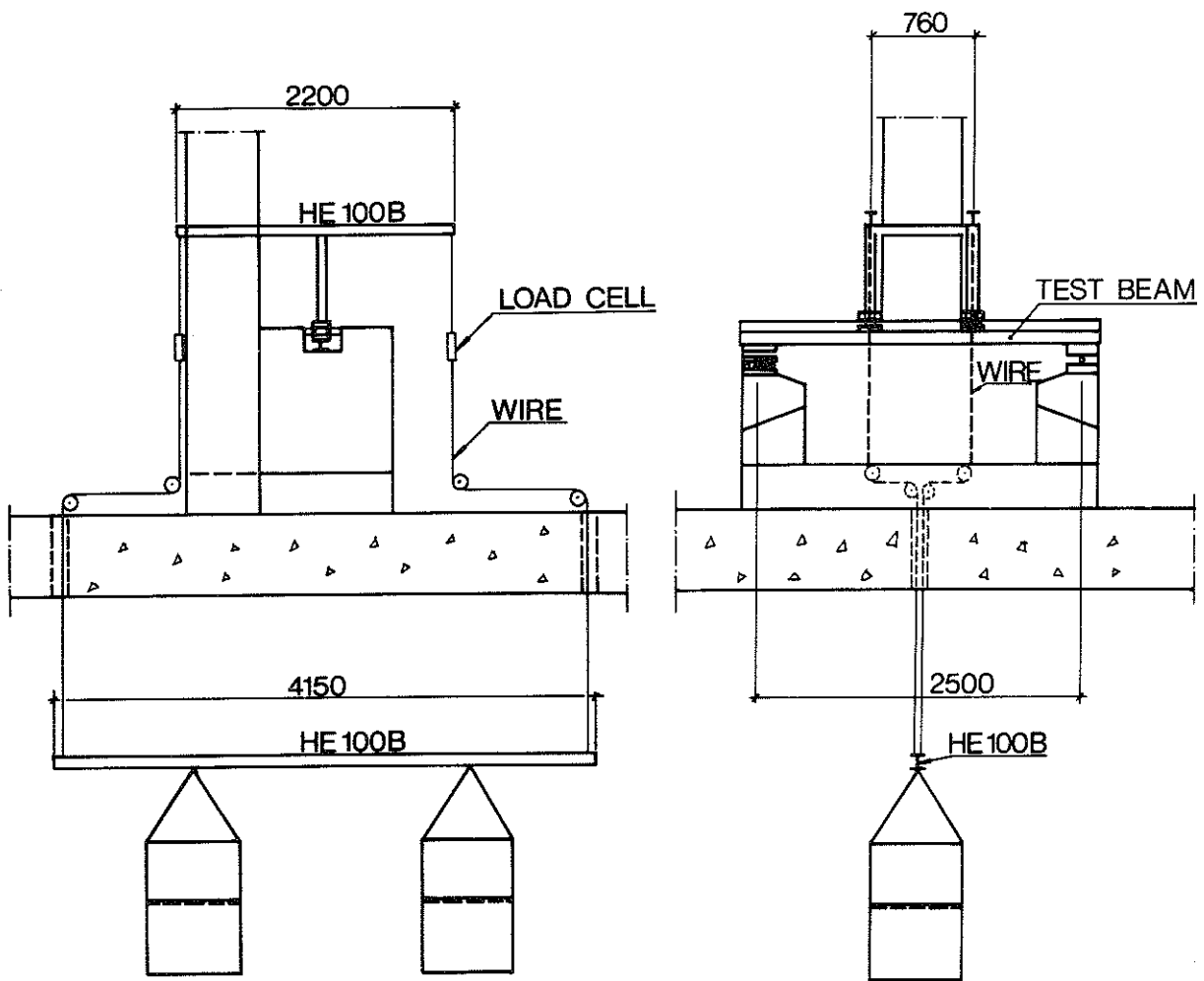


FIG. 18. General arrangement of the loading system.

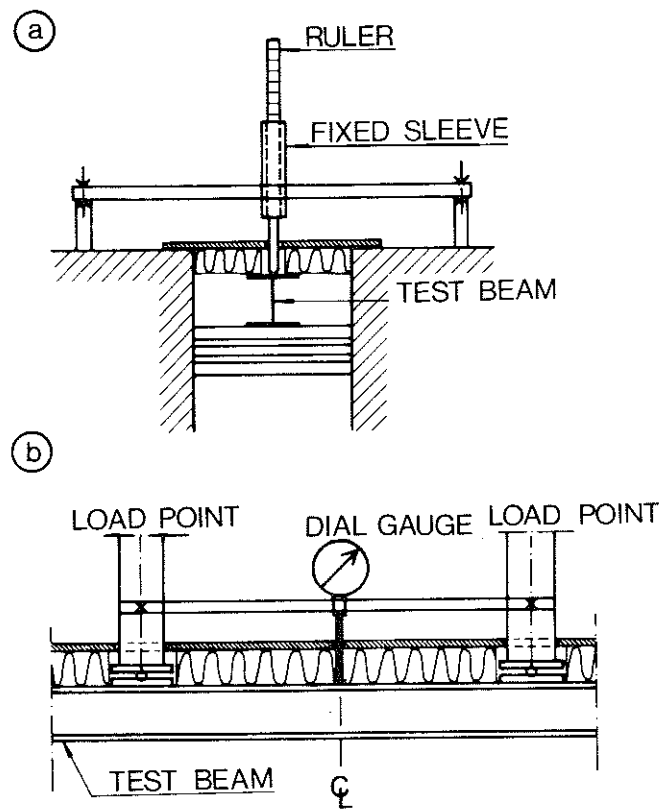


FIG. 19. Measurement of deformations. a) Measurement of the total central deflection of the beam, b) measurement of the difference between the deflection at the centre and those at the points of application of the load.

dial gauge rested on the top flange at the centre of the beam and its reading therefore directly gave the required difference between the deflection at the midpoint and that at the load points. The general arrangement of the measurement system is shown in FIG. 19.

5.1.2 Material data used in the calculations

The deflection curve of the beam was computed for each test by means of the calculation model described in Chapter 4, using the applied load and the recorded beam temperatures as input data. Owing to the large differences in temperature between the centre of the beam and its ends (see FIG. 17), calculation of the deflection curve was confined to the portion between the points of application of the load. The differences in temperature along the beam were considerably less in this portion than between the centre and ends. Another advantage of this procedure was that the moment acting on the beam was constant between these points.

The stress-strain curves according to FIG. 3 were used in the model for calculation of the deformations. As mentioned before, these curves had been determined on the material of the beams used in the tests, and, furthermore, the influence of creep strain may be considered negligible in these curves. The values of the creep parameters $\Delta H/R$, Z and ϵ_t used in Equations (8) and (9) of the calculation model were those listed in TABLE I (Section 3.2) for Steel 1411. These values had been determined on material taken from the beams used in the tests.

The deformation due to elastic strain in a steel beam exposed to the action of fire is small compared with the deformation due to the instantaneous and time dependent plastic strain. Experimental study of the temperature dependence of the modulus of elasticity in the beam material used was therefore considered unnecessary. The relation between the modulus of elasticity E (kgf/cm^2) and the temperature θ ($^{\circ}\text{C}$) which was used in the model was therefore determined on the basis of information in the literature (1), (4), (8), (14). The following simplified relations, which are rough mean values of the relations given in the literature, have been used:

For $\vartheta < 205^{\circ}\text{C}$

$$E = 2,100,000 \quad (23)$$

For $205 < \vartheta < 370^{\circ}\text{C}$

$$E = 2,535,000 - 2,120 \vartheta \quad (24)$$

For $\vartheta > 370^{\circ}\text{C}$

$$E = 3,245,000 - 4,040 \vartheta \quad (25)$$

Reference (8) gives the relation between the relative thermal expansion and the temperature for a structural steel that is largely the same as the material used in the test beams. In the calculation model, this relation has been approximated by two linear relations between the thermal expansion e_t and the temperature ϑ .

For $25^{\circ}\text{C} < \vartheta < 370^{\circ}\text{C}$

$$e_t = 0.0000131 \cdot (\vartheta - 25) \quad (26)$$

For $\vartheta > 370^{\circ}\text{C}$

$$e_t = 0.0000164 \cdot (\vartheta - 370) + 0.0045 \quad (27)$$

5.1.3 The results of tests and calculations

The results of tests and calculations are exemplified in FIG. 20 (a, b, c).

The recorded and calculated deflection-time curves relating to the portion of beam between the points of application of the load are shown for three of the tests. The Figures also show the temperature-time curve recorded at the top and bottom flanges respectively at the midsection. The calculated stress distributions at the beginning and end of each test are also shown.

In all the beam tests, the agreement between recorded and calculated deflections may be said to be very good. This demonstrates that the calculation model described in Chapter 4, using the material data

FIGs. 20 (a, b, c). Comparison of during fire tests recorded (—) and calculated (---) central deflections y_1 for the portion of beam between the points of application of the load, as a function of the time t . The temperature-time ($\vartheta - t$) curves for the top and bottom flange at the midsection are shown by the lower and upper chain lines respectively, (b)

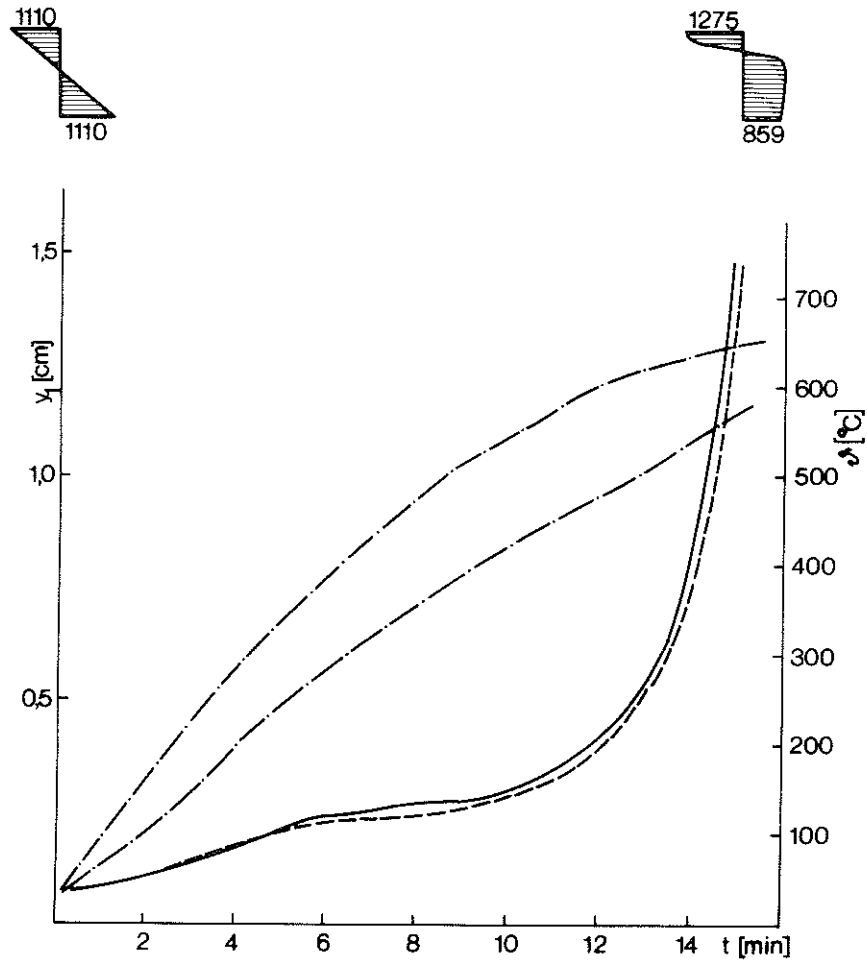


FIG. 20 a.

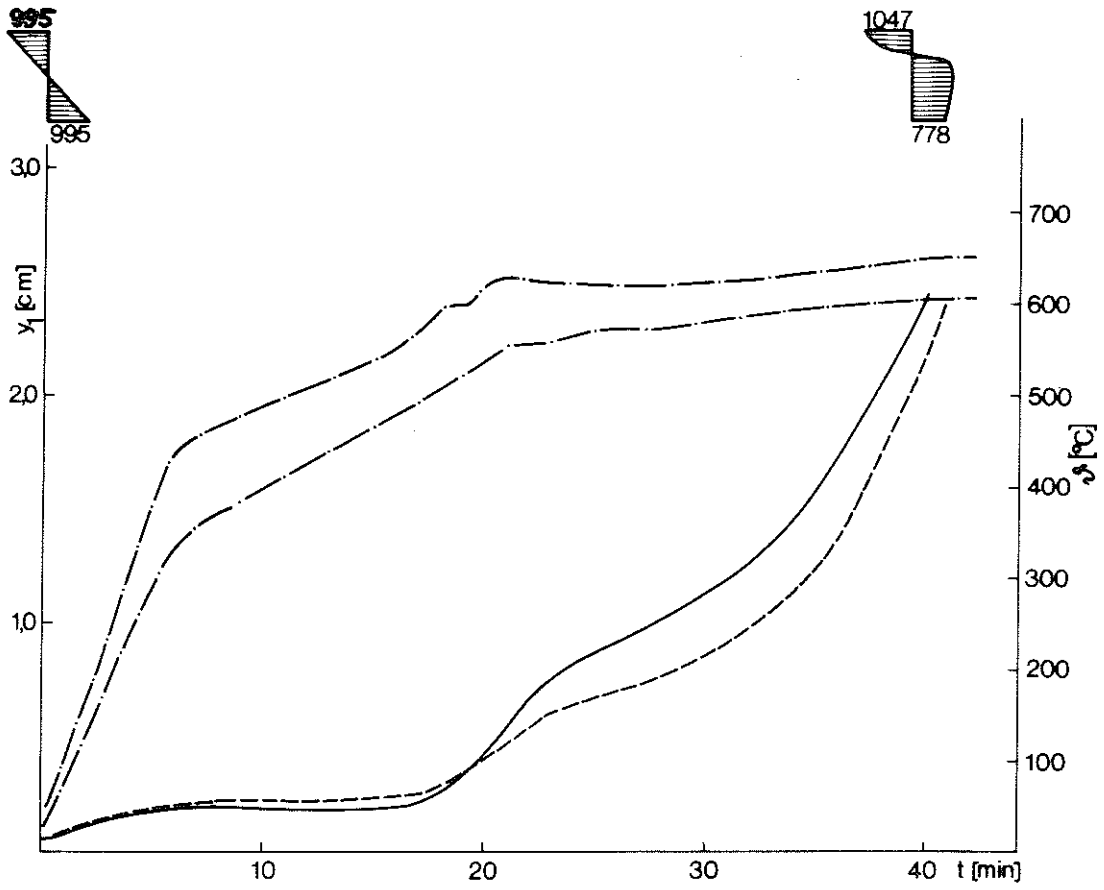


FIG. 20 b.

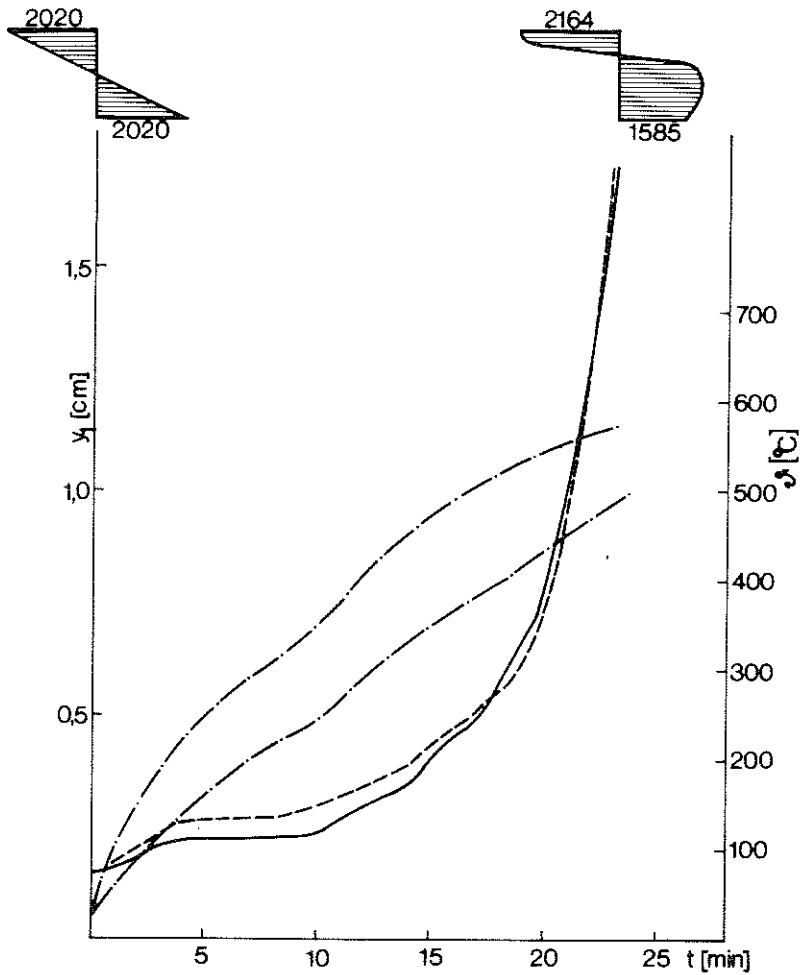


FIG. 20 c.

determined in accordance with Chapters 2 and 3, can be used with satisfactory accuracy for the assessment of the deformation behaviour of steel beams when acted upon by fire.

5.2 Beam tests performed under the aegis of the **European Convention for Constructional Steelwork**

There is very little possibility of utilising the results of fire tests performed on steel beams, which are reported in the literature, for further comparisons of the calculated and recorded deformation processes. Test conditions relating to supports, restraint, loading and temperatures and also the elevated temperature properties of the steel material are in most cases described so sketchily that the deformation process cannot be checked on the model. This was also one of the reasons why the fire tests with simply supported steel beams, described in the previous Section, were carried out.

In spite of the fact that some data necessary for the calculation model had not been given, the results of some fire tests performed on steel beams of HE 220 B section by the **European Convention for Constructional Steelwork (15, 16)** could be made use of for further comparisons between recorded and calculated deformations. Data which were required for the calculations but had not been given had to be estimated. Such data are those concerning the elevated temperature properties of the material in the form of the stress-strain curve at different temperatures and also data relating to the creep properties of the material. Calculation of the deformations was therefore based on material data determined for the beams used in the fire tests described in the previous Section. The material in these beams had a higher yield stress at room temperature than that in the beams used in the **European Convention for Constructional Steelworks tests, however. Fictitious loads, equal to the real load multiplied by the ratio between the yield stress at room temperature for the model material and the actual material, were therefore used in calculating the deformations for these latter beams. As regards the temperatures in these beams, these are quoted only for the bottom flange, web and top flange at the midsection. On the basis of temperatures recorded in other fire**

tests, it may be assumed that the temperatures in the end regions of these beams were lower than in their midregions. Two different calculations were therefore performed for each beam, the assumption in the first case being that the temperature of the midsection was representative for the whole of the beam, and in the second case that the temperature ϑ at the ends of the beam was 75% of the temperatures ϑ_m given at the midsection of the beam. Decrease of temperature along the beam from the middle to the ends was assumed to be in the form of a sine curve. The recorded and calculated deflection-time ($y - t$) curves are compared in FIGs. 21a - 21d. FIGs. 21a and 21b refer to simply supported beams (15), while FIGs. 21c and 21d refer to beams restrained at one end (16). Each Figure shows the temperature-time ($\vartheta_m - t$) curve at the bottom and top flange at the midsection. For the simply supported beams, the difference between calculated deformations for the temperature ratios ϑ/ϑ_m of 1.0 and 0.75 is considerably less than that for the restrained beams. This is explained by the fact that deformation of a simply supported beam is essentially governed by curvature conditions at the midregion of the beam, while for a restrained beam it is the magnitude of curvature at the sections where the beam is restrained which exercises the predominant influence on deformation. It is also evident from the Figures that the deformation curves calculated by means of the model, particularly at the assumed temperature ratio $\vartheta/\vartheta_m = 0.75$, are in good agreement with the recorded deformation curves.

FIGs. 21 (a, b, c, d). Comparison of central deflection-time ($y-t$) curves recorded during fire tests (15, 16) and those calculated for steel beams HE 220 B ϑ = temperatures at the ends, ϑ_m = temperatures at midsection, q = load, q_s = load which causes the most highly stressed section to yield at room temperature.

- recorded central deflection
- . - calculated central deflection for $\vartheta/\vartheta_m = 1.0$
- calculated central deflection for $\vartheta/\vartheta_m = 0.75$
- x - top flange temperature at midsection
- o - bottom flange temperature at midsection

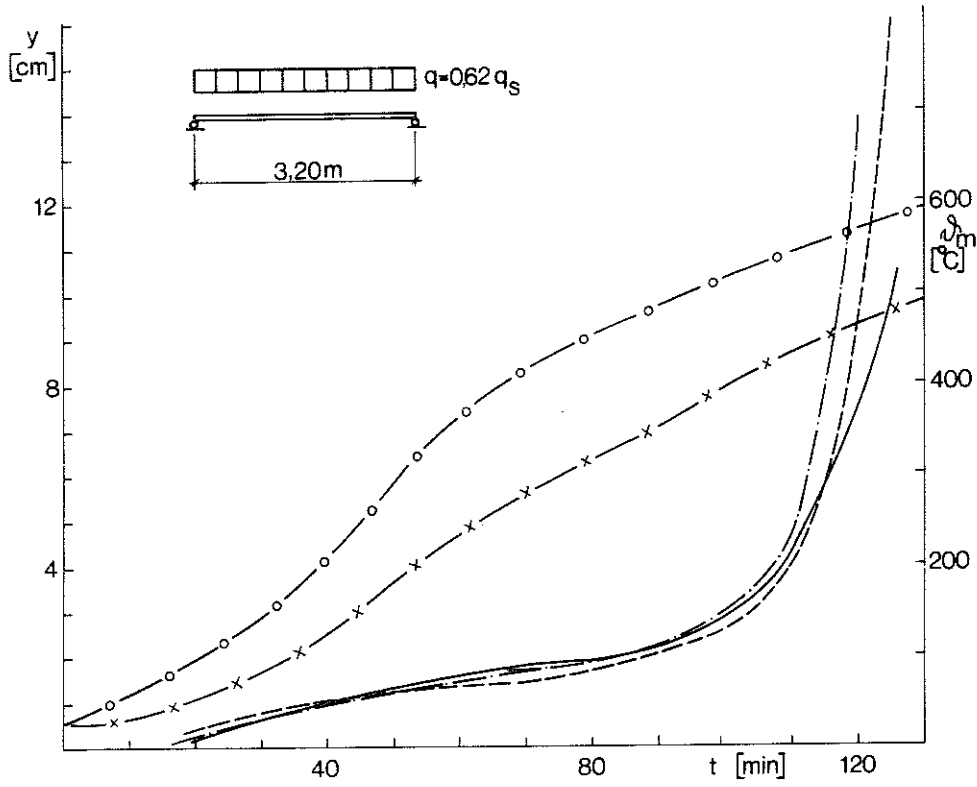


FIG. 21 a.

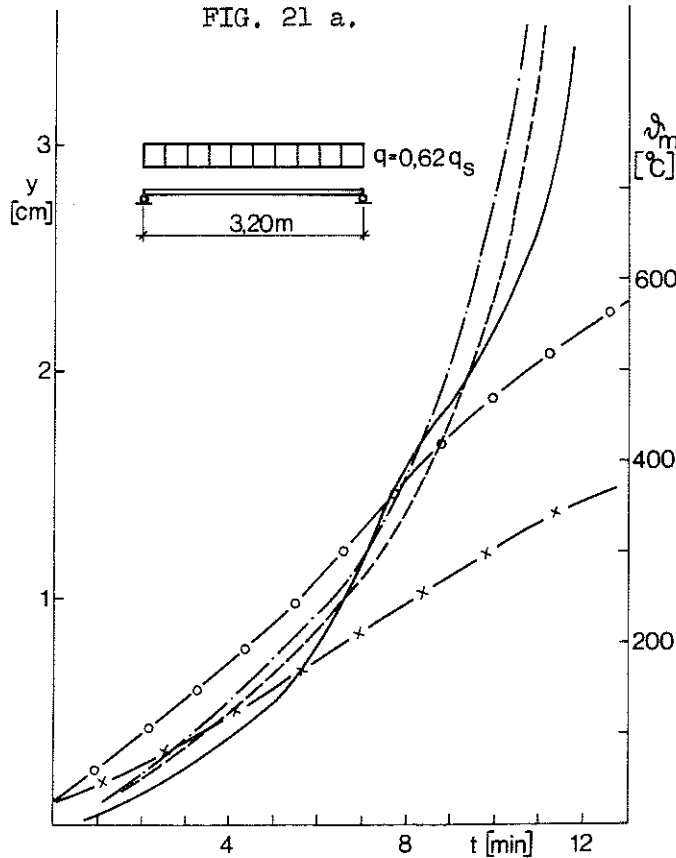


FIG. 21 b.

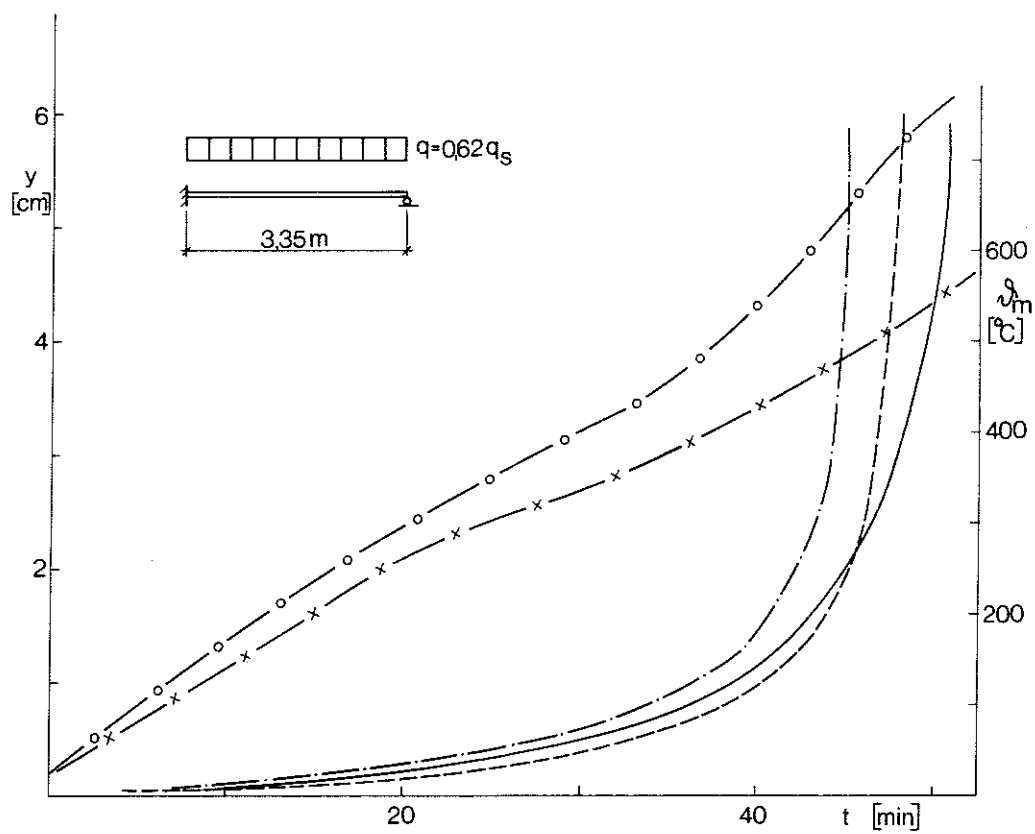


FIG. 21 c.

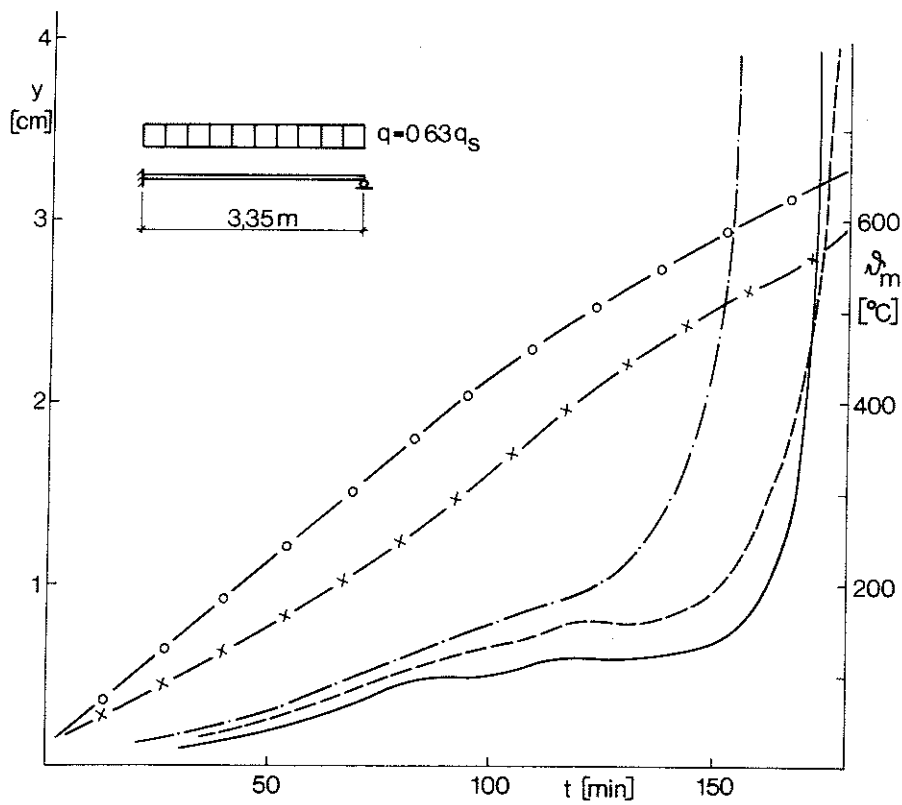


FIG. 21 d.

6 CRITERION OF FAILURE

As will be seen from the stress-strain curves in FIG. 3, at elevated temperatures there is no clearly defined yield region. Since the stress-strain curves are also very softly rounded, assessment on the basis of the 0.2% proof stress of the load carrying capacity of a steel beam which is exposed to fire very often results in an obvious underestimation of the actual load carrying capacity of the beam. Estimation of the load carrying capacity should instead be based on the deformation curve of the beam when it is acted upon by fire. Theoretically, the load carrying capacity of a beam in a fire test may be considered exhausted when its rate of deformation is infinitely high. It is, however, very difficult to decide when the rate of deformation is to be defined as "infinitely high" since the rate of deformation during a test continuously increases as the temperature rises. Furthermore this criterion is impossible to use in connection with a real fire when the deflection of the beam due to creep continues to increase during the cooling down period of the beam. There is therefore a clear need for a definition of failure which is better suited for practical purposes. Various such practical definitions of failure, associated with finite deformations or rates of deformation, are also often applied in fire testing contexts. Robertson and Ryan (17) have proposed the following criteria of failure for statically determinate beams which are exposed to fire

$$y = \frac{L^2}{h \cdot 800} \quad (28)$$

$$\frac{dy}{dt} = \frac{L^2}{h \cdot 150} \quad (29)$$

where L = distance between the points of support of the beam (cm)

h = depth of beam (cm)

y = central deflection of the beam (cm)

t = time (h)

According to Robertson and Ryan, both criteria must be satisfied before failure is to be considered to have occurred. This implies that, provided the rate of temperature rise is sufficiently low, central deflection of the beam may become considerable before the criterion concerning rate of deflection according to Equation (29) is satisfied. When a beam is part of a structure, however, it cannot perform its function when its deformation is excessive since adjacent elements of the structure such as parts

of the floor slab may lose their support etc. The structure would in other words cease to function before the beam itself has attained the criteria of failure according to Equations (28) and (29). Satisfaction of both criteria may also have the consequence that a beam which is heated at a fast rate attains a lower critical temperature than a beam which is heated slowly. This appears to be functionally wrong in view of the fact that a fast rate of heating has a lesser effect on creep than slow heating. In view of this and with regard to the function of the beam as part of a structure, it is therefore appropriate to make use of a criterion of failure which is based only on deflection and not on the rate of deflection.

The deflection criterion of Robertson and Ryan according to Equation (28), $y = L^2/h.800$, is logically constructed, since the deflection y of a beam can always, independently of the loading and restraint conditions of the beam, be written in the form

$$y = \frac{L^2}{h} \cdot \sum_i^n \frac{c_i(e_1 - e_2)_i}{C}$$

where the summation sign implies summation over all the sections into which the beam has been divided in the course of calculation. The symbols e_1 and e_2 denote the expansion in the bottom and top respectively at the appropriate cross section. C and c_i are constants which are functions of restraint conditions, loading and the number n of cross sections.




If a beam exposed to fire is loaded by a bending moment constant along its entire length and if the temperature in all parts of the beam is assumed to be the same at all times, then the deflection criterion according to Equation (28) is equivalent to a strain of 0.5% at the bottom of the beam (11). This is true on condition that the compressive strain due to a compressive force is the same as the positive strain due to a tensile force of the same magnitude. For other loading conditions, for instance a uniformly distributed load or concentrated load, the strain at the bottom of the beam at the section which is most highly stressed must be greater than 0.5% in order that a deflection according to Equation (28) should be attained. The relation between stress and strain is not linear at temperatures which occur during a fire.

The magnitude of the strain required for a deflection according to Equation (28) is therefore not clearly determined by the type of loading in the case of loading conditions other than a constant bending moment. The magnitude of this strain is dependent on the maximum temperature and the rate of heating. In order to obtain a rough idea of which strains satisfy the deflection criterion, a number of deformation calculations were performed with the calculation model. The calculations were made for different temperature effects, both for a beam with a uniformly distributed load and for a beam with a centrally placed concentrated load. In order to make possible direct comparisons with the beam subjected to a constant bending moment, it was assumed during each calculation that the temperature was equal all along the beam at all times. The results of the calculations show that the deflection criterion is equivalent to a strain at the bottom of the beam of 0.8 - 1.0% for a beam with a uniformly distributed load and one of 1.5 - 1.9% for a beam with a central concentrated load. The results are shown in TABLE IIa.

Inequality of temperature in the beam also influences the magnitude of the strain required for the deflection criterion according to Equation (28) to be attained. In order to study this in closer detail, a number of deformation calculations were performed for a beam subjected to a constant bending moment, the temperature being varied along the axis of the beam according to an assumed sinusoidal temperature distribution. The calculations were carried out for ratios between the temperature of the end and central sections of 0.75 and 0.5. The magnitude of the strain which is required at the bottom of the midsection in order that the deflection criterion according to Equation (28) may be attained is not clearly determined by the temperature distribution. As has been mentioned before, the maximum temperature and the rate of heating exercise an influence on the magnitude of this strain. When the ratio between the temperatures at the end section and the midsection is 0.75, the requisite strain is in the region of 0.6 - 1.0%. For a temperature ratio of 0.5, the requisite strain at the bottom of the midsection is in the region of 0.8 - 1.4%. These results are tabulated in TABLE IIb.

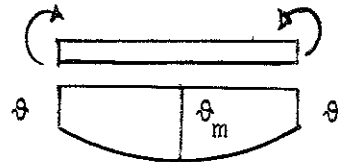
TABLE II. Strain (%) required in the bottom fibres at midsection in order that the deflection criterion $y = L^2/h.800$ should be reached.

a) Different loading conditions, Same temperature in all parts of the beam.

| Loading condition | | |
|---|---|---|
|  |  |  |
| 0.5 | 0.8 - 1.0 | 1.5 - 1.9 |

b) Variable temperature along the beam. Constant bending moment.

Temperature distribution ϑ .



| Temperature distribution | | |
|-------------------------------|--------------------------------|-------------------------------|
| $\vartheta/\vartheta_m = 1.0$ | $\vartheta/\vartheta_m = 0.75$ | $\vartheta/\vartheta_m = 0.5$ |
| 0.5 | 0.6 - 1.0 | 0.8 - 1.4 |

During a fire test, the temperature at the ends of a beam is lower than that around its centre. This is also very often the case in natural fires. It is obvious on the basis of a rough estimate using the values in TABLES IIa and IIb that the strain required at the bottom of the midsection in order that a deflection according to Equation (28) should be attained, is probably in the region of 1 - 2% in most cases. It will be seen from FIG. 3 that the slope of the stress-strain curves at elevated temperatures is comparatively shallow within the 1 - 2% strain region. When this region has been passed, strain and hence deformation therefore generally increase at a fast rate as the stress or temperature rises. For the beams in the fire tests described in Section 5.1, application of Equation (28) to the portion of the beam between the points of application of the load yields a critical deflection of 0.75 cm. It is evident from the calculated and recorded deflection curves that deflection generally increases rapidly when this level of deformation has been passed.

A reasonable requirement which a criterion of failure should generally satisfy is that the deformation should increase at a considerable rate when the load exceeds the load level which satisfies the criterion of failure. Determination of the loads which produce a deflection in agreement with Equation (28), for different steel temperature-time curves (different maximum temperatures and rates of heating and cooling), would provide a possibility of studying more closely this aspect of the deflection criterion according to Equation (28). The increase in deflection due to a certain rise in the critical load determined in the way described above could then be found. Such a study is however difficult to perform purely on the basis of test results, since it is likely that a very large number of tests would be necessary at each temperature-time curve in order that the load which produces a deflection according to Equation (28) may be determined. Further, with the testing equipment described in Section 5.1, it would be practically impossible for the tests to be fully reproducible as regards temperatures. Owing to variations in temperature differences both along and across the beam and also differences in the rates of heating and cooling, it would be impossible to make direct comparisons between the different tests. Such a study is however

possible using the calculation model, and a study has been performed for a simply supported beam with a uniformly distributed load. The results show that the central deflection increases by 60 - 100% for a 10% rise in the loads which, at the temperatures concerned, satisfies the criterion according to Equation (28). A six to tenfold increase in deflection for unit increase in the load may be considered sufficiently large in order that the deflection criterion according to Equation (28) should be accepted as a reasonable criterion of failure; from the above aspect also, for steel beams exposed to fire.

The criteria proposed by Robertson and Ryan, as described in Equations (28) and (29), were originally intended for statically determinate beams. It is however appropriate that the deflection criterion according to Equation (28) should be extended to cover also statically indeterminate beams. It has already been pointed out that, when a beam is subjected to excessive deflection, there is a risk that the parts of the structure connected to the beam, such as parts of the floor slab, will lose their support. Owing to this, it is appropriate that a criterion associated with the magnitude of deflection should be used for the definition of failure, and it is also reasonable that the criteria applied with regard to the maximum permissible deflection should be the same irrespective of the static system. This implies therefore that L in Equation (28) should denote the distance between the points of support of the beam and y the central deflection, even when this Equation is applied to a statically indeterminate beam, for instance one rigidly restrained at one or both ends. On the other hand, however, when the Equation is applied to a cantilever, L must denote twice the length of the cantilever and y the deflection at the free end of the cantilever in order that conditions may be comparable with those in the case of a beam supported at two points.

7 THE INFLUENCE OF VARIOUS FACTORS ON THE DEFORMATION PROCESS OF STEEL BEAMS EXPOSED TO THE ACTION OF FIRE

Deformations of a steel beam which is exposed to the action of fire are influenced by a number of factors. If it is assumed that the temperature-time relation is the same all over the beam and there is no restraint on longitudinal expansion of the beam, then the deformation as expressed by $y \cdot \frac{h}{L^2}$ (y = central deflection, h = depth of beam, L = length of beam) will be governed by the following factors for a certain material and a certain shape of section:

- a) Maximum temperature
- b) Rate of heating and cooling
- c) Statical system
- d) Type of loading
- e) Magnitude of load

Using the calculation model, the influence of these factors on the deformations in beams of carbon steel and of constant I cross section has been studied.

7.1 Maximum temperature

Since the strength and deformational stiffness of steel decrease as the temperature rises, the deformation of a steel beam which is exposed to fire is very largely dependent on the steel temperature attained, as will be seen in FIG. 22. This shows the calculated central deflection y for a simply supported beam with a uniformly distributed load q as a function of the steel temperature ϑ , on the assumption that the action of the temperature is represented by a linear temperature rise of $100^{\circ}\text{C}/\text{min}$ from room temperature to the temperature ϑ . The load q_g is the load at which the section subjected to the highest stress reaches the yield stress at room temperature.

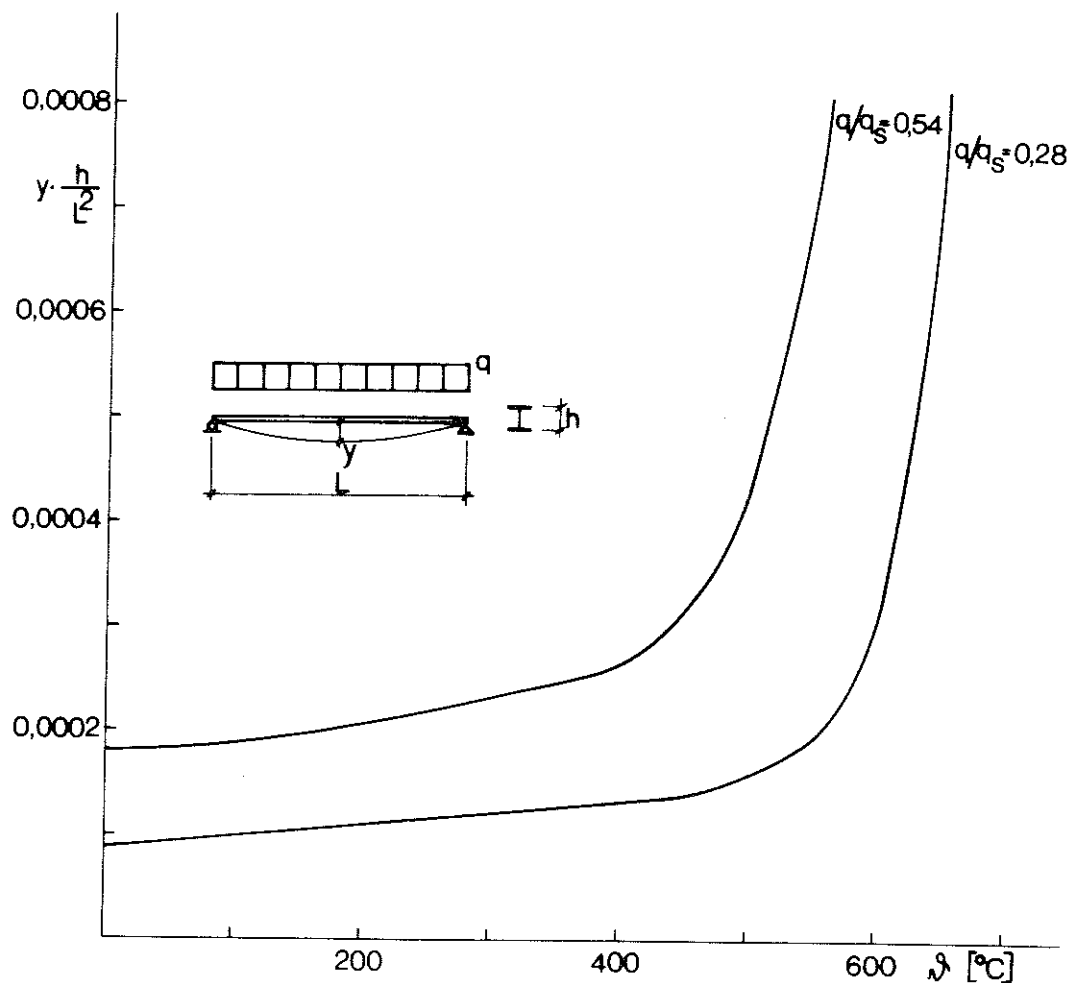


FIG. 22. Calculated central deflection y as a function of the steel temperature ϑ for a simply supported beam with uniformly distributed load q when it is exposed to a temperature action represented by a linear increase in temperature of $100^\circ\text{C}/\text{min}$ from room temperature to the temperature ϑ . It is assumed that the temperature is equal all over the beam and that there is no restraint on longitudinal expansion of the beam. The load q_s is the load at which the most highly stressed section reaches the yield stress at room temperature.

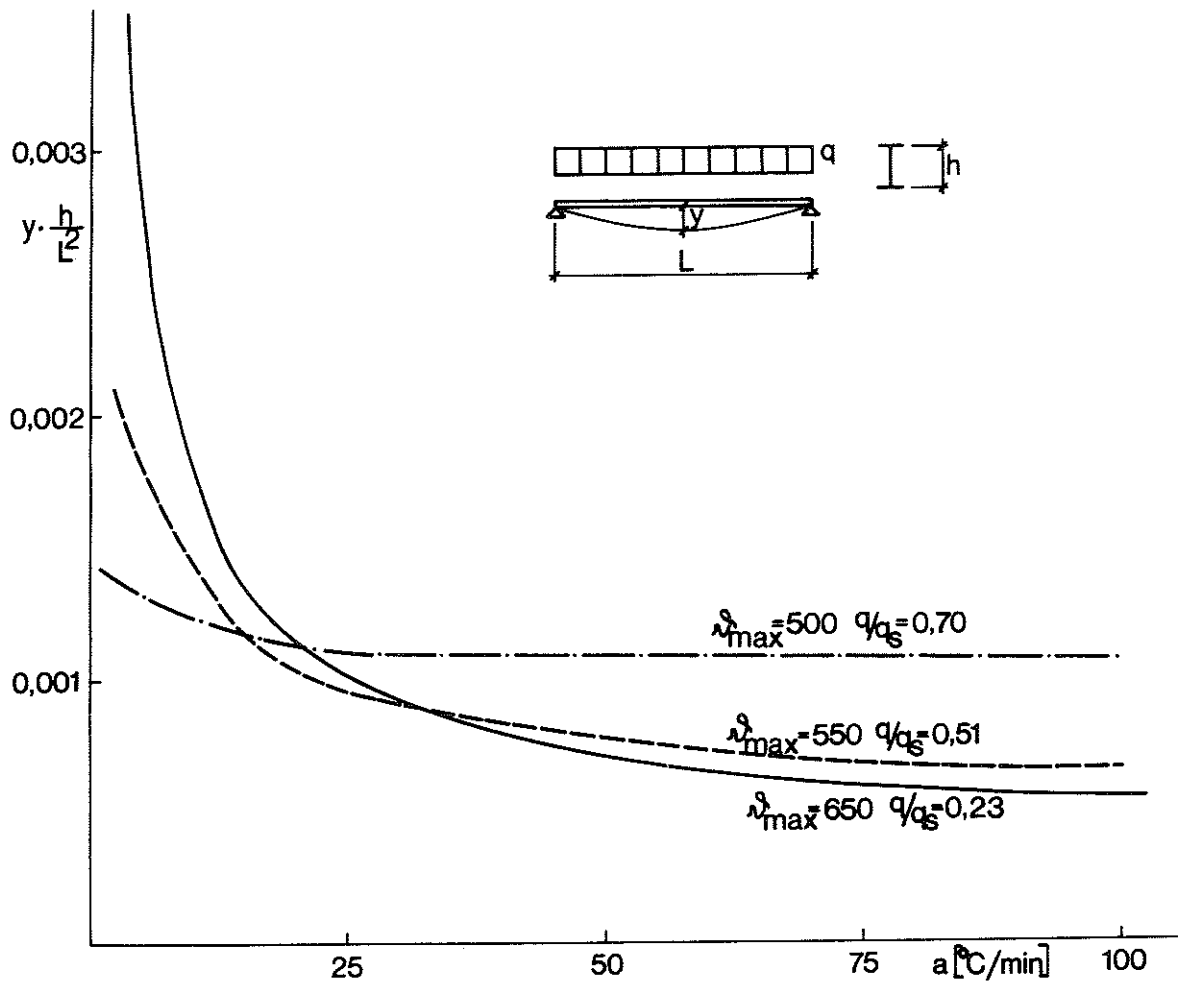


FIG. 23. Calculated central deflection y , under fire exposure conditions, as a function of the rate of heating a for a simply supported carbon steel beam with a uniformly distributed load q . The deflections during the cooling period are included in the calculated deflections. It is assumed that the rate of cooling is one-third of the rate of heating in question, that the temperature is the same all over the beam, and that there is no restraint on longitudinal expansion of the beam. The load q_s is the load at which the most highly stressed section reaches the yield stress at room temperature, and ϑ_{max} the maximum temperature which the beam attains during the fire.

7.2 Rates of heating and cooling

It is not until a temperature of approximately 450°C has been reached that the creep strain of the steel begins to exert an influence on the deformation of a steel beam exposed to fire. Since the magnitude of creep strain is time dependent, deformation at temperatures above 450°C will be the greater, the slower the rates of heating and cooling. FIG. 23 shows the calculated maximum central deflection y for a simply supported beam with uniformly distributed load, which is exposed to fire, as a function of the rate of heating a . The deflection includes that during the cooling period, the assumption being that the rate of cooling is one-third of the rate of heating under consideration. The Figure shows three curves representing different loads q and maximum temperatures ϑ_{max} . The symbol q_s denotes that load at which the section which is most highly stressed reaches the yield stress at room temperature. The loads used in the calculations at the different maximum temperatures have been chosen in such a way that the deflections in the three cases are of the same order and reach values which are critical from the point of view of failure, at a rate of heating of $10\text{-}20^{\circ}\text{C}/\text{min}$. It is evident from the curves that the influence of the rates of heating and cooling on the deformation increases as the temperature rises.

7.3 Statical system

The type of statical system exerts a great influence on the deformation of a steel beam which is exposed to fire. Contrary to the state of affairs in a statically determinate beam, a re-distribution of moments generally occurs in a statically indeterminate beam as the deformation of the beam increases during a fire. This re-distribution of moments has the effect that the moments and stresses in the sections of a beam which are most highly stressed are reduced, and this has a restraining effect on the deformation. The influence of this re-distribution of moments on the deformation of a steel beam which is exposed to fire has already been touched upon to some extent in Section 4.2.

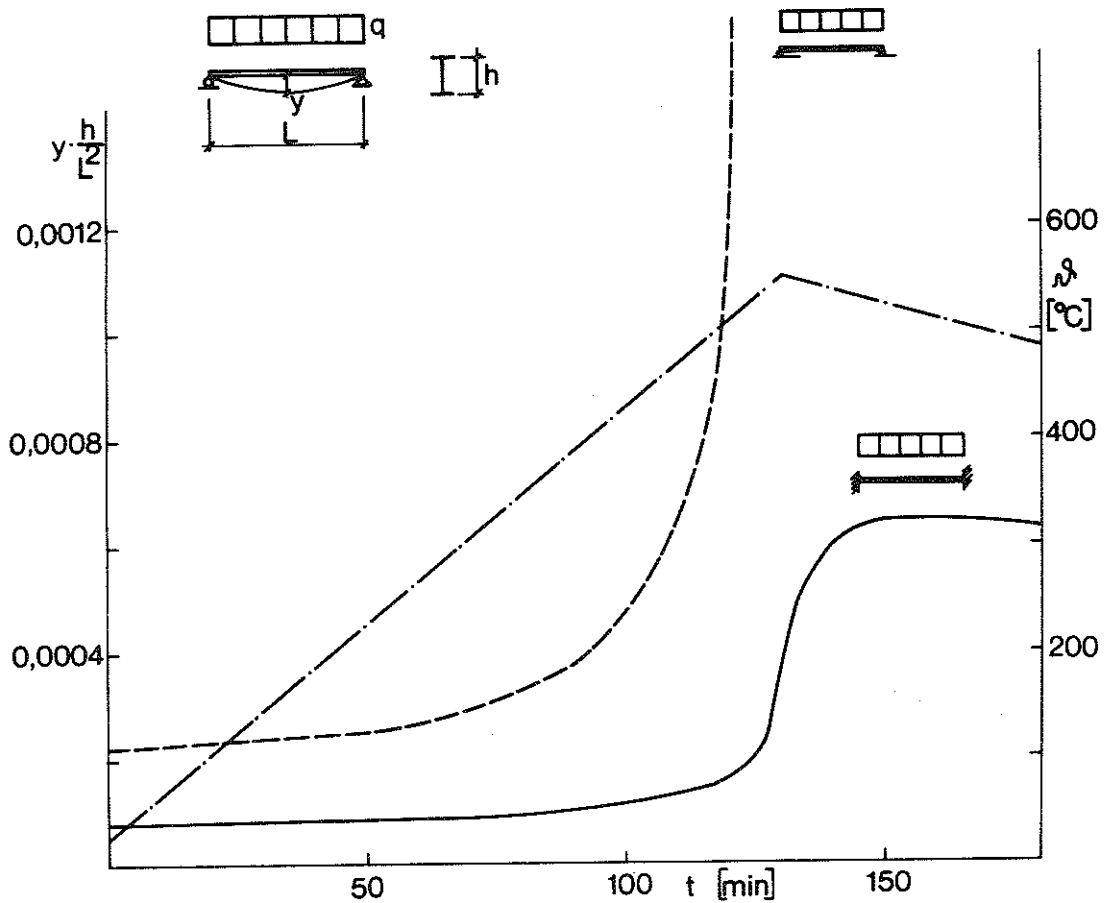


FIG. 24. Comparison of the calculated central deflection y as a function of the time t for a simply supported carbon steel beam (---) and one rigidly restrained at both ends (—), the beams being acted upon by a uniformly distributed load q and exposed to a temperature action, represented by the chain line ($\phi - t$) curve, which is uniform over the whole of the beam. It is assumed that there is no restraint on longitudinal expansion of the beams. The load q is equivalent to 67% of that load in each beam which causes the yield stress to be reached at room temperature at the most highly stressed section.

The calculated central deflection-time ($y - t$) curves for a simply supported beam and for one restrained at both ends, both with a uniformly distributed load and exposed to the same temperature ($\theta - t$) action, are compared in FIG. 24. The load in both cases is 67% of that load q_g which in each beam causes the yield stress to be reached at room temperature in the section which is most highly stressed. It is seen in the Figure that the beam restrained at both ends, in which there is a re-distribution of moments, stands up to the temperature conditions very much better than the simply supported beam.

7.4 Type of loading

The deformation of a beam is dependent on the distribution of curvature along the beam. This implies that the deformation of a steel beam which is exposed to fire will vary in magnitude for different types of loading, even if the maximum moments in the beam are the same for these types of loading. This state of affairs is illustrated in FIG. 25 in which the calculated central deflection-time ($y - t$) curve for a simply supported beam with a uniformly distributed load is compared with that for a simply supported beam with a central concentrated load, both beams being exposed to the action of fire. The temperature-time ($\theta - t$) curve is also shown in the Figure. The maximum moment is the same in both cases, but for a concentrated load the reduction in moment from the mid-section to the supports is larger than for a uniformly distributed load, and the deflection for a concentrated load is therefore less. If there is a linear relationship between stress and strain, the ratio of the deflection for a uniformly distributed load to that for a concentrated load is 1.25. The relationship between stress and strain is not linear at elevated temperatures, however, and this means that the relationship between the deflections at the two types of loading varies with the temperature.

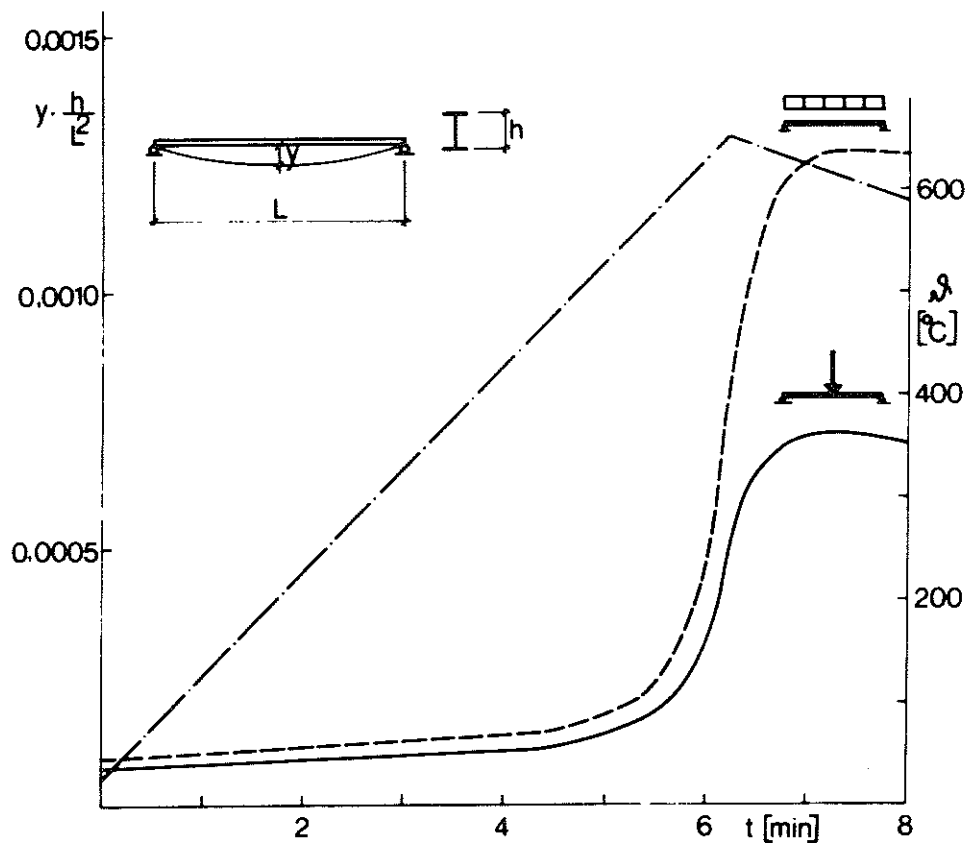


FIG. 25. Comparison, under fire exposure conditions, of the calculated central deflection-time ($y - t$) curve for a simply supported carbon steel beam with a central point load (—) with that for a beam with a uniformly distributed load (---), both beams being exposed to a temperature action, uniform all over the beams, which is represented by the ($\phi - t$) curve shown by a chain line. It is assumed that there is no restraint on longitudinal expansion of the beams. In both cases, the load is 30% of that load which causes the most highly stressed section to yield at room temperature.

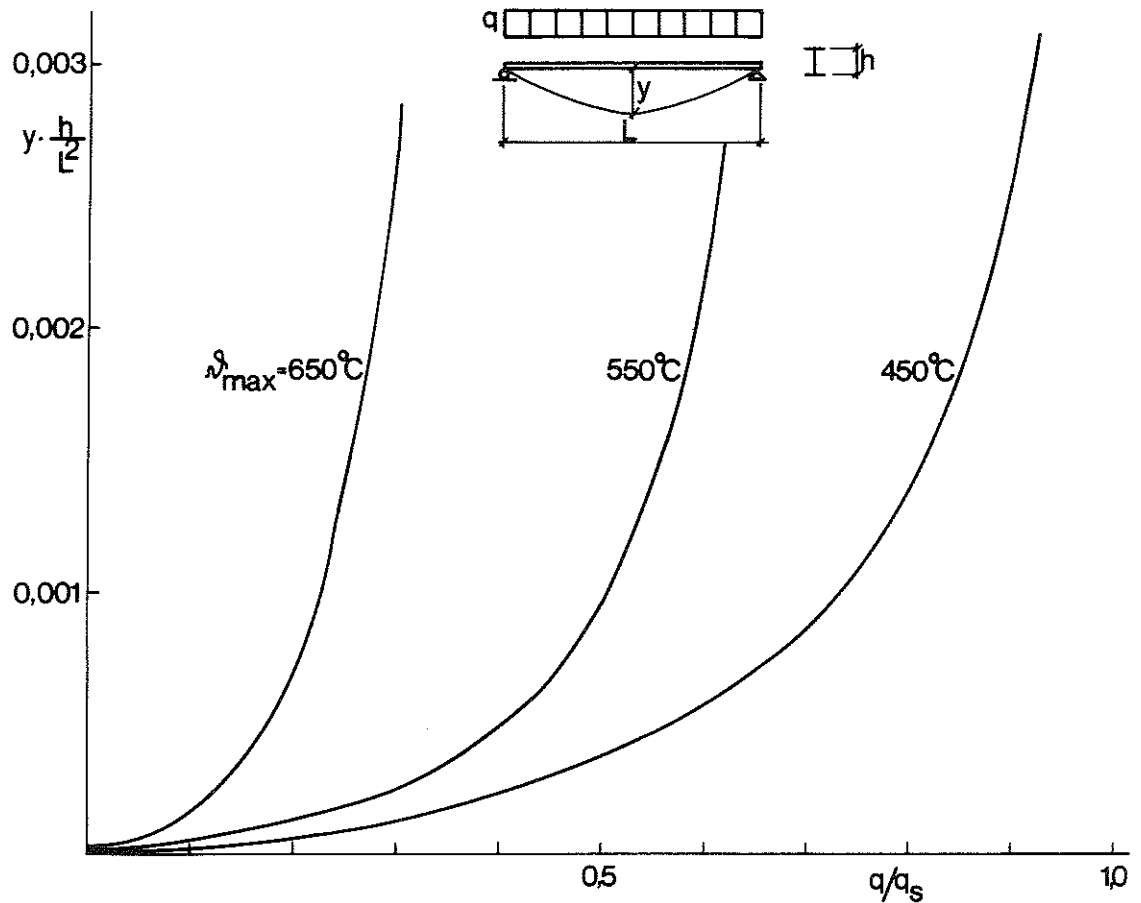


FIG. 26. Calculated central deflection y , under fire exposure conditions, as a function of the load level q/q_s at three different maximum steel temperatures ϑ_{\max} for a simply supported carbon steel beam with a uniformly distributed load.

- q = the load being considered
 q_s = the load which causes the most highly stressed section to yield at room temperature

The calculated deflections which include those during the cooling period, are calculated on the assumption that the rate of heating, which is uniform all over the beam, is $20^\circ\text{C}/\text{min}$ and the rate of cooling is $6.7^\circ\text{C}/\text{min}$. It is also assumed that there is no restraint on longitudinal expansion of the beam.

7.5 Magnitude of load

As will be seen in FIG. 26, the magnitude of the load exerts a great influence on the deformation in a beam exposed to fire. The calculated central deflection y which includes the deflection which occurs during the cooling period is shown for a simply supported beam with a uniformly distributed load as a function of the load level q/q_s , where q denotes the actual load and q_s the load at which the yield stress is reached at room temperature at the section which is most highly stressed. The calculations were performed for three different maximum temperatures ϑ_{\max} at an assumed rate of heating of $20^\circ\text{C}/\text{min}$ and a rate of cooling of $6.7^\circ\text{C}/\text{min}$.

8 CRITICAL LOADS FOR STEEL BEAMS EXPOSED TO THE ACTION OF FIRE AS DETERMINED BY MEANS OF CALCULATED DEFORMATIONS

8.1 Calculation method

By means of systematic calculations with the calculation model - during which the factors listed in the previous Chapter are varied - the load which produces a deflection according to Equation (28) can be determined for different types of loading, different statical systems and different temperature relationships. Due consideration is given in this connection to the argument in Chapter 6 concerning the significance, in conjunction with different statical systems, of the quantities comprised in Equation (28). The critical loads determined in this way are exemplified in FIG. 27 which applies for a simply supported beam of I section loaded by a uniformly distributed load. The Figure gives the value of the coefficient β which is the ratio between the load which produces a deflection according to Equation (28) and the load at which the most highly stressed section reaches the yield stress at room temperature, as a function of the maximum steel temperature ϑ_{\max} attained during the fire for three different rates of heating and cooling. For purposes of comparison, the Figure also shows values of β on the assumption that there is no creep, i.e. the rates of heating and cooling are infinitely great. The coefficient β is calculated on the assumption that the temperature is equal all over the beam and that its longitudinal expansion is not prevented. For a simply supported beam of I section with a uniformly distributed load, as shown in the Figure, the critical load is

$$q_{\text{cr}} = \beta \cdot \frac{8 \cdot W \cdot \sigma_s}{L^2} \quad (30)$$

where q_{cr} = critical load (kgf/cm)
 β = coefficient according to FIG. 27
 W = elastic modulus of section (cm³)
 σ_s = yield stress of the material at room temperature (kgf/cm²)
 L = length of beam (cm)

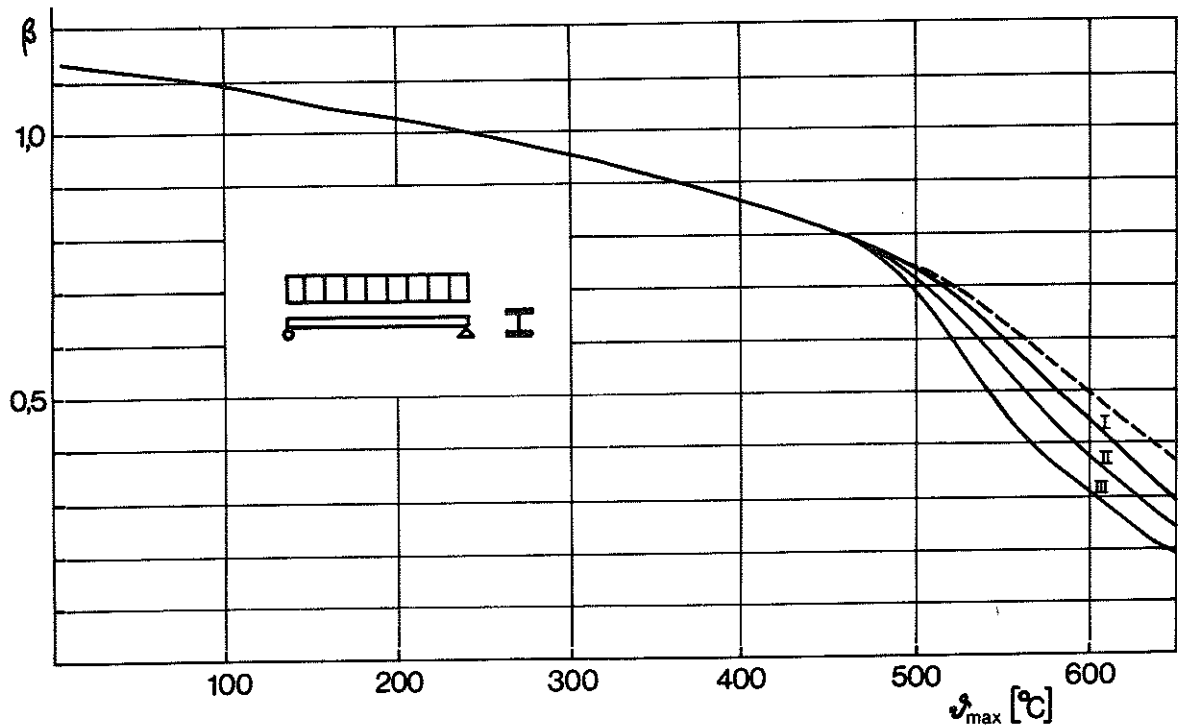


FIG. 27. The coefficient β for calculation, according to Equation (30), of the critical load q_{cr} for a simply supported I section beam of carbon steel with a uniformly distributed load, as a function of the maximum steel temperature δ_{\max} for three different rates of heating and cooling (I, II, III). The value of β for infinitely fast rates of heating and cooling is also given for purposes of comparison.

| <u>Curve</u> | <u>Rate of heating ($^{\circ}\text{C}/\text{min}$)</u> | <u>Rate of cooling ($^{\circ}\text{C}/\text{min}$)</u> |
|--------------|---|---|
| I | 100 | 33.3 |
| II | 20 | 6.67 |
| III | 4 | 1.33 |
| --- | | |

It is assumed that the temperature is the same all over the beam and that there is no restraint on longitudinal expansion of the beam.

Section 8.2 discusses diagrams constructed in the same way for determination of the critical load for a number of types of loading and statical systems.

In FIG. 27 and in the diagrams in Section 8.2, the coefficient β is the ratio between the load which produces a deflection according to the deflection criterion Equation (28) and the load which causes the most highly stressed section to reach the yield stress at room temperature. Another possibility would be to make β represent the relation between the load which causes a deflection according to Eq. (28) and the limiting load of the beam at room temperature, as calculated by the limit state theory. In this way, initial values of the β curves at a temperature of 0°C would always be unity irrespective of the type of loading, statical system or shape of cross section. The main reason why the former method has been chosen is that design of steel beams at room temperature conditions is at present generally based on the elastic theory. By using in the diagrams a value of β equal to the extreme fibre stress at the most highly stressed section according to the elastic theory, divided by the yield stress of the material at room temperature, the maximum temperature which the beam in question can withstand without the deflection exceeding that according to Equation (28), can be directly determined.

8.2 Diagrams for determination of the critical load for certain given conditions

The diagrams for determination of the critical loads of steel beams exposed to fire, which are discussed in this Section and shown in FIG. 30, are based on the conditions given in the subsections a) - f) below. The effect on the critical load when certain conditions are different from those below is discussed in Section 8.3.

a) Type of load, statical system

The type of load and the statical system are shown in the diagrams. See Subsection 8.3.1 with regard to types of loading which are not included. See Subsection 8.3.2 with regard to continuous beams.

b) Grade of steel

The diagrams can be used for structural steels to Swedish Standards Steel 1311, 1312, 1411, 1412, 1413, 1414 or for steels of similar composition and strength. See Subsection 8.3.3 with regard to steels with compositions or strengths which show major deviations from these steels.

c) Shape of cross section

The diagrams apply to I beams of constant cross section. See Subsection 8.3.4 with regard to beams of different cross sections and Subsection 8.3.5 with regard to beams of variable cross section. The diagrams are further valid only on condition that there is no risk of instability failure (see Subsections 8.3.4 and 8.3.5).

d) Rates of heating and cooling

The diagrams are based on a steel temperature relationship which entails linear increase in temperature from room temperature to the appropriate maximum temperature ϑ_{\max} and subsequent linear cooling at a rate which is one-third of the rate of heating. The values of β are shown for three different rates of heating and cooling, viz. $100^{\circ}\text{C}/\text{min}$ and $33.3^{\circ}\text{C}/\text{min}$, $20^{\circ}\text{C}/\text{min}$ and $6.67^{\circ}\text{C}/\text{min}$, and $4^{\circ}\text{C}/\text{min}$ and $1.33^{\circ}\text{C}/\text{min}$. It is only at temperatures in excess of approximately 450°C , where creep strain begins to be felt, that the rates of heating and cooling have a noticeable influence on the critical load. If the maximum steel temperature ϑ_{\max} , in the course of practical design, is determined by calculation of the entire steel temperature process (4, 18), the appropriate rate of heating will also be obtained. If, on the other hand, the max. steel temperature ϑ_{\max} is determined from diagrams presented in (5) or (18) which give ϑ_{\max} directly as a function, inter alia, of the fire load and the opening factor of the fire cell, the rate of heating must be estimated separately. This can be done with the help of FIG. 28 which gives the average rate of heating of the beam as a function of the fire load q for different values of the opening factor $A\sqrt{h}/A_t$ and the maximum steel temperature ϑ_{\max} . The rates of heating for values of the opening factor and maximum temperatures other than those in the Figure may be estimated by means of linear interpolation.

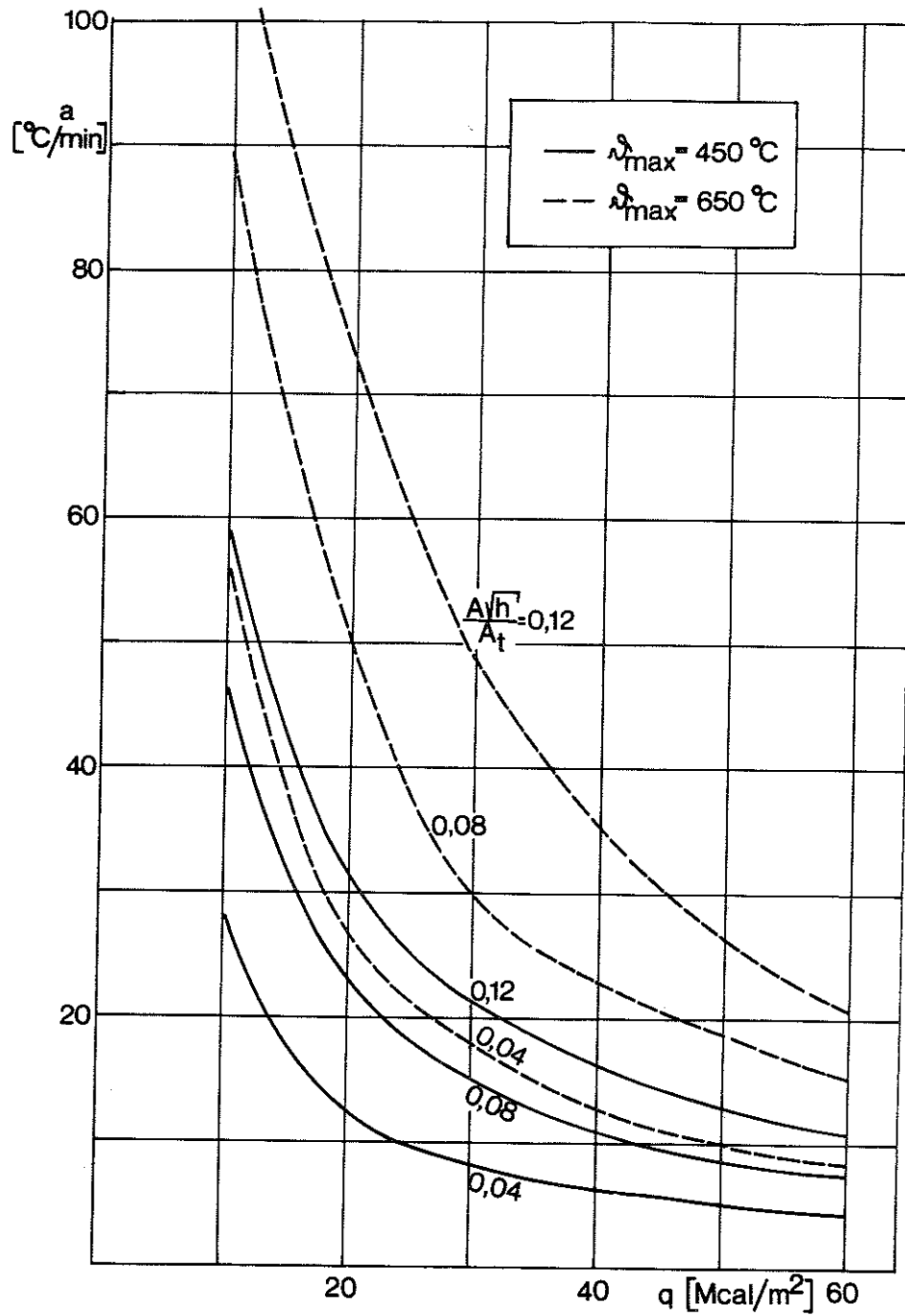


FIG. 28. Average rate of heating a as a function of the fire load q for different values of the opening factor $\frac{\sqrt{h}}{A_t}$ of the fire cell and for different maximum steel temperatures ϕ_{max} .

A = total opening area of the fire cell (m²)

h = mean value of the vertical extents of the openings, weighted in view of their sizes (m)

A_t = total surface area of the fire cell (m²).

The curves in FIG. 28 have been determined on the basis of the following considerations. The gas temperature-time ($\theta - t$) curve for a fire cell, for which the thermal properties of the structures bounding the fire cell are given, is determined by the magnitudes of the fire load and the opening factor. The gas temperature-time ($\theta - t$) curve for a fire cell is shown schematically by the full line in FIG. 29. The temperature-time process in an uninsulated steel structure, for a given gas temperature development, is determined by the ratio between the area of the steel section which is exposed to the fire and the volume of the section. The dashed line in FIG. 29 shows schematically the steel temperature development for an uninsulated steel structure. The point of intersection between this curve and the gas temperature curve gives the maximum temperature θ_{\max} in the steel and the time t_{\max} at which this temperature is reached. If the maximum temperature θ_{\max} of an uninsulated steel structure is thus known, the time t_{\max} corresponding to this temperature can be determined, since the gas temperature-time curve is known. The average rate of heating is obtained by division of θ_{\max} by t_{\max} .

For an insulated steel structure at a given gas temperature development, the steel temperature development depends on the thermal resistance and heat capacity of the insulation and on the ratio between the mean surface area of the insulation and the volume of the steel section. The steel temperature curve for an insulated steel structure is shown schematically by the chain line in FIG. 29. Owing to the effect of the heat capacity of the insulation, the maximum steel temperature in this case is not given by the point of intersection between the steel temperature and gas temperature curves. Since the heat capacity of commonly used insulation materials is normally negligible in comparison with that of the steel section, the difference in time between t_{\max} and the time at which the steel temperature and gas temperature curves intersect is usually very small in relation to the time t_{\max} . In view of this and the fact that, with regard to the relevant circumstances, the average rate of heating can only be estimated roughly, FIG. 28 can be used for insulated steel structures also. As a rule, the maximum steel temperature is also calculated without consideration of the heat capacity of the

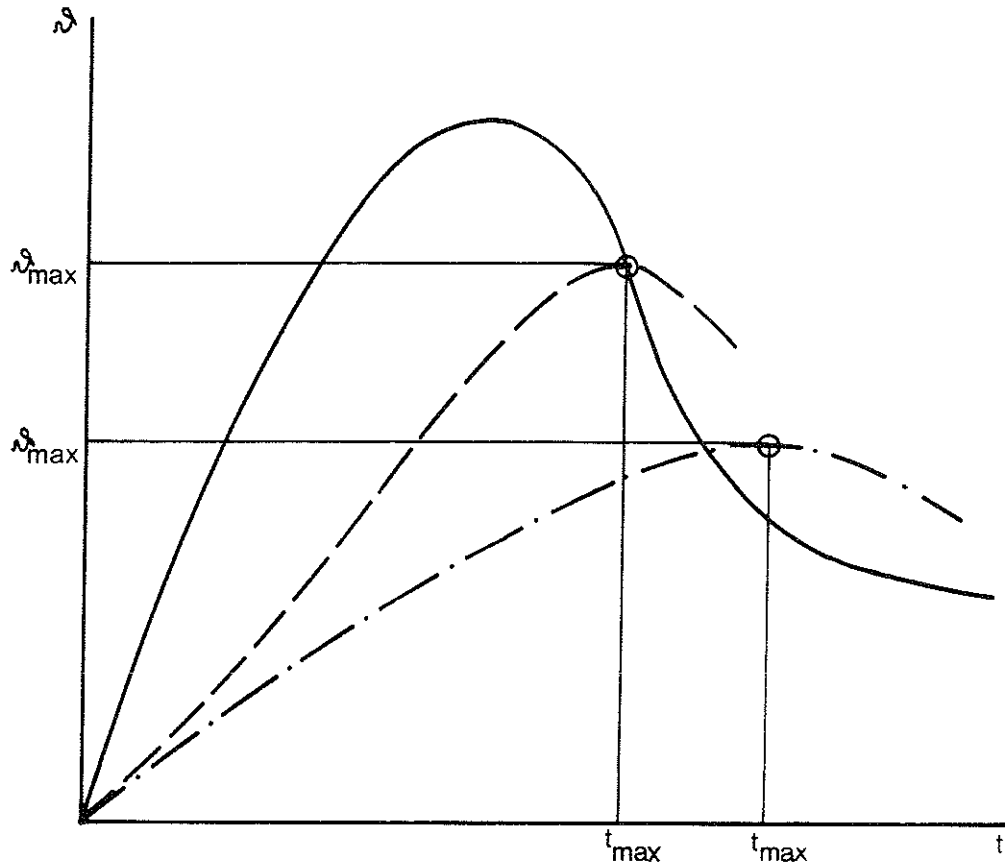


FIG. 29. Schematic temperature-time ($\theta - t$) curves.

- Gas temperature development in a fire cell
- Steel temperature development in an uninsulated steel structure
- . - Steel temperature development in an insulated steel structure

insulation. The calculated maximum temperature is therefore a little above the actual maximum temperature, which, from the safety point of view, more than makes up for any errors in the estimated rate of heating.

With regard to ratios other than 3:1 between the rates of heating and cooling, see Subsection 8.3.6.

e) Temperature distribution along and across the beam

It is assumed that the temperature is the same in all parts of the beam. See Subsection 8.3.7 with regard to variations in temperature across the cross section of the beam and Subsection 8.3.8 with regard to variations in temperature along the beam.

f) Longitudinal expansion

The diagrams assume that longitudinal expansion of the beam is not prevented. See Subsection 8.3.9 with regard to a restraint on longitudinal expansion.

8.3 Estimation of critical load under conditions different from those in Section 8.2

8.3.1 Other types of loading

The deflection becomes less and the values of β therefore become larger, the smaller the moments in different cross sections of a beam exposed to fire are in relation to the maximum moment in the beam. This is also evident from FIG. 30. The values of β are for instance higher for a simply supported beam loaded with a point load than for a simply supported beam in which the bending moment is constant along the beam. The latter type of loading produces the lowest values of β of all types of loading.

In conjunction with types of loading other than those given in FIG. 30, the value of β applicable for a constant bending moment and the temperature in question can therefore be used for an estimation, on the safe side, of the critical load. This value

FIGs. 30 (a-1). The coefficient β - as a function of the maximum steel temperature ϑ_{\max} for different rates of heating and cooling (I, II, III) - for determination of the critical load in steel beams under fire exposure conditions. Conditions as enumerated in Subsections a) - f) in 8.2.

| Curve | Rate of heating ($^{\circ}\text{C}/\text{min}$) | Rate of cooling ($^{\circ}\text{C}/\text{min}$) |
|-------|---|---|
| I | 100 | 33.3 |
| II | 20 | 6.67 |
| III | 4 | 1.33 |

Symbols

$M_{\text{cr}}, q_{\text{cr}}, P_{\text{cr}}$ = critical load (kgf cm), (kgf/cm), (kgf)
 L = length of beam (cm)
 W = elastic modulus of section (cm^3)
 σ_s = yield stress of the material at room temperature (kgf/cm^2)

It is evident from the diagrams that the values of β at temperatures within the range $100\text{-}400^{\circ}\text{C}$ are in some cases higher than those at room temperature. This implies that the load at which a deflection according to Equation (28) is reached in these cases is higher than the load for which the yield point will be reached at room temperature at the most highly stressed cross section. This is explained by the fact that, in the temperature range $100\text{-}400^{\circ}\text{C}$, the stresses which correspond to the stress-strain curves determined by means of tensile tests at elevated temperatures exceed the corresponding stresses at room temperature for sufficiently large values of the strain, and the fact that the strain required in order that a deformation according to Equation (28) should be reached varies according to the type of loading and the statical system. The influence of some other factors on the appearance of the β curves is discussed in section 8.3.

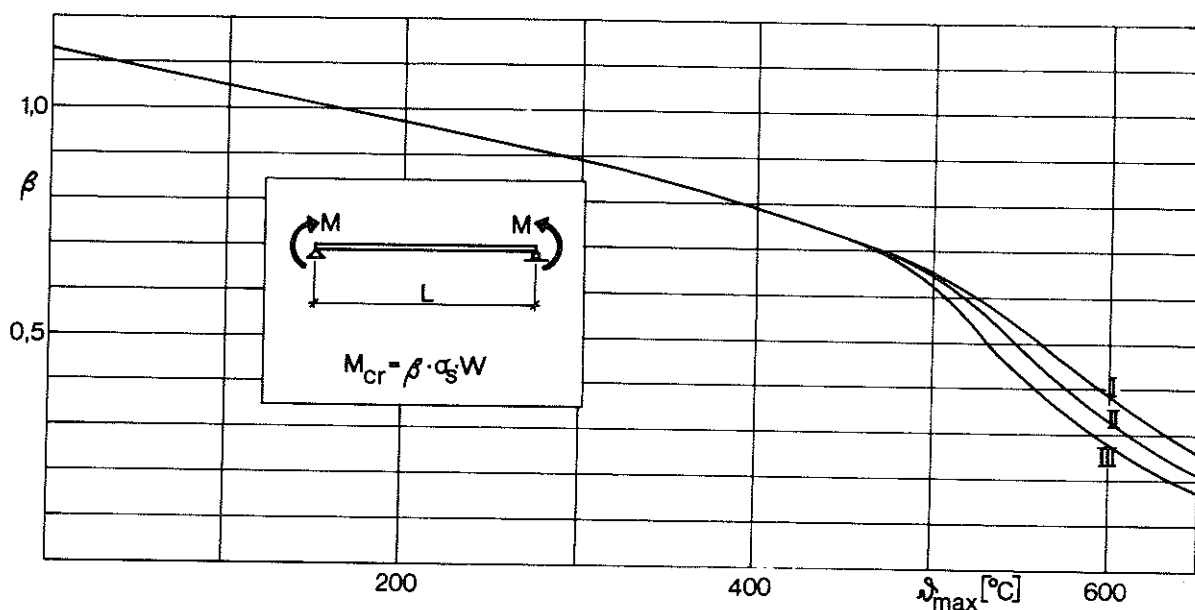


Fig. 30 a.

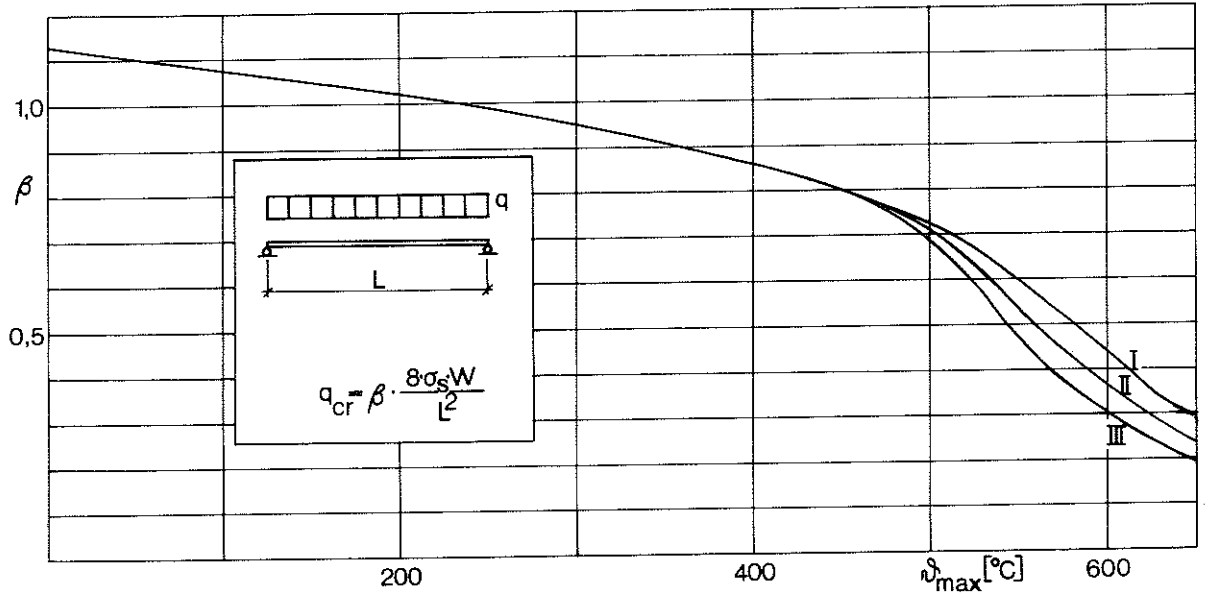


FIG. 30 b.

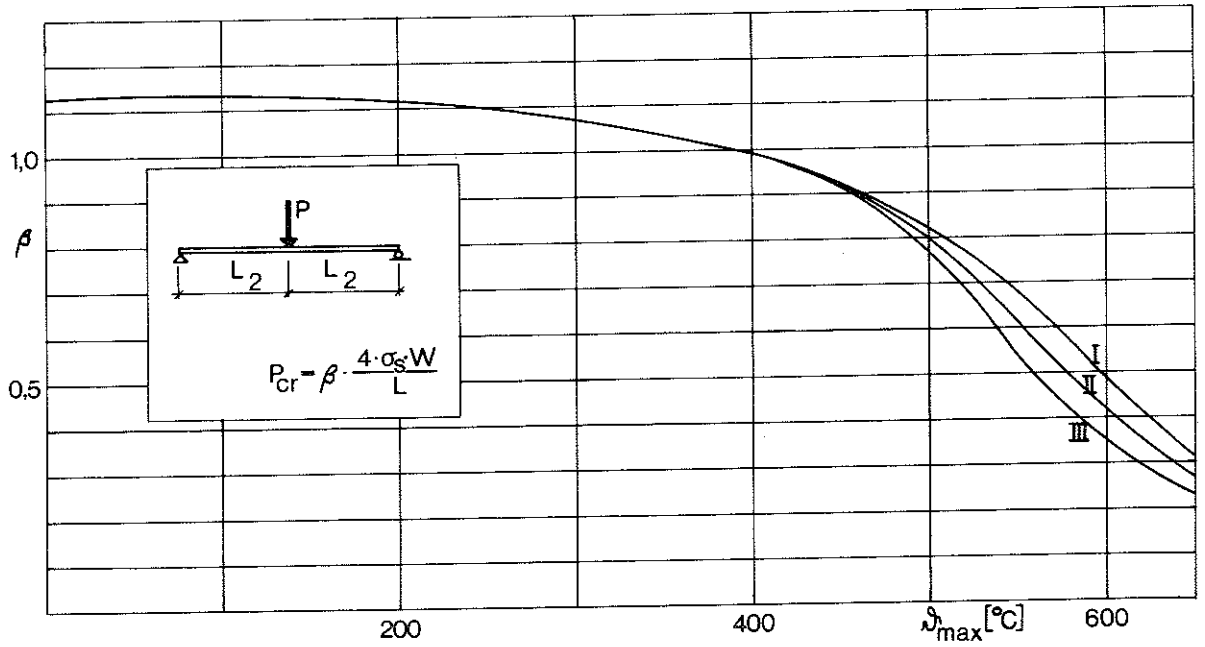


FIG. 30 c.

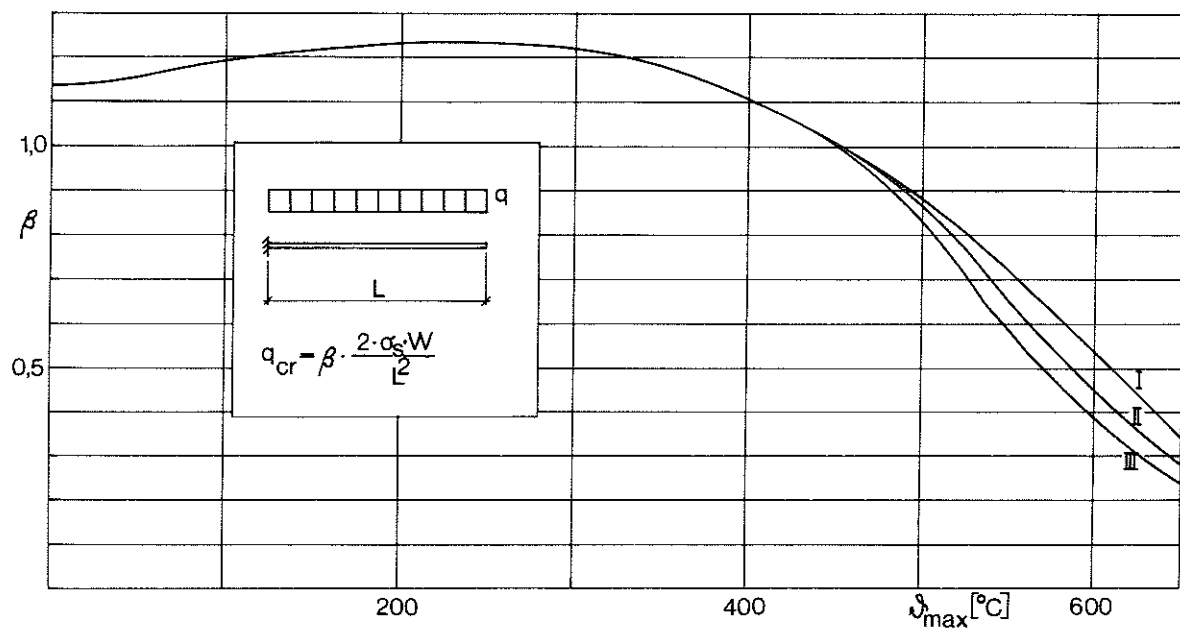


FIG. 30 d.

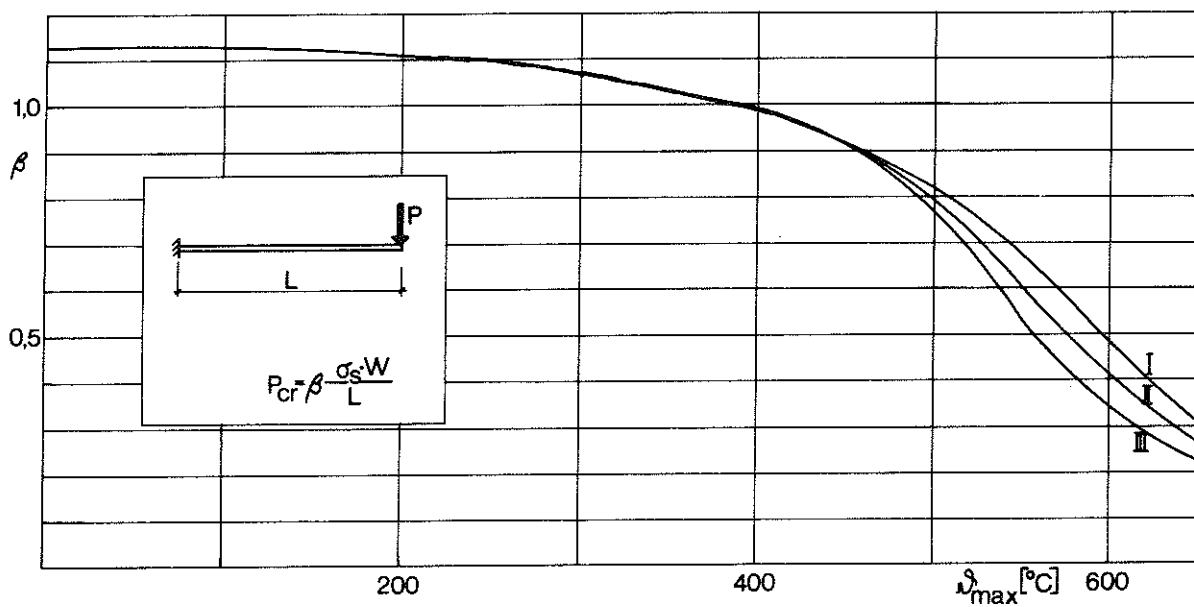


FIG. 30 e.

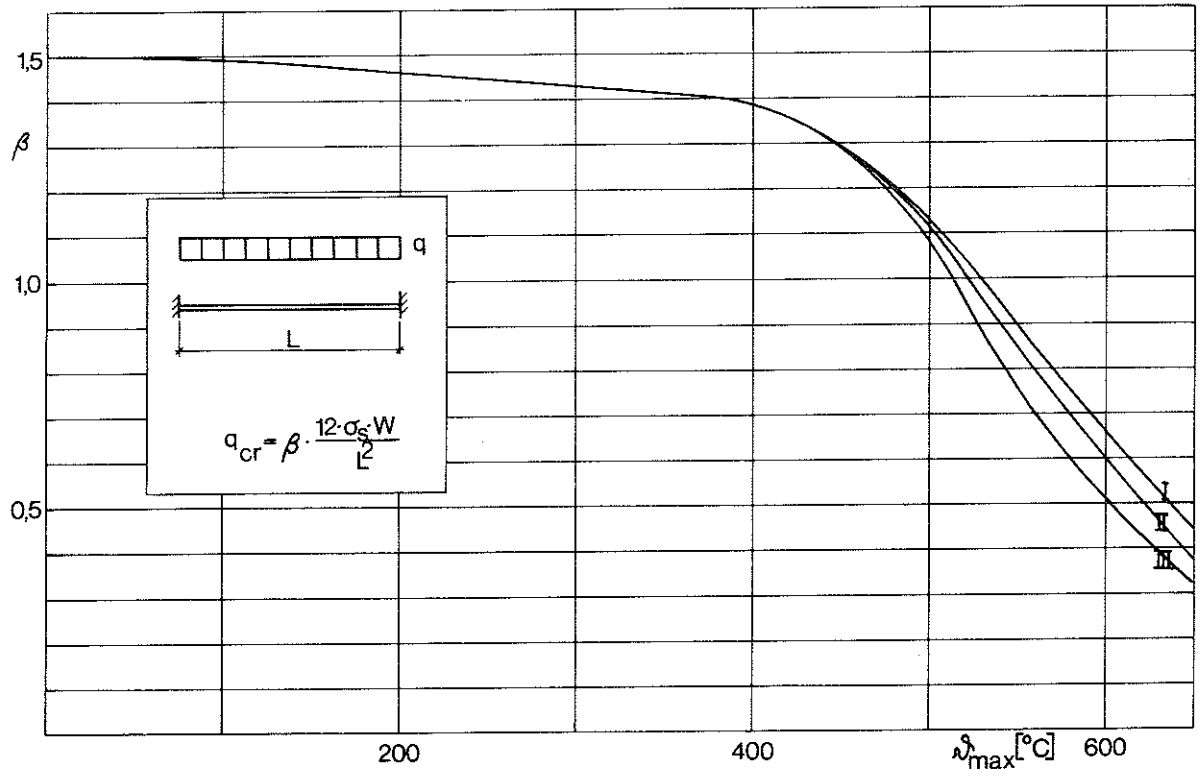


FIG. 30 f.

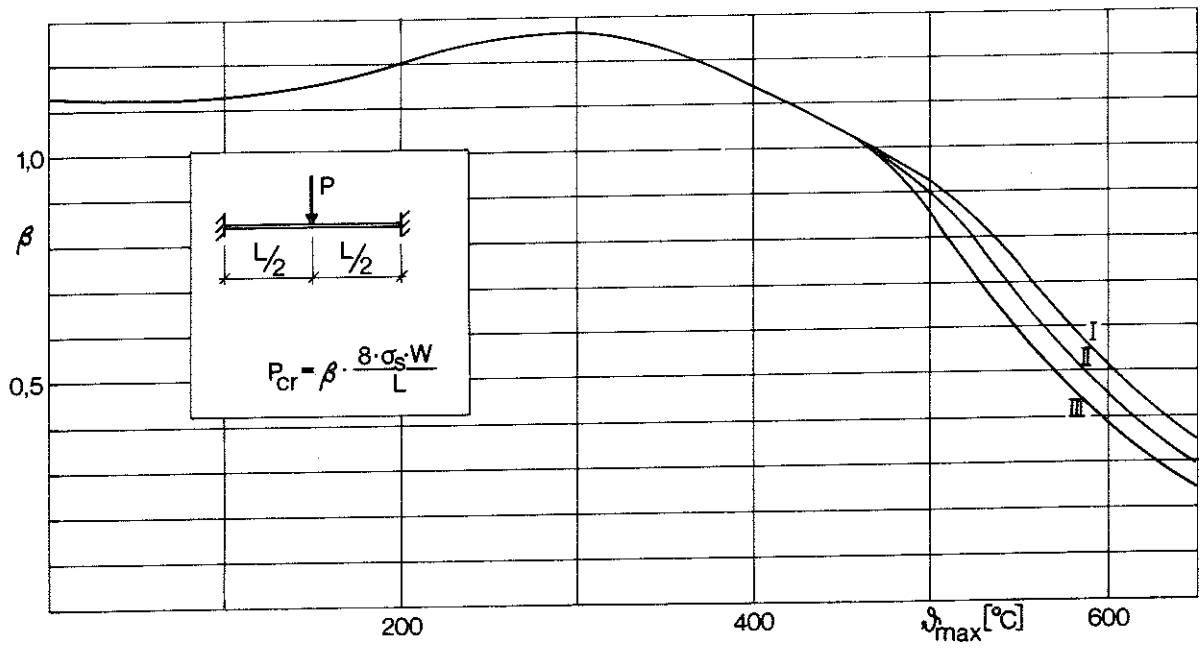


FIG. 30 g.

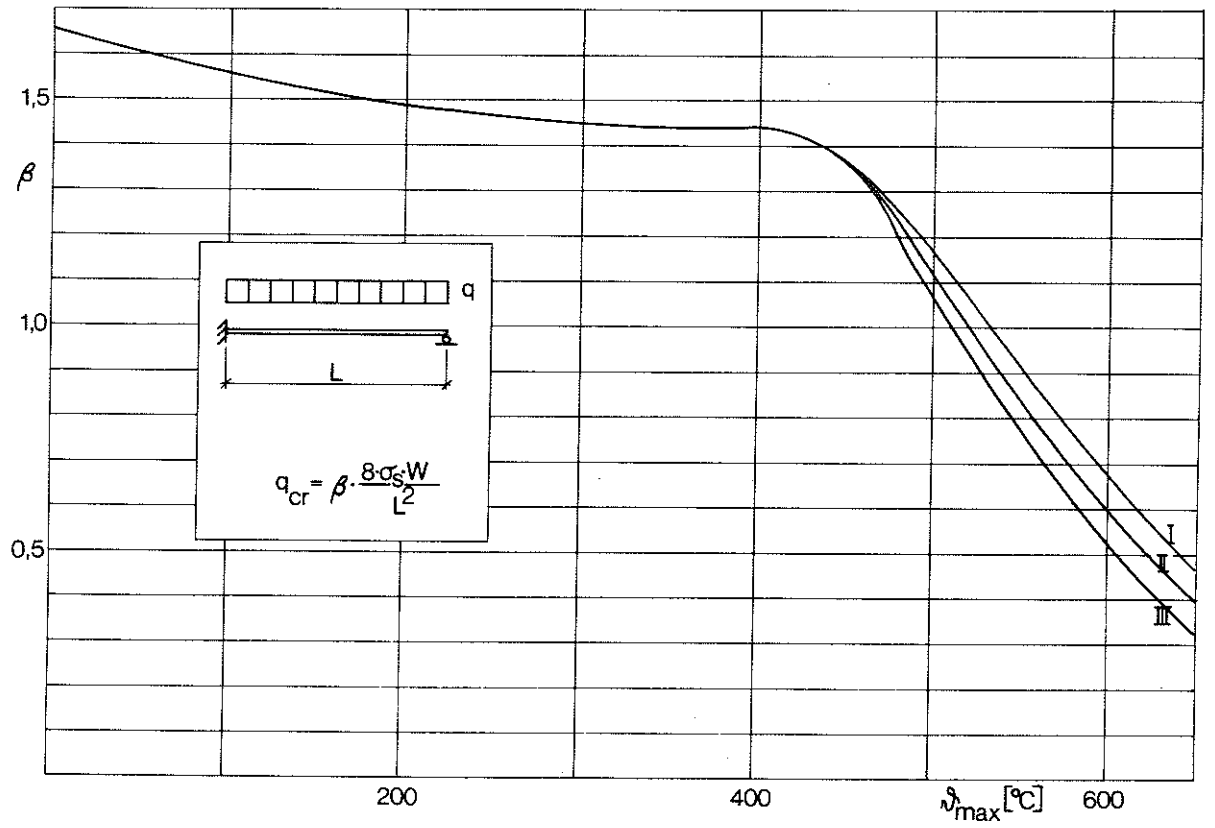


FIG. 30 h.

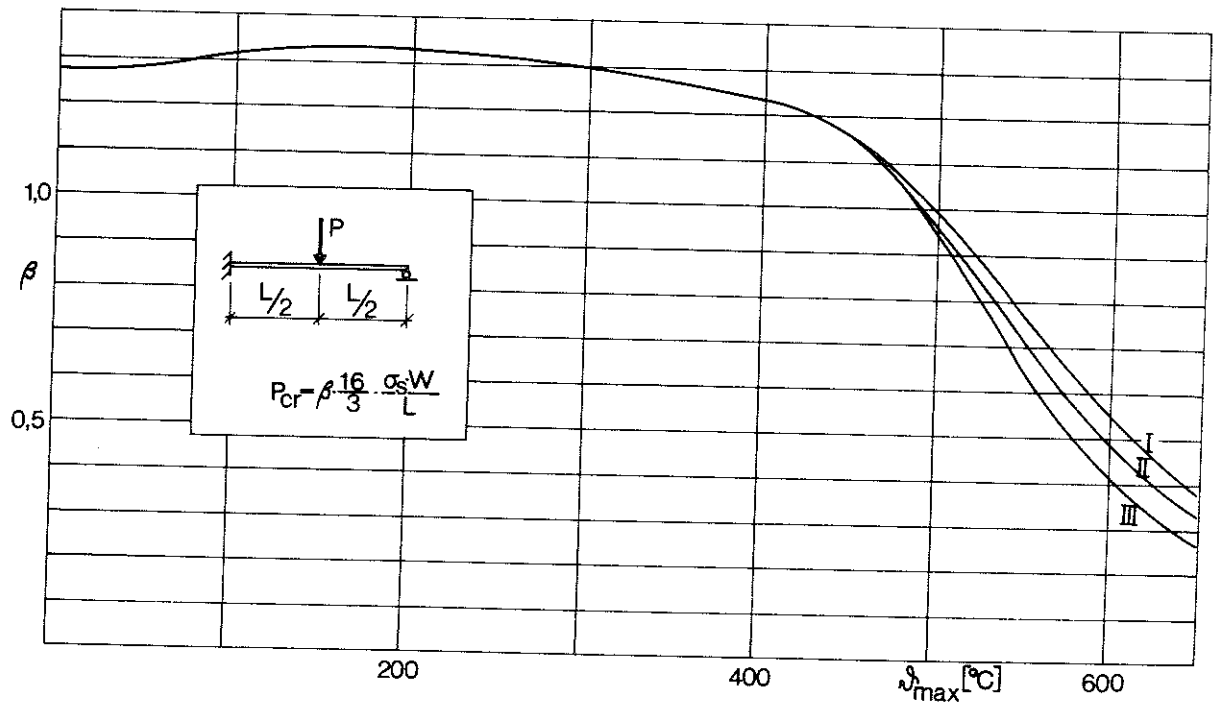


FIG. 30 i.

of β is then to be multiplied by that load which, for the type of loading in question, produces incipient yield at room temperature at the section which is most highly stressed.

8.3.2 Continuous beams

It is seen in FIGs. 30 f, g, h and i that the values of β for beams with end restraint at one or both ends are about the same at the same type of loading, although the values of β are somewhat higher when the beam is restrained only at one end. The reason for this is that moment re-distribution occurs more easily in this case. The relationship between the restraining moment M according to the elastic theory and the moment M_g according to the limit state theory provides a measure of the theoretical moment re-distribution possibilities.

For a beam with a UDL,

$$\begin{aligned} \text{Restrained at both ends:} \quad M &= \frac{qL^2}{12} & M_g &= \frac{qL^2}{16} \\ M/M_g &= 1.33 \end{aligned}$$

$$\begin{aligned} \text{Restrained at one end:} \quad M &= \frac{qL^2}{8} & M_g &= \frac{qL^2}{11.7} \\ M/M_g &= 1.47 \end{aligned}$$

For a beam with a central point load,

$$\begin{aligned} \text{Restrained at both ends:} \quad M &= \frac{PL}{8} & M_g &= \frac{PL}{8} \\ M/M_g &= 1.0 \end{aligned}$$

$$\begin{aligned} \text{Restrained at one end:} \quad M &= \frac{3PL}{16} & M_g &= \frac{PL}{6} \\ M/M_g &= 1.12 \end{aligned}$$

For a continuous beam, the magnitude of the support moment calculated by the elastic theory is usually between those for beams restrained at one and both ends respectively. Estimation, on the safe side, of the critical load for a continuous beam of

constant I section which is loaded with a uniformly distributed load or a central concentrated load can thus be based on the values of β for a beam restrained at both ends which is loaded with a UDL or a central point load. The value of β corresponding to the actual temperature and load - uniformly distributed or point load - is then to be multiplied by that load which, at room temperature, causes incipient yield in the most highly stressed section of the continuous beam.

8.3.3 Other grades of steel

The diagrams in FIG. 30 have been constructed on the basis of material data determined by means of tensile tests at elevated temperatures and by means of creep tests, on test pieces taken from the steel beams used in the fire tests described in Section 5.1. (6). The material in these beams was Steel 1411 according to SIS 14 14 11. Critical loads for steel beams which are exposed to the action of fire have however also been calculated with the model on the basis of material data (3) for an American steel A 36. With regard to its material analysis and strength properties, this steel corresponds to Steel 1412 according to SIS 14 14 12. The creep parameters and stress-strain relations at different temperatures, which are given in (3) for the A36 steel, indicate the differences from the corresponding data for the 1411 steel. The fact that there is good agreement between the β values for these steels, i.e. between the ratios of the critical load on exposure to fire to the load at which the most highly stressed section yields at room temperature, shows however that the strength and deformation properties of the two steels are similar under fire exposure conditions. The calculated values of β for the two steels are compared in FIGs. 31 and 32, for simply supported beams and beams restrained at both ends, for a constant I section and a uniformly distributed load.

Reference (12) gives an account of an experimental and theoretical study of the creep properties of different structural steels under fire exposure conditions. In addition to the A36 and 1411 steels mentioned above, the carbon steels comprised in the study were two 1312 steels to SIS 14 13 12. The theoretically calculated

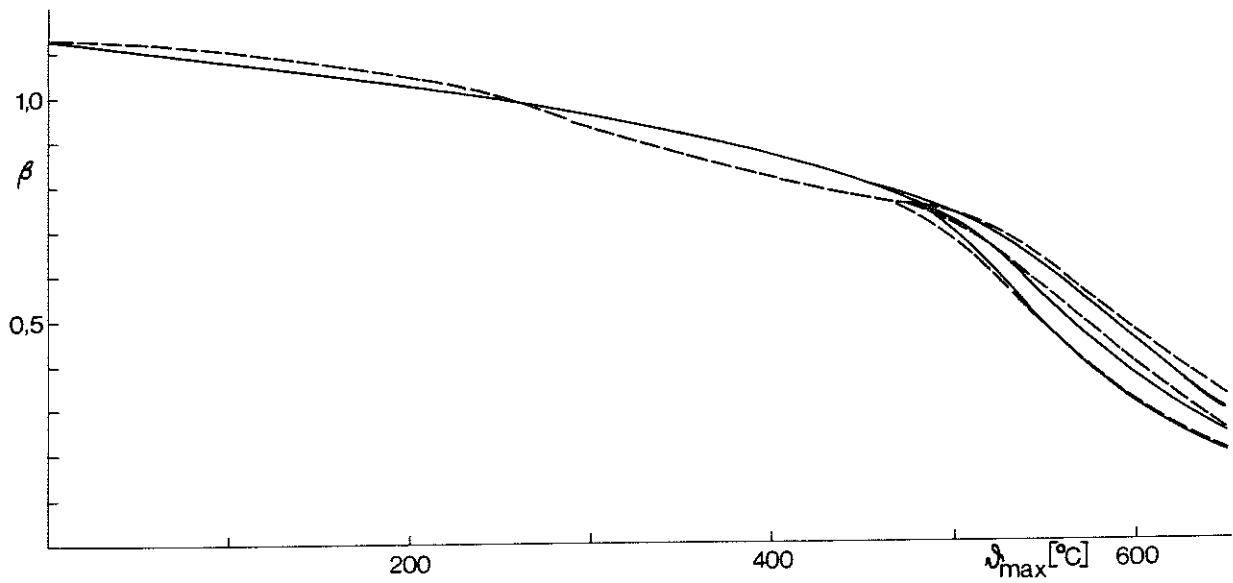


FIG. 31. Comparison of calculated values of β for a simply supported beam of constant I section with uniformly distributed load, the materials being Steel A36 (---) and Steel 1411 (—).

It is assumed that longitudinal expansion of the beams is not restrained and that the temperature is the same all over the beams.

The different branches of the curve correspond to rates of heating and cooling according to curves I, II and III in FIG. 30.

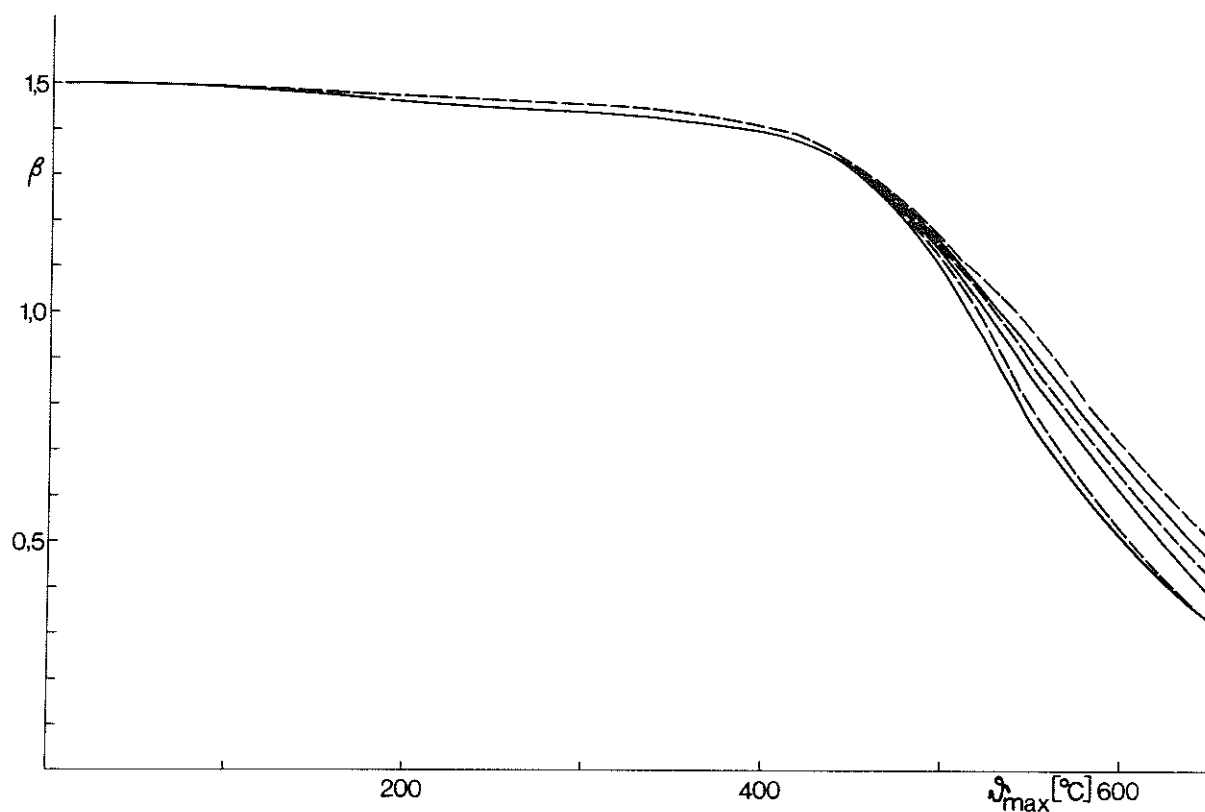


FIG. 32. Comparison of calculated values of β for a beam of constant I section with a uniformly distributed load which is rigidly restrained at both ends, the materials being Steel A36 (---) and Steel 1411 (—).

It is assumed that longitudinal expansion of the beams is not restrained and that the temperature is the same all over the beams.

The different branches of the curve correspond to rates of heating and cooling according to curves I, II and III in FIG. 30.

creep processes for these four steels, which were based on the creep parameters determined for each steel, were found to be in very good agreement at stresses of the same magnitude in relation to the yield stress of the steels at room temperature. This fact and the good agreement between the calculated values of β for the A36 steel and the 1411 steel (FIGs. 31 and 32) show that the diagrams in FIG. 30 which were constructed on the basis of material data for the 1411 steel can be used for all steels with analyses and strengths similar to those of a 1411 steel, i.e. for all ordinary carbon steels. The differences in the yield stresses of the steels are taken into consideration by means of the equations given in the diagrams for calculation of the critical loads. Most often, however, the actual yield stress of the material in a steel beam is unknown, and estimation of the load carrying capacity in the event of fire must in such cases be based on the nominal yield stress of the material. In most cases, this entails a not inconsiderable underestimation of the real load carrying capacity, since, statistically, the actual yield stress exceeds the nominal value in 95% of the cases.

The study reported in (12) also comprised two carbon-manganese steels corresponding to Steel 2172 according to SIS 14 21 72 and also two grain-refined steels with a basic analysis the same as that of the carbon-manganese steels. The theoretically calculated creep processes for these different steels, which were based on the creep parameters determined for each steel, were found to be in good agreement within each steel group at stresses of the same magnitude in relation to the yield stresses of these steels at room temperature. In addition, the creep processes in the grain-refined steels were largely the same as those in the carbon steels. This indicates that the diagrams in FIG. 30 can be used, with sufficient accuracy, also for the estimation of the critical loads in beams exposed to fire which consist of grain-refined material of the same basic analysis as an ordinary carbon-manganese steel. On the other hand, however, the carbon-manganese steels which had not received grain refining treatment exhibited an appreciably lower tendency to creep than the carbon steels and the grain-refined steels. Systematic calculations of the critical loads in beams exposed to the action of fire were also carried out, therefore,

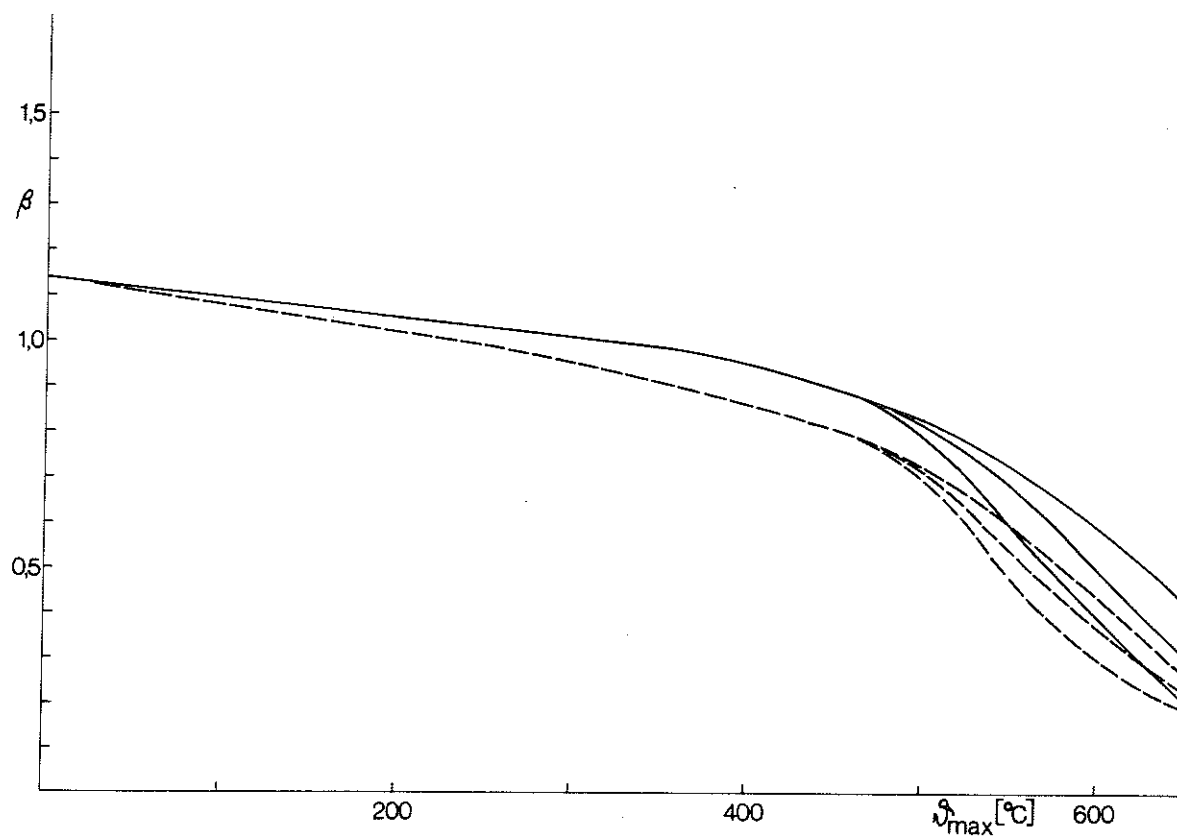


FIG. 33. Comparison of values of β for a simply supported beam of constant I section with uniformly distributed load, the materials being carbon-manganese steel (—) and carbon steel (---). It is assumed in both cases that the temperature is the same all over the beam and that longitudinal expansion is not restrained.

The different branches of the curve correspond to rates of heating and cooling according to curves I, II and III in FIG. 30.

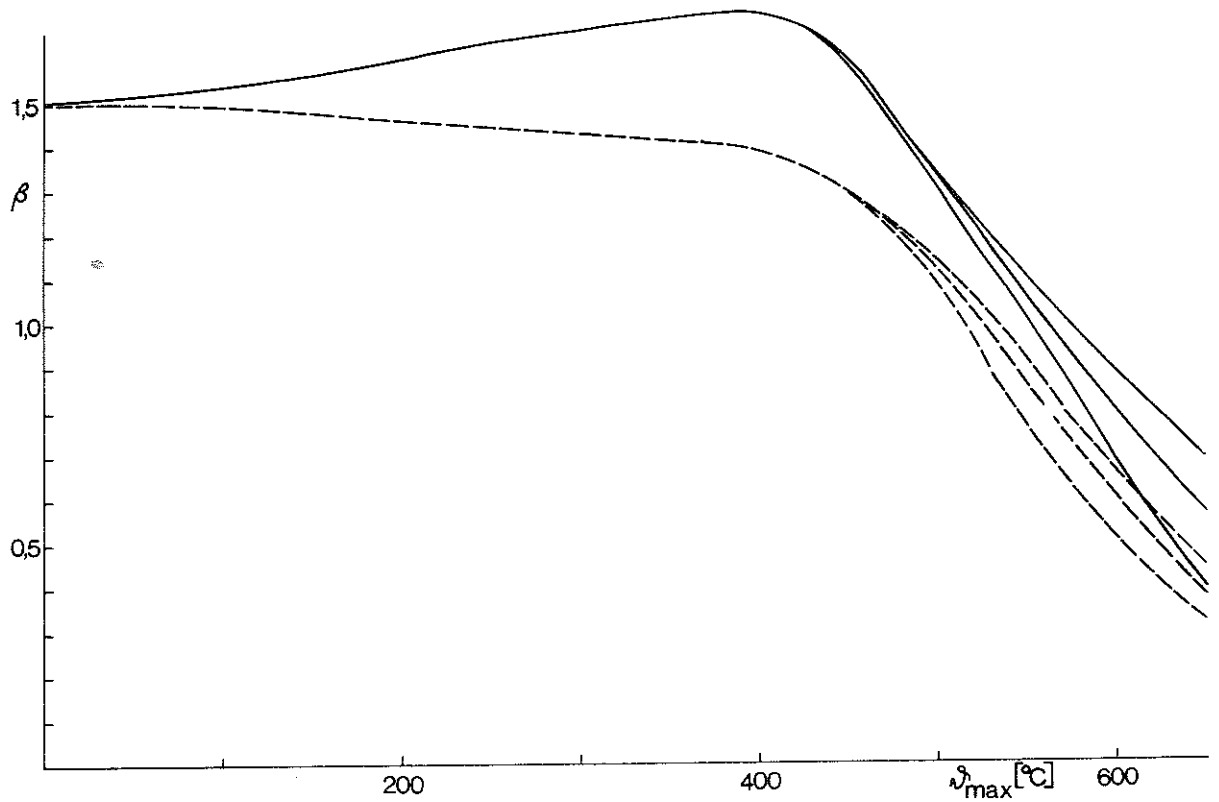


FIG. 34. Comparison of values of β for a beam of constant I section with a uniformly distributed load which is rigidly restrained at both ends, the materials being carbon-manganese steel (—) and carbon steel (---). It is assumed in both cases that the temperature is the same all over the beam and that longitudinal expansion is not restrained.

The different branches of the curve correspond to rates of heating and cooling according to curves I, II and III in FIG. 30.

on the basis of the material data presented in (3), for one of the carbon-manganese steels comprised in the above study. The calculations were confined to simply supported beams and beams restrained at both ends, of constant I sections and loaded with a uniformly distributed load. The results are shown in FIGs. 33 and 34 in which the values of β for beams of carbon-manganese steel and carbon steel are compared. It is evident from the Figures that the values of β are consistently higher for beams of carbon-manganese steel than those of carbon steel. It is also evident from FIG. 34 that the value of β for the restrained beam of carbon-manganese steel has a maximum at about 400°C , while there is no corresponding maximum for the beam of carbon steel. This may be explained as follows. Within the temperature range of approx. $100-450^{\circ}\text{C}$, at sufficiently large strains, the stresses corresponding to the stress-strain curves drawn on the basis of tensile tests at elevated temperatures exceed the corresponding stresses at room temperature. This applies to both carbon-manganese steel and carbon steel, but the strains which cause the stresses to become higher are smaller in the carbon-manganese steel than in the carbon steel. The strains required in order that the restrained beam should attain a deflection according to Equation (28) are evidently sufficiently large at some sections for the above effect to be felt in beams of carbon-manganese steel, but are not sufficiently large for this to be manifested in beams of carbon steel. As will be seen in FIG. 33, β has no maximum at elevated temperatures in any of the steels in the simply supported beam. The strains required in order that the simply supported beam should attain a deflection according to Equation (28) are evidently less than the strains required in the carbon-manganese steel in order that the stresses at elevated temperatures should exceed those according to the stress-strain curve determined at room temperature.

8.3.4 Different shape of cross section

During deformation of a beam which is exposed to the action of fire, there is a redistribution of stresses over the cross section as a result of plastic strains (6, 11). The stresses at the extreme fibres become smaller while those inside the section increase. The

decrease in the extreme fibre stresses limits deflection of the beam, and the greater this reduction in the extreme stresses, the smaller the deflection will be. One of the factors which influences the extent to which the extreme stresses are reduced is the shape of the cross section. The greater the ratio of the plastic section modulus W_p of the cross section to the elastic section modulus W , the greater the reduction in extreme fibre stresses during a fire. Since estimation of the critical load is based on the deflection, the increase in critical load is a function of the increase in the value of W_p/W . According to the limit state theory, which assumes that the most highly stressed cross section of the beam is fully plastic, the load carrying capacity is directly proportional to the value of W_p/W . For ordinary I sections, the value of W_p/W is 1.13-1.15, and for rectangular sections it is 1.50. According to the limit state theory, therefore, the ratio of the load carrying capacity of a beam of rectangular section to that of a beam of I section is 1.31-1.33, on the assumption that the elastic section moduli are the same in both sections. During a fire, however, the deformations of a beam must be very large before the most highly stressed section becomes fully plastic, the reason being the very softly rounded shapes of the stress-strain curves at elevated temperatures. At a deflection according to the deflection criterion formulated in Equation (28), the most highly stressed section of a steel beam is not fully plastic under fire exposure conditions, which implies that the critical load in the event of fire is not directly proportional to the W_p/W value of the cross section. This is also demonstrated in FIG. 35 in which the values of β for a simply supported beam of carbon steel, of constant rectangular section and with a uniformly distributed load, are compared with those for a similar beam of constant I section. At room temperature, the ratio of the critical loads for the two beams is 1.33, which is the same as the ratio of W_p/W for the rectangular section to that of the I section. As the temperature rises, the ratio between the critical load for the beam of rectangular section and that for the beam of I section becomes smaller and drops to 1.20-1.25 within the temperature range 400-650°C. Roughly the same state of affairs can be seen in FIG. 36 in which the values of β for a beam of

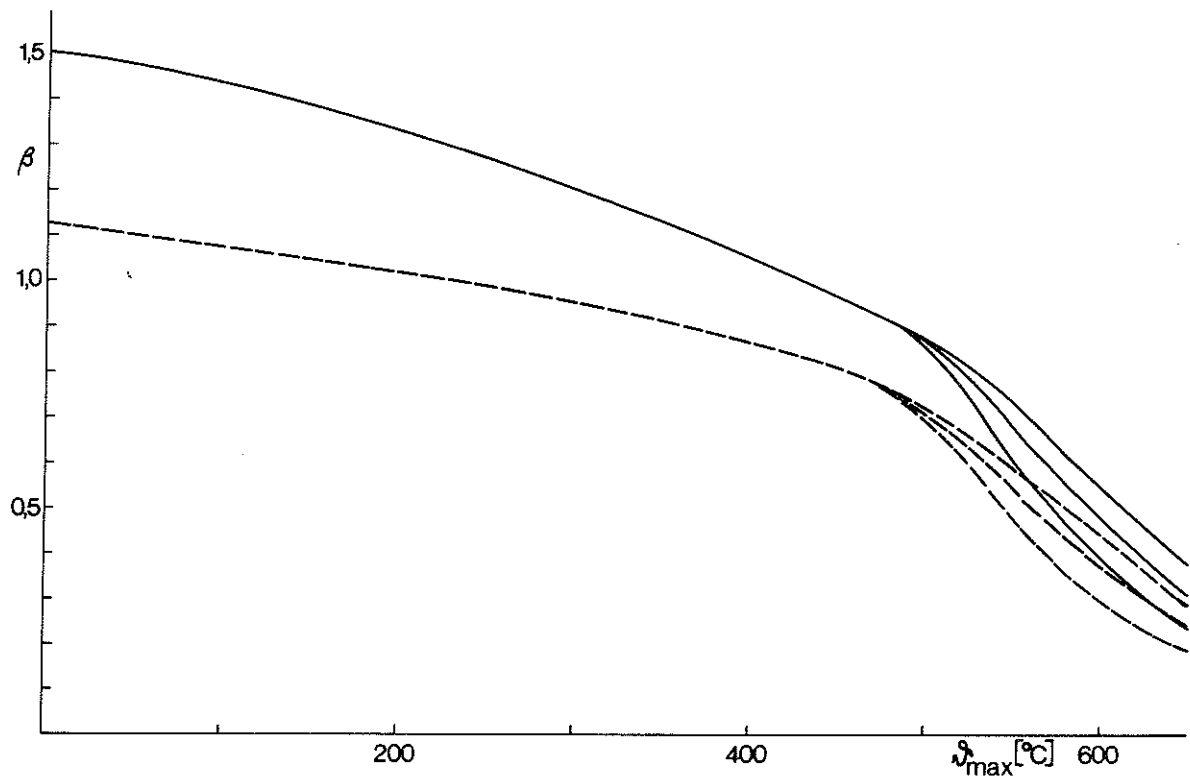


FIG. 35. Comparison of the values of β for a simply supported carbon steel beam with a uniformly distributed load, the cross section being constant and rectangular (—) and I-shaped (---). It is assumed in both cases that the temperature is the same all over the beam and that longitudinal expansion is not restrained.

The different branches of the curve correspond to rates of heating and cooling according to curves I, II and III in FIG. 30.

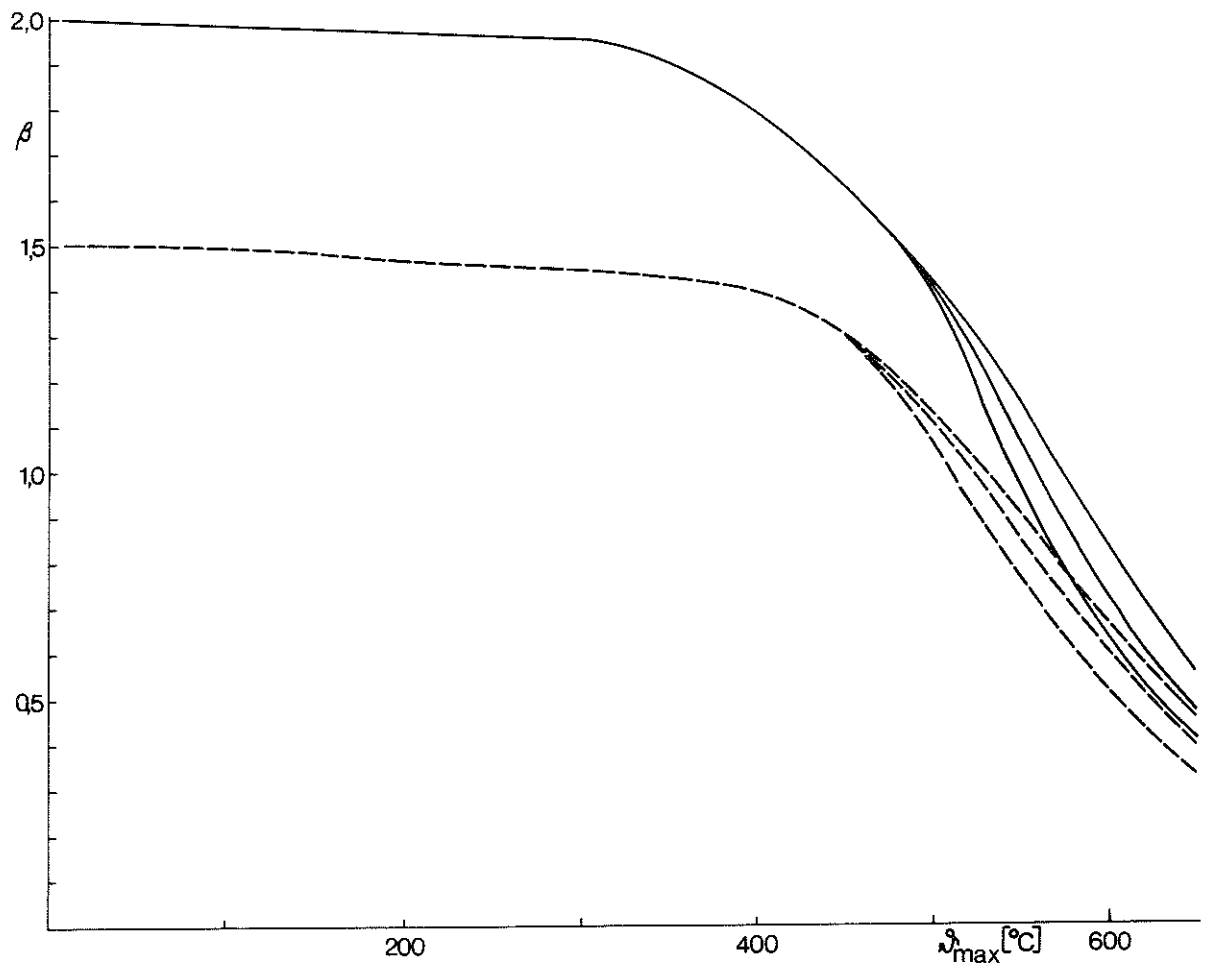


FIG. 36. Comparison of the values of β for a carbon steel beam with a uniformly distributed load which is rigidly restrained at both ends, the cross section being constant and rectangular (—) and I-shaped (---). It is assumed in both cases that the temperature is the same all over the beam and that longitudinal expansion is not restrained.

The different branches of the curve correspond to rates of heating and cooling according to curves I, II and III in FIG. 30.

carbon steel of constant rectangular cross section, restrained at both ends and loaded with a uniformly distributed load, are compared with those for a similar beam of constant I section.

One of the conditions stipulated in conjunction with the diagrams in FIG. 30 was that there must be no risk of instability failure. In the case of a beam section where the flange width is much greater than the flange thickness, or the depth of web is much greater than the web thickness, certain local instability phenomena may be critical with regard to the load carrying capacity of the beam. If, however, the shape of the cross section is such that there is no risk of a local instability failure at room temperature, then it is also unlikely that there will be any such risk at elevated temperatures. The load at which local instability failure occurs is greatly dependent on the magnitude of the modulus of elasticity, the proportional decrease in which as the temperature rises is less than that in the yield stress or the 0.2% proof stress. (4, 14). The ratio between the risk of a local instability failure and the risk of a flexural failure should therefore become smaller as the temperature rises. However, owing to the softly rounded shapes of the stress-strain curves at elevated temperatures and the fact that the load carrying capacity with regard to instability is governed both by the modulus of elasticity - or tangent modulus - and also the yield stress or the 0.2% proof stress, it is likely that the reduction in this risk ratio on a rise in temperature is less than the ratio between the proportional reduction in the magnitude of the 0.2% proof stress and that in the magnitude of the modulus of elasticity.

8.3.5 Variation in the cross section along the beam

The deflection of a steel beam which is exposed to fire primarily depends on the stress distribution along the beam and not on the moment distribution. If the section modulus of a simply supported beam subject to a certain load is varied along the beam in such a way that the extreme fibre stresses are the same all along the beam, the deflection development on exposure to fire will be the same in this beam as that in a beam of constant section modulus which is loaded by a constant bending moment, on condition that

the stresses and the steel temperature development are the same in the two cases. Since the deflection processes are identical, the ratio between the critical load under fire exposure conditions and that at room temperature is also the same in the two cases. An estimation, on the safe side, of the critical load for a simply supported beam of variable cross section along the beam can thus always be based on the values of β applicable to the loading condition of constant bending moment, according to FIG. 30a. The appropriate value of β is to be multiplied by that load which, for the cross sectional variation in question, causes the yield stress to be reached at room temperature at the most highly stressed section.

Variation of the cross section along a beam is more usual in a rigidly restrained or continuous beam than in a simply supported one. If a rigidly restrained beam is designed so that the extreme fibre stresses at the section where the span moment is the maximum are the same as at the restraint sections, then the capacity of the beam with regard to moment redistribution is exhausted. Naturally, the values of β for a simply supported beam can be used for the estimation of the critical load in such cases, but this results in many cases in an estimation of the risk of failure which is rather too much on the safe side. In spite of the fact that no redistribution of moments occurs, the moment distribution in a rigidly restrained beam is still considerably more favourable than in a simply supported beam. This state of affairs is illustrated to some extent in FIG. 37. This compares the calculated values of β for a beam restrained at both ends, which has a section modulus in the span that is only one-half that at the restraint sections, with the values of β for a beam of constant cross section that is rigidly restrained at both ends, and also with the values of β for a simply supported beam of constant cross section. The load in all cases is assumed to be uniformly distributed. Only the values of β for the slowest temperature development according to curve III in FIG. 30 are shown. In the case of the beam of variable cross section, it is assumed that the transition between the different forms of cross section coincides with the points of contraflexure in the beam at room temperature. It is seen in the

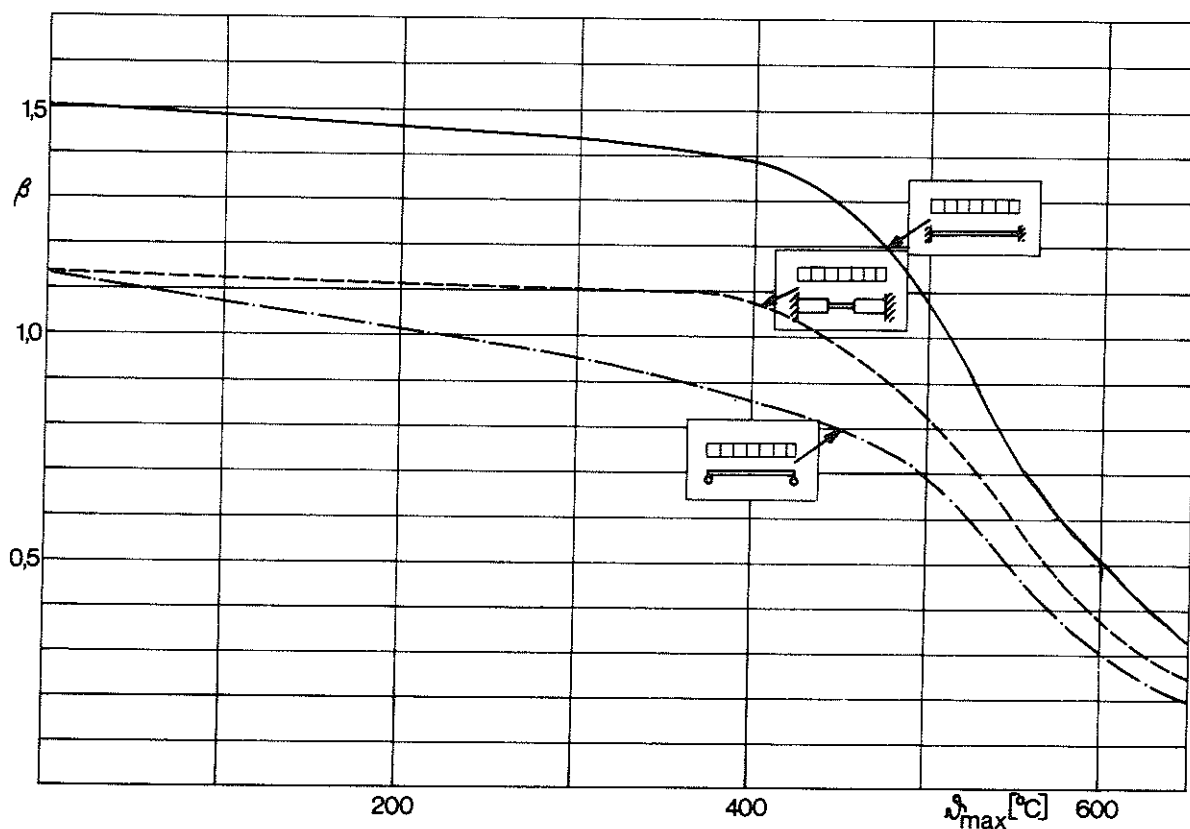


FIG. 37. Comparison in beams of carbon steel of the calculated values of β . All the beams carry a uniformly distributed load, and the curves refer to a simply supported beam of constant I section (- · -), a beam of I section rigidly restrained at both ends in which the modulus of section in the span is one-half that at the end sections (---), and a beam of constant I section rigidly restrained at both ends (—). It is assumed in all cases that there is no restraint on longitudinal expansion of the beams and that the temperature is the same all over the beams. The values of β apply for the slowest rate of heating according to curve III in FIG. 30.

Figure that the values of β are the same at room temperature for the restrained beam of variable cross section and the simply supported beam, but that the values of β at elevated temperatures are higher in the restrained beam. In the temperature range of 500-650°C, the ratio between the values of β in the two beams is about 1.20-1.25.

8.3.6 Different ratio between the rates of heating and cooling

The diagrams in FIG. 30 are based on a steel temperature development for which the rate of heating was assumed to be three times the rate of cooling. On the basis of the theoretically calculated steel temperature processes for uninsulated and insulated steel beams, performed at the Division of Structural Mechanics and Concrete Construction of Lund Institute of Technology, and the steel temperature curves determined in the course of tests, it is found that this relationship between the rates of heating and cooling is representative of that in actual fire conditions.

In order to get an idea of what will be the result of a change in the relationship between the rates of cooling and heating, the critical load for a simply supported beam with a uniformly distributed load has been calculated on the assumption that the rate of cooling is only one-sixth of the rate of heating. According to this assumption, the calculated critical load at a maximum temperature ϕ_{\max} of 650°C is approximately 95% of that applicable to a rate of cooling that is one-third of the rate of heating. The difference between the critical loads in the two cases becomes less as the maximum temperatures decrease. At 500°C, the critical load at the lower rate of cooling is about 99% of that at the higher rate of cooling. The reduction in critical load owing to a lower rate of cooling than that assumed in the diagrams in FIG. 30 is thus fairly moderate. This reduction is in addition more than counterbalanced by the rise in critical load as a result, inter alia, of the uneven distribution of temperature along the beam. (See Subsections 8.3.7 and 8.3.8).

The temperature developments comprising a linear rise in temperature up to the actual maximum temperature and a subsequent linear decrease in temperature, which have been assumed in calculating the deformation curves and in evaluating the critical loads, are naturally an approximation of the steel temperature developments which occur during an actual fire. The above comparisons between critical loads at rates of cooling higher and lower than that assumed, and some calculations performed with non-linear temperature developments more in agreement with actual conditions, show however that the linear temperature developments employed for the sake of simplicity can be accepted with an accuracy that is sufficient in conjunction with exposure to fire.

8.3.7 Variation in temperature across the cross section

When a beam is exposed to the action of fire, the temperature at the top of the beam is generally lower than that at the bottom of the beam. The magnitude of this difference in temperature depends on a number of factors such as room geometry, the design of the insulation, dissipation of heat to the floor slab, etc. On the basis of recorded temperatures during fire tests, it appears that the difference in temperature between the top and bottom flanges of a steel beam which is exposed to fire is normally in the range of 50-200°C.

This difference in temperature between the top and bottom flanges causes a deformation in the beam irrespective of whether or not the beam is loaded. However, the top flange which is at a lower temperature takes a larger proportion of the load and thus relieves the hotter and therefore weaker bottom flange. This redistribution of stresses has the result that the deflection is less than when the top flange has the same temperature as the bottom flange. This is particularly noticeable at elevated temperatures when the creep strain predominates. The deflection-time ($y - t$) curves for a simply supported beam of I section and with a uniformly distributed load, for the assumptions that the temperature is the same all over the beam and that the temperature of the top flange is 100°C lower than that of the bottom flange, are compared in FIG. 38. In the latter case, the temperature is assumed to be constant from the

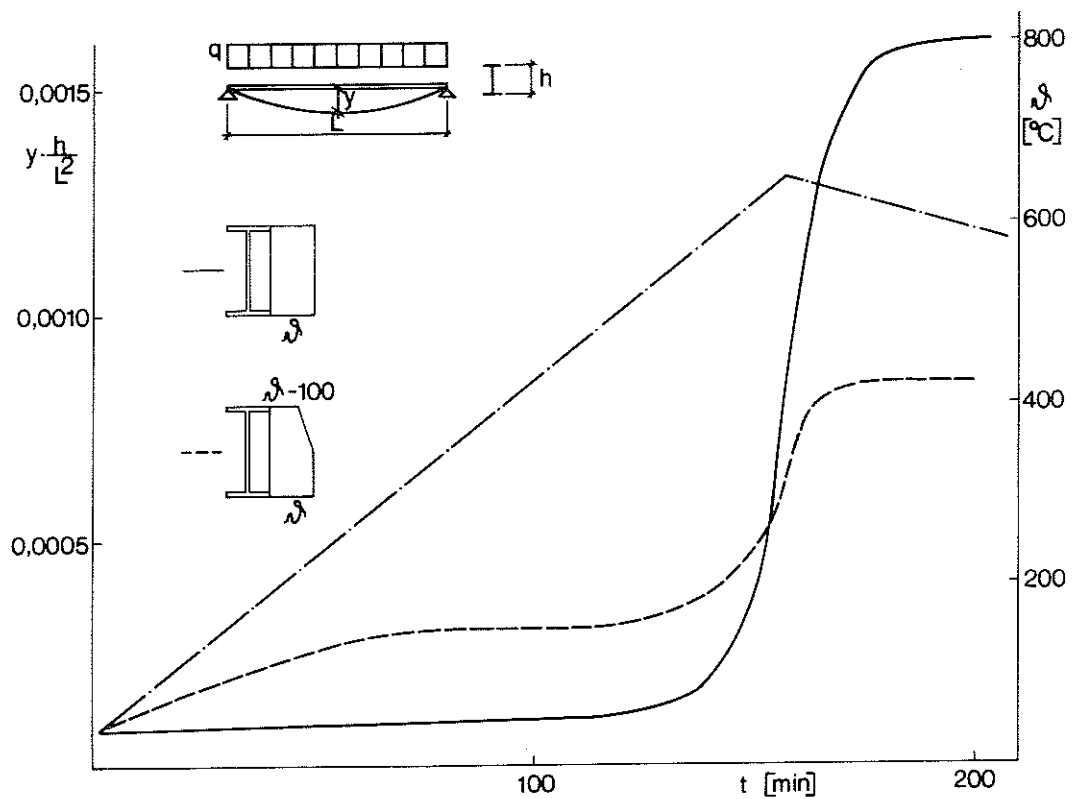


FIG. 38. Deflection-time ($y - t$) curves for a simply supported carbon steel beam with a uniformly distributed load, calculated on the assumption that the temperature is the same all over the beam (—) and that the temperature across the cross section varies as shown in the inset (---). The maximum temperature ϕ of the beam as a function of the time t is shown by the chain line. In the case of the beam in which the temperature varies over the cross section, it is assumed that the temperature of the top flange, before the bottom flange has attained a temperature of 125°C , is constant at 25°C . It is assumed in both cases that there is no restraint on longitudinal expansion of the beam. The load q is equivalent to 20% of that load which causes the yield stress to be reached at room temperature at the most highly stressed section.

bottom flange up to the middle of the web and to decrease linearly from there to the top flange. The temperature θ in the bottom flange is given in the Figure as a function of the time t . At the beginning of the fire, before the temperature of the bottom had attained 125°C , the temperature of the top flange of the beam with variable temperature was assumed to be constant at 25°C .

It will be seen from FIG. 38 that the deflection of the beam in which the temperature varies over the cross section is initially greater than that of the beam in which the temperature is constant over the cross section. This is due, as mentioned above, to the additional deformation caused by the difference in temperatures in the beam. Owing to the favourable redistribution of the stresses over the cross section, deflection of the beam with the temperature variable over the cross section will however gradually become less than that of the beam in which the temperature is constant over the cross section.

Since redistribution of the stresses exerts an influence on the development of deformations, the shape of the cross section is significant with regard to the magnitude of the difference between the deformations in the beam where the temperature varies over the cross section and those in the beam where the temperature is constant over the cross section. Calculations also show that the deformations in a beam of rectangular cross section, for the same difference in temperatures, are somewhat less than in a beam of I section. The state of affairs in the case of a statically indeterminate beam is similar to that in a statically determinate beam, but the influence which the difference in temperatures exerts on the deformations is a little greater in the former case. This is due to the fact that the variation in temperature over the cross section, with the top flange cooler than the bottom one, causes the restraining moments to become larger and the span moment consequently to become smaller than is the case in a similar beam of constant temperature.

By means of systematically performed calculations, the critical load was determined for beams in which the temperature varies over the cross section. The results show that the critical load - as

defined by the deflection criterion in Equation (28) - is consistently larger for a beam in which the top flange is cooler than the bottom flange than for a beam in which the temperature of the whole beam is equal to that of the bottom flange. Since, however, there is a limit to redistribution of stresses in a cross section, there is also a limit above which an increase in the temperature difference over the cross section causes no increase in the critical load. The critical load at a temperature difference between the top and bottom flange of 200°C is only slightly larger than that at a temperature difference of 100°C , the maximum temperatures being the same in the two cases.

Summarising, the following recommendations can be made on the basis of the calculation results with regard to the increase in the critical load for beams in which the top flange is $100\text{-}200^{\circ}\text{C}$ cooler than the bottom flange in relation to that in similar beams in which the temperature over the cross section is constant.

a) Simply supported beam with a uniformly distributed load

For beams of I section, the increase in critical load is of the order of 5% at a maximum temperature of 450°C and is about 15% at a maximum temperature of 650°C . The corresponding figures for beams of rectangular section are 10% and 25%.

b) Beam restrained at both ends, uniformly distributed load
(I section)

At a maximum temperature of 450°C , the increase in critical load is of the order of 10%, and at a maximum temperature of 650°C it is about 20%.

8.3.8 Variation in temperature along the beam

In the course of fire tests on steel beams, it has been found that the temperature in the end regions of the beams is considerably lower than in their midregions. A similar state of affairs may also be expected in the case of a beam subjected to the action of a real fire if the supports of the beam are on or near the walls which confine the fire. The fact that the temperature is lower in the end regions of a beam means that the deflection is less

than if the whole beam had the same temperature as its midregion. The reason for this is that the curvature of the beam becomes less as the temperature is smaller, and that the deflection of the beam is dependent on the curvature along the entire beam. How much less the deflection is in a beam in which there is a certain temperature difference between the ends and the centre than in a similar beam with a constant temperature is governed, inter alia, by the nature of loading and the statical system.

Since the critical load is based on the magnitude of the deflection, a variation in temperature along the beam will also exert an influence on the magnitude of the critical load. Systematic calculations have been performed of the critical load in a simply supported beam with a uniformly distributed load which is exposed to the action of fire, the temperature of the end sections being assumed to be 100°C lower than that of the midsection. The results show that the critical load at a maximum temperature of 450°C is about 5% greater than in a similar beam of constant temperature. The assumption made in the case of a beam in which the temperature varies along the span is that the variation is linear between the temperature of the midsection and that of the end sections. At a maximum temperature of 650°C , the critical load in beams of variable temperature is approximately 10% greater than in beams of constant temperature. Similar calculations of the critical load, on the assumption that the temperature of the end sections is 200°C lower than that of the midsection, show that the increase in critical load in relation to that at constant temperature along the beam is about 7% at a maximum temperature of 450°C and about 17% at a maximum temperature of 650°C . The temperature of the end sections, before the temperature of the midsection had attained 125°C or 225°C , was assumed constant at 25°C .

For a statically indeterminate beam the increase in critical load due to a lowering of the temperature at the end sections is considerably greater than that in a statically determinate beam. This is due to the fact that the moment taken by the sections at which the beam is restrained is the higher, the lower their temperature, and the span moment diminishes correspondingly. Calculations made for a beam with a uniformly distributed load

which is rigidly restrained at both ends show that the critical load, at a maximum temperature of 450°C and a temperature difference of 100°C , is about 10% greater than in a similar beam of constant temperature. The assumption made in the case of temperature varying along the beam is that the variation between the midsection and the end sections is linear. At a maximum temperature of 550°C , the increase in critical load is about 25% and at a maximum temperature of 650°C it is about 65%. At a temperature difference between the midsection and end sections of 200°C , the increase in critical load in relation to that at a constant temperature distribution is about 20% at a maximum temperature of 450°C . At a maximum temperature of 550°C , the corresponding increase is about 55% and at a maximum temperature of 650°C it is about 150%. In the same way as in the case of the simply supported beam, it was assumed that the temperature of the end sections is constant at 25°C as long as the temperature of the midsection is less than 125°C or 225°C .

8.3.9 Restraint on longitudinal expansion

If the longitudinal expansion of a steel beam due to the action of fire is wholly or partly prevented - for instance due to limitation of movement at the supports - forces are imposed on the beam. The magnitude of these imposed forces depends on a number of factors such as temperature conditions, the degree of restraint on longitudinal expansion, the stiffness of the beam, the magnitude of transverse loading etc.

In practical construction, movement at the supports is usually subject to considerable limitations. This is for instance the case in conjunction with floor slabs of high in-plane stiffness which limit the movements in a horizontal direction of the supporting columns and hence of the beam supports. It is likely that some movement nevertheless occurs, for instance due to a clearance or plastic deformation at the points of attachment. An other thing is that there also had to be some expansion of the beam in order to prevent forces to be imposed even when the supports are absolutely immovable. That is because the neutral axis of a deformed beam is longer than the distance between the points of support and the deflection increases during a fire.

At the beginning of a fire, when the deflection of a steel beam is small, the difference between the lengths of the neutral axis and the chord is less than the expansion due to the rise in temperature. If the supports are immovable, the beam is therefore initially subjected to a compressive force. In those cross sections of the deformed beam where the resultant of the compressive force is above the centroid of the section, the moment acting on the beam is increased. If, therefore, the resultant of the compressive force coincides with, or is situated above, a line connecting the centroids of the end cross sections, the moment is increased along the entire beam. An increase in the moment acting on the beam causes an increase in deflection. At all times, the compressive force is so large that the difference between the length of the neutral axis of the deflected beam and the length of the chord between the points of support is equal to the expansion of the beam due to the rise in temperature, less its shortening due to elastic and plastic contraction. When the deflection has become so large that the difference between the lengths of the neutral axis and the chord exceeds the thermal expansion less any residual contraction owing to plastic compressive strain, the beam is instead subjected to a tensile force. This tensile force reduces the moment acting on the beam and thereby exerts a limiting influence on continued deformation of the beam. This state of affairs is illustrated in FIG. 39, which compares the calculated deflection y of a simply supported beam whose supports are absolutely immovable in the horizontal direction with the calculated deflection of a similar beam whose expansion is not subject to any restraint, both beams being acted upon by fire and loaded with a uniformly distributed load. In the case of the beam subjected to restraint, it is also assumed that the resultant of the imposed forces coincides with a line between the centroids of the end cross sections. The deflection is plotted as a function of the steel temperature θ . The calculations have been performed for two different load levels and three ratios between the depth h and length L of the beam. As will be seen in the Figure, the points of intersection between the deformation curves for the beam which cannot move at the supports and those for the beam which is free to move occur at different temperatures and deflections,

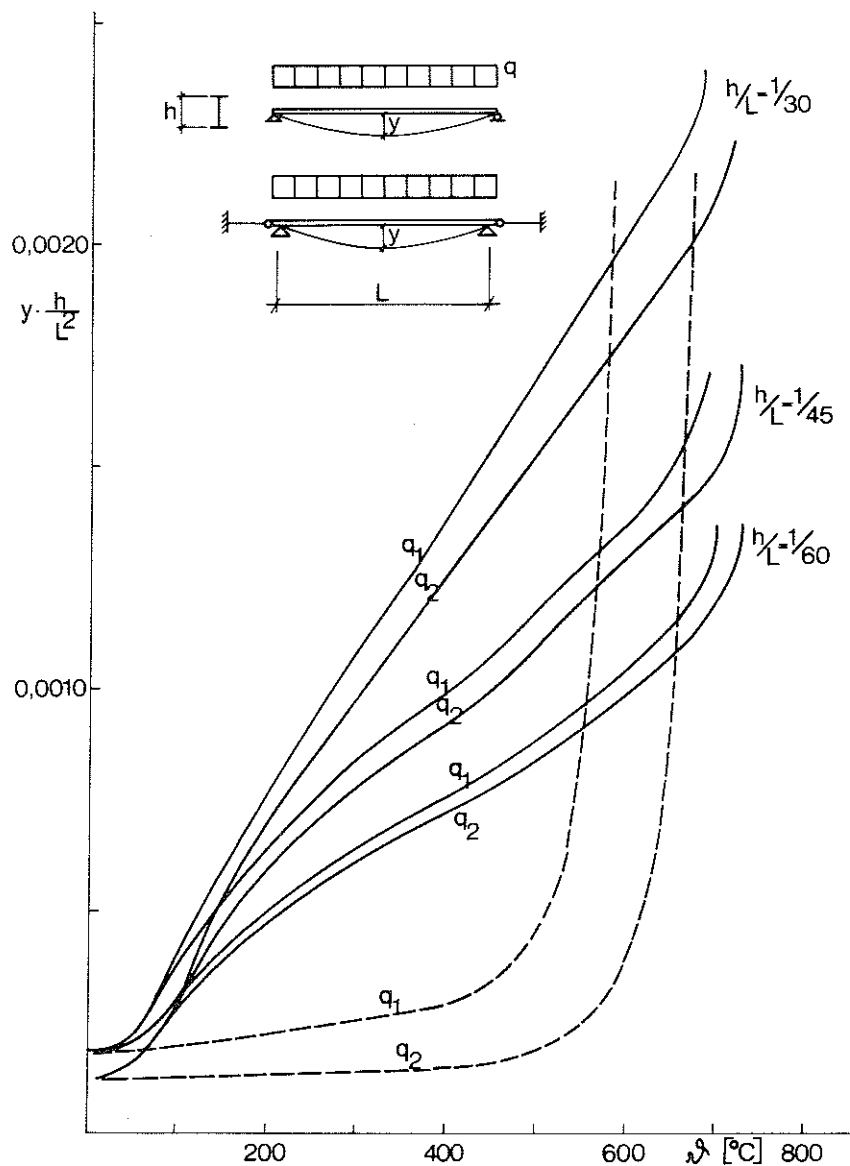


FIG. 39. Calculated deflection y as a function of a temperature θ which is uniform all over the beam, for a simply supported beam with a uniformly distributed load q , on the assumption that the supports of the beam are absolutely immovable (—) in the horizontal direction and that there is no restraint on longitudinal expansion of the beam (---). The loads q_1 and q_2 are 60% and 35% of the load which causes the most highly stressed cross section to reach the yield stress at room temperature. The deflections are calculated without consideration of the creep strain. In the beam which is restraint on longitudinal expansion, it is assumed that the resultant of the imposed forces coincides with a line through the centroids of the end cross sections.

depending on the load acting on the beam and on the stiffness of the beam. The points of intersection in the different cases indicate the change in the imposed force from compression to tension. The higher the load, the lower the temperature which is required in order that the deflection necessary for this change may be attained. The more slender the beam, the lower the temperature at which the deflection required for this change in sign occurs. The deflection curves shown in FIG. 39 have been computed without consideration of the effect of creep. The situation will however be similar even when creep is taken into consideration, although the deflection necessary for the change is attained at a lower temperature owing to the influence of creep. That also means that the deflection necessary for this change will be less.

In the course of model tests (19) on loaded frames which were heated in a furnace, one of the factors studied was the effect on the deflection process of preventing horizontal movements of the joints in the frame. The results are exemplified in FIG. 40 in which the recorded deflection y as a function of the steel temperature ϑ is compared for a frame in which the joints cannot move and one in which there is no restraint on horizontal movement of the joints. The state of affairs with regard to deformations is similar in a frame in which movement of the joints is prevented and in a beam which cannot move at the supports. At low temperatures, when the deflection is small, the horizontal member of the frame is acted upon by compressive forces, and consequently the deflection is greater than in a similar frame in which the joints can move horizontal. When the temperatures and hence the deflections become larger, the restraint on movement of the frame joints causes the horizontal frame member to be acted upon by a tensile force, and the deflection of the frame with restrained frame joints is then less than that of the frame in which movement of the joints is not prevented. It was also found in the study (19) that the critical temperature in frames where horizontal movement of the joints was prevented was consistently higher than for frames in which there was no restraint on horizontal movement of the joints.

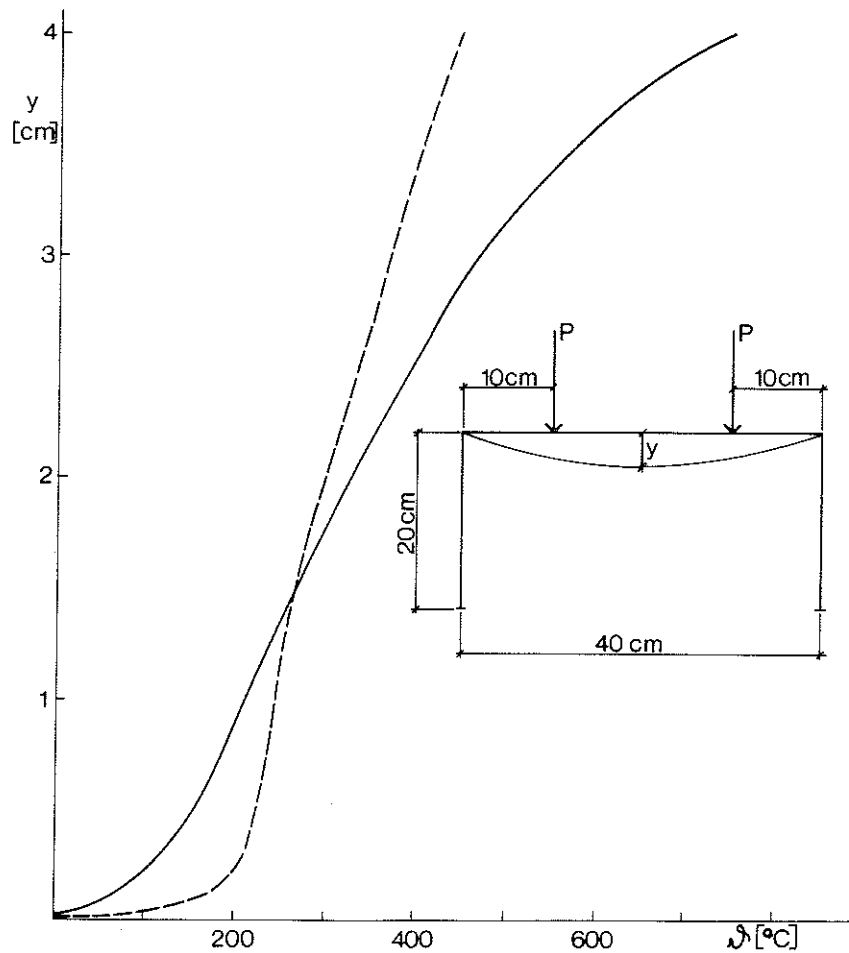


FIG. 40. Comparison of the recorded central deflections y , as functions of the temperature ϑ , in a model frame in which horizontal movement of the joints is prevented (—) and one in which there is no restraint on horizontal movement of the joints (---). The width of the horizontal portion of the frame is 0.63 cm and its depth is 0.42 cm. The dimensions of the legs of the frame are 0.63 x 0.63 cm. The load P is 72.5% of the limiting load for the frame at room temperature, calculated by means of the limit state theory, and the rate of heating is approximately $8^{\circ}\text{C}/\text{min}$. Owing to the relatively slow heating and the small dimensions of the frame, it may be assumed that the temperature is uniform over the frame.

If the deflection criterion $y = L^2/h.800$ according to Eq. (28) is applied as the criterion of failure also to a beam which is completely prevented from moving horizontally at its supports, then, as shown in FIG. 39, the critical temperature for such a beam will be either higher or lower than that for a similar beam whose expansion is not restrained, depending, inter alia, on the magnitude of the load and the stiffness. The greater the load and the more slender the beam, the greater the probability that the critical temperature in the beam which cannot move at the supports will be higher than in the beam whose movement is not prevented.

One of the reasons why the deflection criterion according to Equation (28) can be considered suitable as the criterion of failure for a steel beam under fire exposure conditions (6) is that the increase in the deflection of the beam, on a rise in temperature, is sufficiently large once a deflection according to Equation (28) has been reached. As will be seen in FIG. 39, this evidently does not apply for a beam which cannot move at its supports. The increase in deflection, after the deflection has become so large that tensile forces arise, is considerably slower than in a beam which can expand longitudinally without restraint. A certain modification of the criterion of failure may therefore be necessary in the case of beams which cannot move axially at their supports. In practice, however, it is difficult to make a quantitative assessment of much accuracy of the movements in a beam when this is exposed to fire. Owing to e.g. clearance at the points of attachment and plastic flow in these, it is probable that actual conditions are often intermediate between full restraint on axial movement at the supports and complete freedom to do so. Owing to the difficulty of making a relevant assessment of the possibility of movement at the supports, it would seem therefore appropriate from the practical point of view to base estimation of the load carrying capacity of a steel beam under fire exposure conditions on the assumption that there is no restraint on longitudinal expansion of the beam. This implies that the deflection of a beam whose axial movement at the supports is limited may be a little greater than that corresponding to the deflection criterion of $y = L^2/h.800$, particularly when the depth of the beam is large in relation to its length and the load is small.

The ultimate load of such a beam, however, - if the term ultimate load is taken to mean the highest load which the beam itself is capable of supporting at a certain temperature without consideration of the magnitude of the deflection - is always greater than that of a similar beam which can expand longitudinally without restraint.

An approximate calculation of the conditions at which the deflection in a beam in which axial movements are completely prevented at the supports will be greater than that in a beam whose longitudinal movement is not restrained, can be made in the following way. In order that there should be no imposed forces, the length of the neutral axis of the deflected beam less the length of the chord between the rigid points of support of the beam must be the same as the expansion which would have taken place in the beam if it had been completely free to move axially on a rise in temperature. This disregards any plastic contraction along the neutral axis of the beam, and the results of deflection calculations also show that this contraction is normally very limited. It is possible to draw up a relationship between the central deflection y of the beam, its depth/span ratio h/L and the temperature ϕ , such that the above condition, that there should be no imposed forces, will be satisfied. The particular form of this relation depends on the shape which it is assumed the deflection curve has along the beam. If the deflection curve is approximated to two straight lines, from each support to the centre of the deflected beam, then the relation is

$$y \cdot \frac{h}{L^2} = \frac{\sqrt{\{0.26 \cdot \phi + 0.0013 \cdot \phi^2\}}}{200} \cdot \frac{h}{L} \quad (31)$$

where y = central deflection (cm)

h = depth of beam (cm)

L = length of beam (cm)

ϕ = temperature ($^{\circ}\text{C}$)

The coefficient of longitudinal expansion has been assumed to have a mean value of 13×10^{-6} per $^{\circ}\text{C}$.

If the deflection curve is assumed to be circular, then the relation will be

$$\vartheta = \frac{\left[\frac{\left(\frac{h}{2L}\right)^2 + \left(y \cdot \frac{h}{L^2}\right)^2}{y \cdot \frac{h}{L^2} \cdot \frac{h}{L}} \cdot \sin^{-1} \frac{y \cdot \frac{h}{L^2} \cdot \frac{h}{L}}{\left(\frac{h}{2L}\right)^2 + \left(y \cdot \frac{h}{L^2}\right)^2} \right] - 1}{0.000013} \quad (32)$$

In order, therefore, that there should be no imposed forces on the beam, the values of y , h , L and ϑ must satisfy Equation (31) or Equation (32), depending on the shape of the assumed deflection curve. Normally, the deflection curve of a beam which is exposed to fire is somewhere between these two assumed curves. The relations according to Equations (31) and (32) are reproduced in FIG. 41 for three different values of the stiffness h/L . The curves in this Figure will give an approximate idea of the deflection at which the imposed forces in a beam exposed to fire, in which axial movement at the supports at the level of the centroid is fully prevented, change from compression to tension. At deflections larger than this, the increase in deflection in such a beam is slower than in a similar beam whose longitudinal expansion is not prevented. It is seen from FIG. 39 that the change from compression to tension, for a beam with a load q_1 and a depth/span ratio of $1/30$, occurs for a deflection of $0.0019 \cdot h/L^2$ and a temperature of 575°C . At the lower load q_2 , the corresponding figures are just over $0.0020 \cdot h/L^2$ and 675°C . These figures are in good agreement with the relations illustrated in FIG. 41. Furthermore, FIG. 40 shows that the change from compression to tension takes place in the model frame at a deflection of 1.4 cm - which is equivalent to a value of $y \cdot h/L^2$ of around 0.0035 - and a temperature of 260°C . The value of the ratio h/L for the frame is approximately $1/100$. Even these relations between deflection and temperature are in good agreement with the relations illustrated in FIG. 41.

If movement of a beam under fire exposure conditions is limited at the supports and it is in addition sufficiently slender in the direction of the minor axis, then there is a risk that the beam will deflect laterally owing to the action of the imposed forces. There is however no question whatever of a buckling failure, since the compressive force decreases as the beam deflects, and an

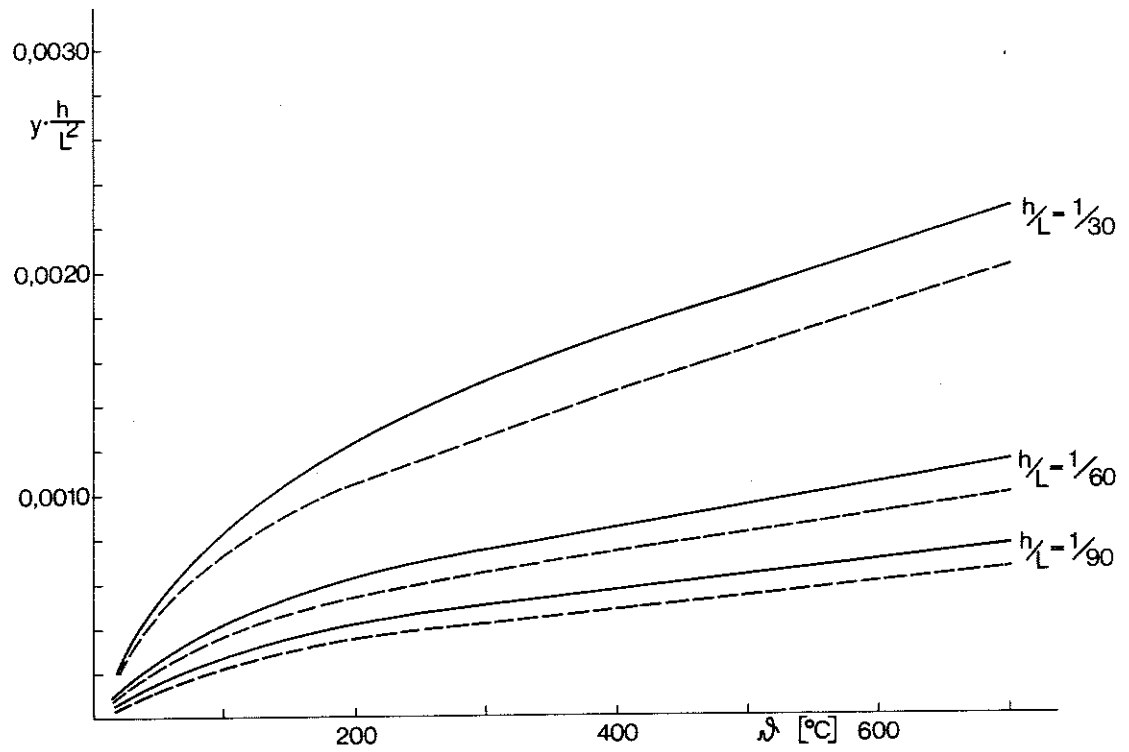


FIG. 41. Relations between central beam deflection y , length of beam L , depth of beam h and temperature Δ , according to Equation (31) (—) and Equation (32) (---).

equilibrium position is attained. This is the fundamental difference in relation to the state of affairs in a column, where an increase in deflection causes an increase in the moment, due to the fact that the vertical load on the column subjects this to an axial compressive force during the whole of the deflection process. The increased moment may therefore, in turn, result in yet larger deflections, and so on.

Even though a steel beam which is acted upon by imposed forces owing to a restraint on its longitudinal expansion as a result of exposure to fire cannot fail by buckling, lateral deflection may nevertheless cause the beam to be subjected to torsional moments. If, however, the restraint on longitudinal expansion of the beam is due to its connection with a stiff floor slab, this slab will in most cases provide effective lateral support for the beam and lateral deflection of this is therefore prevented or greatly reduced.

As has been pointed out before, the risk of lateral deflection, under fire exposure conditions, of a beam which cannot move axially at the supports and is not restrained laterally by a floor slab or in a similar manner, is not directly comparable with the risk of buckling in a column. In spite of this, comparison with columns may give an idea of the factors which have an effect on the risk of lateral deflection in such a beam. During calculation of the beam deflections shown in FIG. 39, the magnitudes of the imposed stresses σ_t were also obtained for the various beams as a function of the temperature ϑ . On the basis of the design diagrams presented in (5), the buckling stress σ_k has therefore been determined as a function of the temperature ϑ for columns which have slenderness ratios the same as those of the beams in the direction of the minor axis. In calculating the slenderness ratios λ , it was assumed that the beams are pin jointed at both ends.

FIG. 42 illustrates the relationship between the stresses σ_t and σ_k , calculated as above, as a function of the temperature ϑ . It is evident from the curves in the Figure that the risk of lateral deflection, under fire exposure conditions, of a steel beam which is prevented from moving at the supports and is not restrained

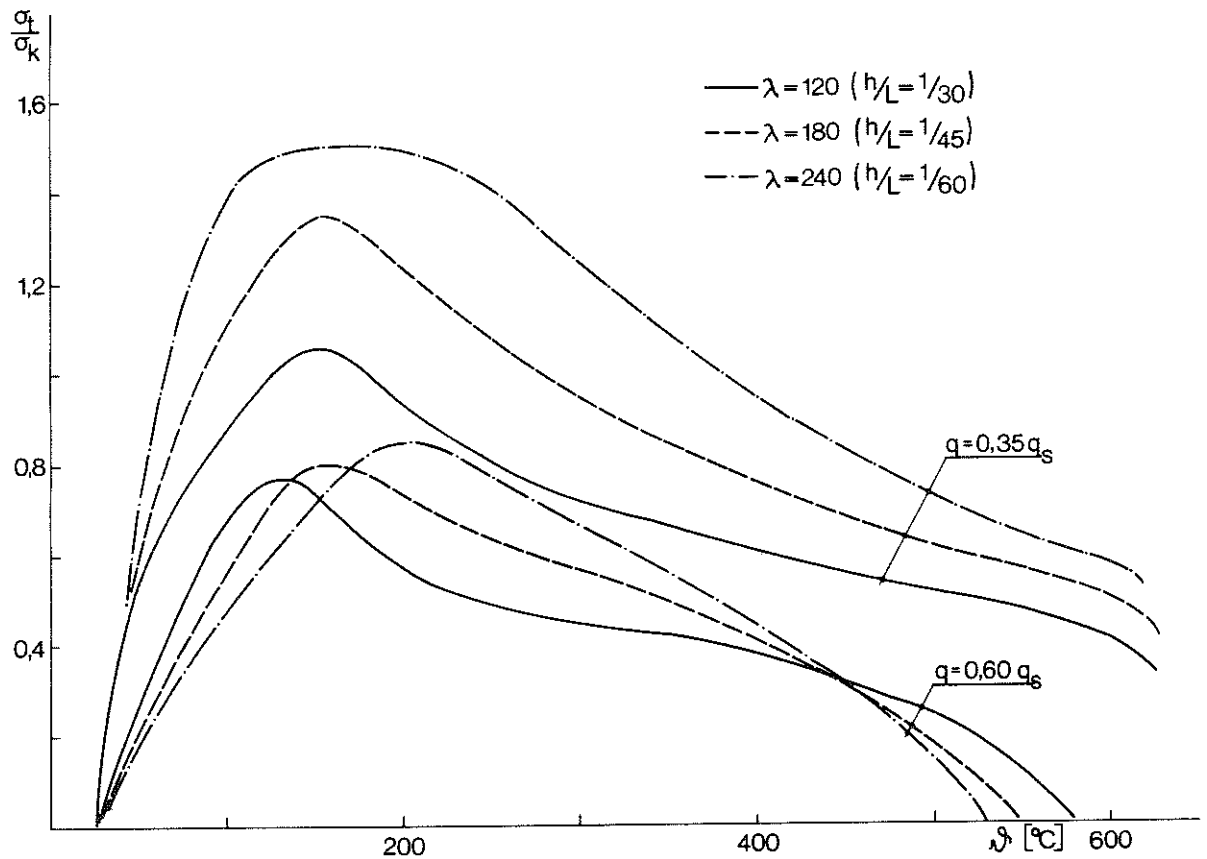


FIG. 42. Relationship between the imposed stress σ_t , under fire exposure conditions, in beams where movement is completely prevented at the supports, with the buckling stress σ_k in columns of different slenderness ratios, calculated on the basis of the diagrams shown in (5). The ratio of σ_t to σ_k is plotted as a function of the temperature ϑ . In calculating the values of σ_k , it was assumed that the slenderness ratio of the columns is equal to that of the beams in the direction of the minor axis and that the beams are pin jointed at both ends. The transverse load on the beam is denoted by q , while q_s is the load which causes the yield stress to be reached at room temperature in the most highly stressed cross section. The depth of the beam is denoted h and its length L .

in the lateral direction, appears to increase as the slenderness ratio λ increases and to decrease as the vertical load q increases. The Figure also shows that the greatest risk of lateral deflection occurs within the temperature range of 100-200°C. The difference between a beam and a column which is of fundamental significance in this context, i.e. that the column buckles at a stress equal to σ_k while the beam, owing to its deflection, is subjected to a gradually diminishing imposed stress, must however be borne in mind.

9 COMPARISON, FOR STEEL BEAMS EXPOSED TO THE ACTION OF FIRE,
OF THE CRITICAL LOADS DETERMINED FROM CALCULATED DEFORMATIONS
WITH THOSE DETERMINED ON THE BASIS OF THE YIELD STRESS OR 0.2%
PROOF STRESS AT ELEVATED TEMPERATURES

Estimation of the load carrying capacity of a steel beam under fire exposure conditions is often based on the limit state theory. Since ordinary structural steels have no clearly defined yield regions at elevated temperatures, the yield stress is replaced by the 0.2% proof stress. The actual stress-strain curves at the different temperatures are simplified in the course of calculations to ideal elasto-plastic stress-strain curves which are assumed to be elastic up to the 0.2% proof stress at the temperature in question. FIG. 43 shows the 0.2% proof stress and the modulus of elasticity as functions of the temperature (4). The 0.2% proof stress was determined in this case on the basis of tensile tests at elevated temperatures in which the load was applied slowly, and a not inconsiderable proportion of the 0.2% proof stress at elevated temperatures is therefore due to creep strain.

For a simply supported beam of length L which is loaded with a central concentrated load P, the maximum moment is

$$M = \frac{PL}{4} \quad (33)$$

According to the limit state theory, it is assumed that the load carrying capacity of the beam is completely exhausted when the whole cross section has become plastic. The maximum capacity M_g of the cross section to resist a moment at a temperature ϑ can therefore be written

$$M_g = \sigma_{s\vartheta} \cdot W_p \quad (34)$$

where $\sigma_{s\vartheta}$ = yield stress (0.2% proof stress) at the temperature ϑ

W_p = plastic section modulus of the cross section

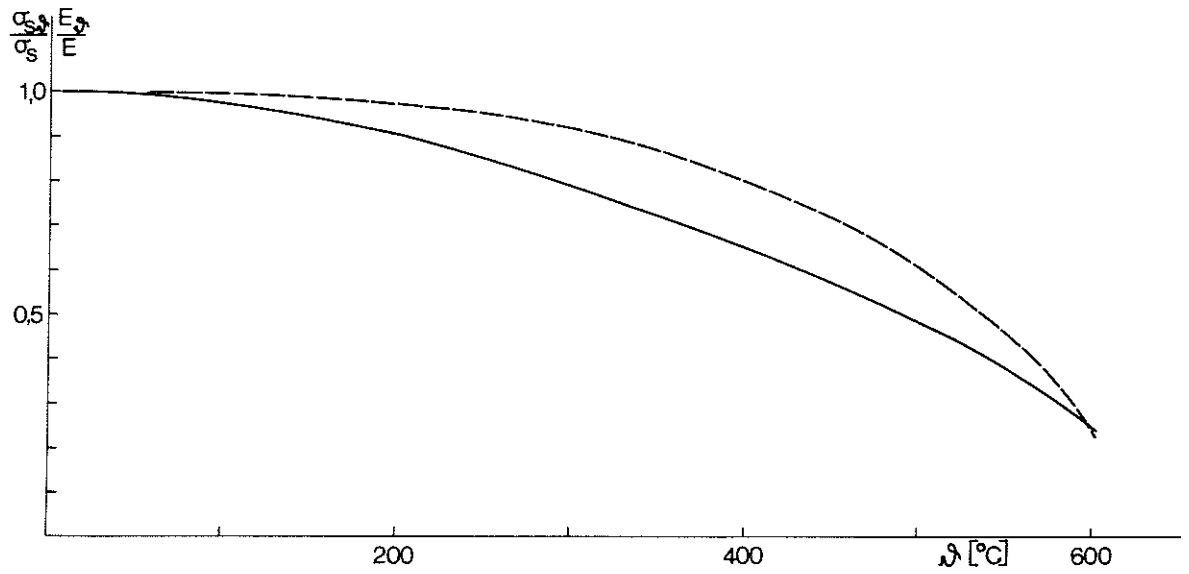


FIG. 43. Variation of the 0.2% proof stress $\sigma_{s\theta}$ (—) and of the modulus of elasticity E_θ (---) with the temperature θ in an ordinary carbon steel (4). The symbols σ_s and E denote the yield stress and modulus of elasticity respectively at room temperature.

By combining Equations (33) and (34), the limiting load P_g of the beam is obtained as

$$P_g = \frac{\sigma_{s\theta} \cdot W_p \cdot l}{L} \quad (35)$$

The load P_s which, at the most highly stressed cross section, gives rise to an extreme fibre stress equal to the yield stress σ_s at room temperature can be written

$$P_s = \frac{\sigma_s \cdot W \cdot l}{L} \quad (36)$$

where σ_s = yield stress at room temperature

W = elastic section modulus of the cross section

If Equation (35) is divided by Equation (36), we obtain the ratio β_1 between the critical load under fire exposure conditions - estimated on the basis of the limit state theory - and the load P_s which causes the most highly stressed cross section to reach the yield stress at room temperature

$$\beta_1 = \frac{\sigma_{s\theta} \cdot W_p}{\sigma_s \cdot W} \quad (37)$$

For an I section, the ratio W_p/W may be put at 1.13. The coefficient β_1 is comparable with the coefficient β in the diagrams in FIG. 30, but it is based on an estimation of failure according to the limit state theory instead of deflection calculations.

The values of β_1 and β are compared in FIG. 44 for a beam with a central concentrated load. The values of the ratio $\sigma_{s\theta}/\sigma_s$ given in FIG. 43 have been used in calculating the values of β_1 according to Equation (37). As will be evident on comparing the values of β and β_1 in FIG. 44, the critical load determined on the basis of the limit state theory is considerably lower than the equivalent load determined on the basis of deflection calculations. This may be explained by the fact that the stress-strain curves at elevated temperatures are softly rounded, which means that the load carrying capacity is not exhausted in spite of the fact that the stresses in a cross section are the same as the 0.2% proof stress.

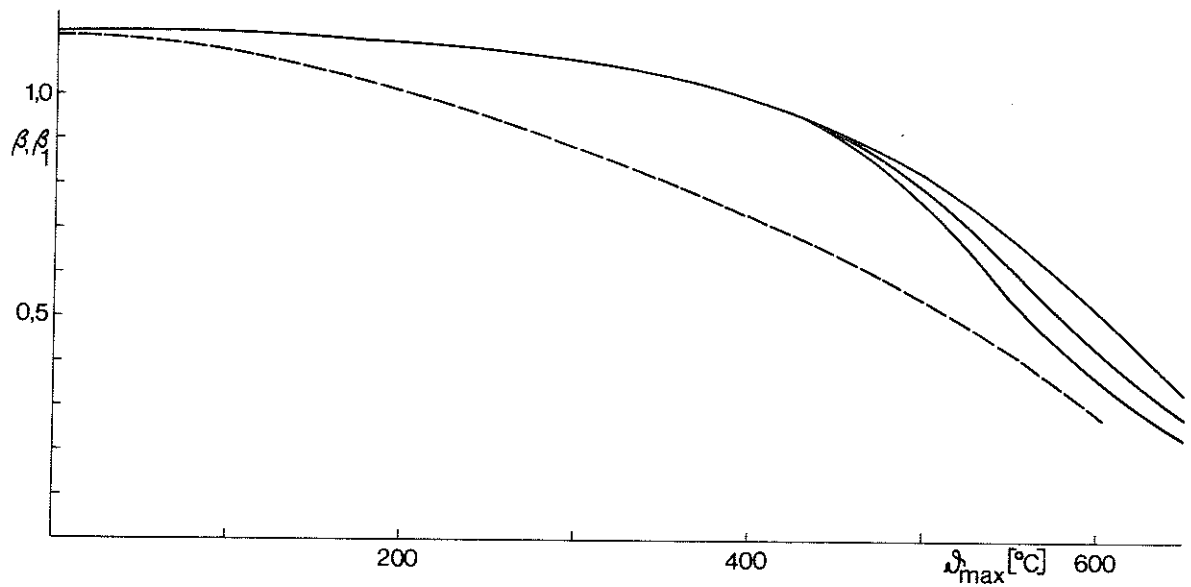


FIG. 44. Comparison, in a simply supported beam of carbon steel of constant I section with a central concentrated load, of the values of β (—) and those of β_1 (---) as functions of the maximum steel temperature ϑ_{\max} . It is assumed that there is no restraint on longitudinal expansion of the beam and that the temperature is the same all over the beam. The different branches of the β curve correspond to the rates of heating and cooling according to curves I, II and III in FIG. 30.

Another difference between these two methods of estimating the critical load is that it is difficult, in estimating the load on the basis of the limit state theory, to take into account the influence of the creep strain satisfactorily. It is further evident from Equation (37) that the value of β_1 and hence of the critical load, when this is estimated according to the limit state theory, is directly proportional to the value of the ratio W_p/W for the cross section. According to the discussion in Subsection 8.3.4, this is not the case when the load carrying capacity is estimated on the basis of deflection calculations.

The relation applicable to β_1 in the case of a beam rigidly restrained against rotation at both ends, which is loaded with a uniformly distributed load, is

$$\beta_1 = \frac{\frac{16 \cdot \sigma_{s\theta} \cdot W_p}{L^2}}{\frac{12 \cdot \sigma_s \cdot W}{L^2}} \approx 1.33 \cdot \frac{W_p}{W} \cdot \frac{\sigma_{s\theta}}{\sigma_s} \quad (38)$$

The corresponding relation for a beam with a uniformly distributed load which is rigidly restrained at one end is

$$\beta_1 = \frac{\frac{11.7 \cdot \sigma_{s\theta} \cdot W_p}{L^2}}{\frac{8 \cdot \sigma_s \cdot W}{L^2}} \approx 1.47 \cdot \frac{W_p}{W} \cdot \frac{\sigma_{s\theta}}{\sigma_s} \quad (39)$$

It will be evident from Equations (38) and (39) that the value of β_1 is directly proportional to the moment redistribution capacity of the beam, as expressed by the ratio of the support moments calculated according to the elastic theory to those calculated on the basis of the limit state theory. As discussed in Subsection 8.3.2, this is not the case as regards the value of β . Complete equalisation of the moments according to the limit state theory has not taken place when the deflection is in accordance with the failure criterion expressed by Equation (28). This state of affairs is also illustrated in FIG. 45 in which the values of β and β_1 are plotted as functions of the temperature θ_{\max} for a beam with a uniformly distributed load when it is rigidly restrained at one end and at both ends respectively. The ratio between the values of

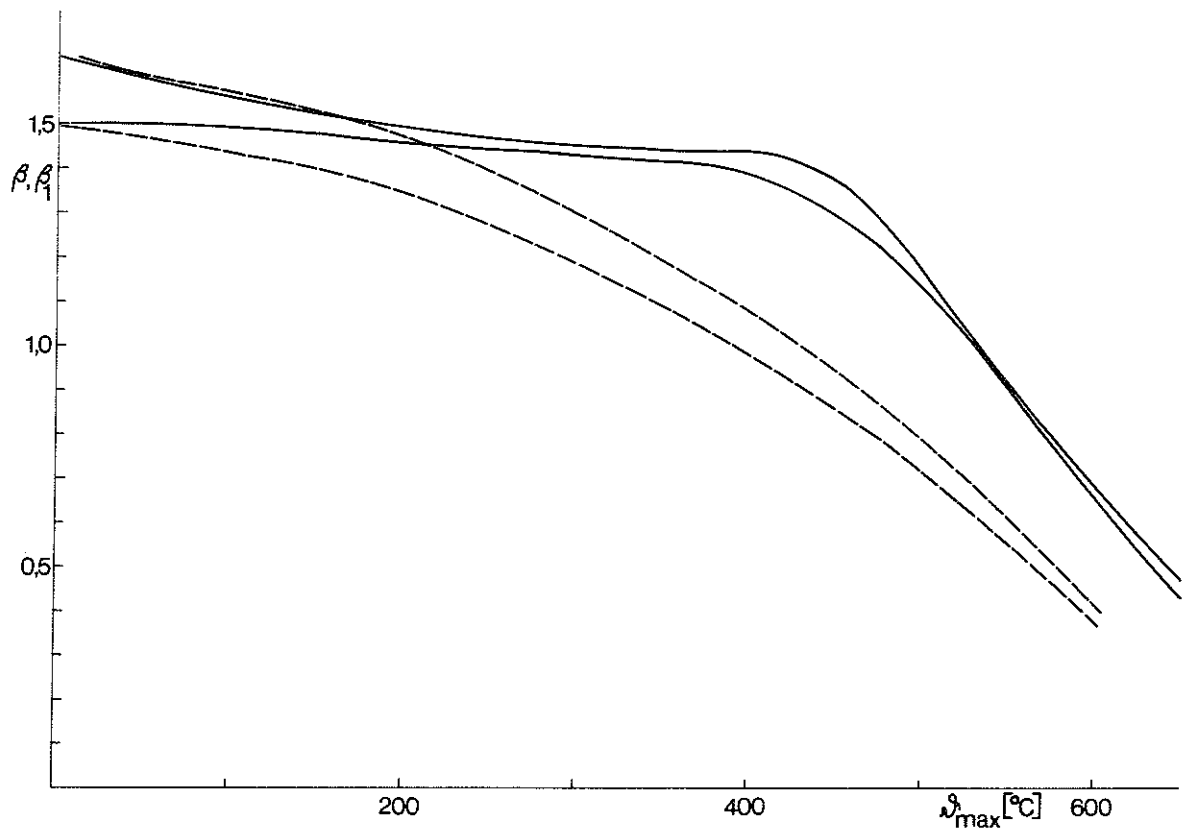


FIG. 45. The values of β (—) and of β_1 (---) for beams of carbon steel of constant I section with a uniformly distributed load. The upper full and dashed curves refer to the case when the beam is rigidly restrained at one end, while the lower full and dashed curves refer to a beam rigidly restrained at both ends. It is assumed that there is no restraint on longitudinal expansion of the beams and that the temperature is the same all over the beams. The values of β are shown only for the lowest rates of heating and cooling according to curve III in FIG. 30.

β_1 for the beam when it is rigidly restrained at one end and at both ends is equivalent - independently of the temperature - to the ratio of the moment redistribution capacity of the beam when it is restrained at one end only to its capacity when restrained at both ends. The ratio of the value of β for the beam when it is restrained at one end to that when the beam is restrained at both ends is however less than the ratio between the values of β_1 , although the absolute values of β are consistently higher than the corresponding values of β_1 .

Summing up, it may be stated that the estimation of the load carrying capacity of a beam under fire exposure conditions can be made with considerably greater accuracy by calculating the deflections of the beam during the fire than by means of the limit state theory on the basis of idealised stress-strain curves. By using the former method, it is also possible to take into account the influence exerted, on the deflection and the load carrying capacity, of creep strains and differences from the assumed ideal conditions regarding, for instance, the temperature distribution in the beam and the extent to which it can move horizontal. The ability to calculate the deformations of a beam during a fire facilitates the prediction of the extent of damage and also makes possible a more reliable assessment of the economical consequences of a fire.

REFERENCES

- (1) Bletzacker, R W: Effect of Structural Restraint on the Fire Resistance of Protected Steel Beam and Floor and Roof Assemblies. Building Research Laboratory, Final Report EES 246/266, Ohio State University, 1966.
- (2) Bono, J A: New Criteria for Fire Endurance Test. Underwriters' Laboratories Inc., 1969.
- (3) Harmathy, T Z and Stanzak, W W: Elevated-Temperature Tensile and Creep Properties of Some Structural and Prestressing Steels. Research Paper No 424, Division of Building Research, Ottawa, 1970.
- (4) Witteveen, J: Brandveiligheid Staalconstructies. Centrum Bowen in Staal, Rotterdam, 1966.
- (5) Magnusson, S E and Pettersson, O: Kvalificerad brandteknisk dimensionering av stålbärverk (Rational Structural Fire Engineering Design of Load-Bearing Steel Structures). Byggmästaren, No 9, 1969.
- (6) Thor, J: Statiskt bestämda stålbalkars deformation och bär-förmåga vid brandpåverkan - experimentell och teoretisk undersökning. (Deformation and Loadbearing Capacity of Statically Determinate Steel Beams Affected by Fire - an Experimental and Theoretical Study). Jernkontorets Forskning, Serie D, No 54, Stockholm 1972.
- (7) Dorn, J E: Some Fundamental Experiments on High Temperature Creep. Journal of the Mechanics and Physics of Solids, Vol, 3, 1954.
- (8) Harmathy, T Z: Deflection and Failure of Steel-Supported Floors and Beams in Fire. National Research Council, Canada, Division of Building Research, Paper No 195, Ottawa 1966.
- (9) Westerberg, G and Wahlberg, G: Korttidskrypprov för utvärdering av ståls egenskaper under brandförhållanden. (Short-Time Creep Tests for Evaluation of the Properties of Steels under Exposure to Fire). Domnarvet Tekniskt Meddelande U 17/70, 1970.
- (10) Thor, J: Krypdata för stål SIS 2172, utvärdering från konventionella krypförsök. (Creep Data for steel SIS 2172, Evaluation on the Basis of Conventional Creep Tests). Stålbyggnadsinstitutets rapport No 22:3, Stockholm 1970.
- (11) Thor, J: Effect of Creep on the Loadbearing Capacity of Steel Beams Exposed to Fire, Publication No 24, Swedish Institute of Steel Construction, Stockholm 1971.
- (12) Thor, J: Undersökning av olika konstruktionsståls krypegen-skaper under brandförhållanden. (Study of the Creep Properties of Different Structural Steels under Fire Exposure Conditions). Jernkontorets forskning, Serie D, No 40, Stockholm 1972.

- (13) Thor, J: Beräkning av brandpåverkade statistiskt bestämda och statistiskt obestämda stålbalkars deformation och kritiska belastning. (Calculation of the Deformation och Critical Load of Statically Determinate and Indeterminate Steel Beams under Fire Exposure Conditions). Swedish Institute of Steel Construction, Report No 22:9, Stockholm 1972.
- (14) Pettersson, O: Den byggnadstekniska brandforskningen i dag och i framtiden. (Present and Future Structural Fire Engineering Research). Brandtekniska Laboratoriet, Statens provningsanstalt, Stockholm 1964.
- (15) Ehm, H and Arnault, P: Versuchsergebnisse an statisch bestimmt gelagerten Trägern in Maizières les Metz. Europäische Konvention der Stahlbauverbände, Brandversuche an statisch bestimmt gelagerten Trägern mit und ohne Ummantelung. Doc. C.E.D.M. - 3.1/71-1.
- (16) Ehm, H and Arnault, P: Brandversuche an statisch bestimmt und statisch unbestimmt gelagerten Stahlträgern. Europäische Konvention der Stahlbauverbände. Doc. C.E.C.M. - 3.1/69-30.
- (17) Robertson, A F and Ryan, I V: Proposed Criteria for Defining Load Failure of Beams, Floors and Roof Constructions during Fire Tests. Journal of Research, National Bureau of Standards, Vol. 63C, 1959.
- (18) Magnusson, S-E and Pettersson, O: Brandteknisk dimensionering av stålkonstruktioner. (Fire Engineering Design of Steel Structures). Stålbyggnadshandboken. Norrbottens Järnverk AB, 1972.
- (19) Witteveen, J and Koning, C H M: Model-Furnace Tests on the Behaviour of Steel Frames in Fire. Report II for Committee 3.1 of the Convention of European Constructional Steelwork Associations, 1969.

D:16 1973

**This document refers to Grant C 742 from the Swedish Council for Building Research to the Swedish Institute of Steel Construction
The proceeds of the sales go to the Building Research Fund.**

**Distribution: Svensk Byggtjänst, Box 1403, S-111 84 Stockholm,
Sweden**

Price: Sw. Kr. 23